Title: The 7-year WMAP Observations: Cosmological Interpretation

Date: Apr 27, 2010 02:00 PM

URL: http://pirsa.org/10040021

Abstract: We have announced the results from 7 years of observations of the Wilkinson Microwave Anisotropy Probe (WMAP) on January 26. In this talk we will present the cosmological interpretation of the WMAP 7-year data, including the detection of primordial helium, images of polarization of microwave background around temperature peaks, and new limits on inflation and properties of neutrinos. We also report a significant detection of the Sunyaev-Zel'dovich effect and discuss implications for the gas pressure in clusters of galaxies.

The 7-Year *WMAP* Observations: Cosmological Interpretation

Eiichiro Komatsu (Texas Cosmology Center, UT Austin)

Cosmology Seminar, Perimeter Institute, April 27, 2010

The **7**-Year *WMAP* Observations: Cosmological Interpretation

Eiichiro Komatsu (Texas Cosmology Center, UT Austin)

Cosmology Seminar, Perimeter Institute, April 27, 2010

The **7**-Year *WMAP* Observations: Cosmological Interpretation

Eiichiro Komatsu (Texas Cosmology Center, UT Austin)

Cosmology Seminar, Perimeter Institute, April 27, 2010

The **7**-Year *WMAP* Observations: Cosmological Interpretation

Eiichiro Komatsu (Texas Cosmology Center, UT Austin)

Cosmology Seminar, Perimeter Institute, April 27, 2010

The **7**-Year *WMAP* Observations: Cosmological Interpretation

Eiichiro Komatsu (Texas Cosmology Center, UT Austin)

Cosmology Seminar, Perimeter Institute, April 27, 2010

The **7**-Year *WMAP* Observations: Cosmological Interpretation

Eiichiro Komatsu (Texas Cosmology Center, UT Austin)

Cosmology Seminar, Perimeter Institute, April 27, 2010

The **7**-Year *WMAP* Observations: Cosmological Interpretation

Eiichiro Komatsu (Texas Cosmology Center, UT Austin)

Cosmology Seminar, Perimeter Institute, April 27, 2010

The **7**-Year *WMAP* Observations: Cosmological Interpretation

Eiichiro Komatsu (Texas Cosmology Center, UT Austin)

Cosmology Seminar, Perimeter Institute, April 27, 2010

The **7**-Year *WMAP* Observations: Cosmological Interpretation

Eiichiro Komatsu (Texas Cosmology Center, UT Austin)
Cosmology Seminar, Perimeter Institute, April 27, 2010

The **7**-Year *WMAP* Observations: Cosmological Interpretation

Eiichiro Komatsu (Texas Cosmology Center, UT Austin)
Cosmology Seminar, Perimeter Institute, April 27, 2010

The **7**-Year *WMAP* Observations: Cosmological Interpretation

Eiichiro Komatsu (Texas Cosmology Center, UT Austin)

Cosmology Seminar, Perimeter Institute, April 27, 2010

The **7**-Year *WMAP* Observations: Cosmological Interpretation

Eiichiro Komatsu (Texas Cosmology Center, UT Austin)
Cosmology Seminar, Perimeter Institute, April 27, 2010

The **7**-Year *WMAP* Observations: Cosmological Interpretation

Eiichiro Komatsu (Texas Cosmology Center, UT Austin)

Cosmology Seminar, Perimeter Institute, April 27, 2010

The **7**-Year *WMAP* Observations: Cosmological Interpretation

Eiichiro Komatsu (Texas Cosmology Center, UT Austin)
Cosmology Seminar, Perimeter Institute, April 27, 2010

The **7**-Year *WMAP* Observations: Cosmological Interpretation

Eiichiro Komatsu (Texas Cosmology Center, UT Austin)

Cosmology Seminar, Perimeter Institute, April 27, 2010

The **7**-Year *WMAP* Observations: Cosmological Interpretation

Eiichiro Komatsu (Texas Cosmology Center, UT Austin)

Cosmology Seminar, Perimeter Institute, April 27, 2010

The **7**-Year *WMAP* Observations: Cosmological Interpretation

Eiichiro Komatsu (Texas Cosmology Center, UT Austin)

Cosmology Seminar, Perimeter Institute, April 27, 2010

The **7**-Year *WMAP* Observations: Cosmological Interpretation

Eiichiro Komatsu (Texas Cosmology Center, UT Austin)

Cosmology Seminar, Perimeter Institute, April 27, 2010

The **7**-Year *WMAP* Observations: Cosmological Interpretation

Eiichiro Komatsu (Texas Cosmology Center, UT Austin)

Cosmology Seminar, Perimeter Institute, April 27, 2010

The **7**-Year *WMAP* Observations: Cosmological Interpretation

Eiichiro Komatsu (Texas Cosmology Center, UT Austin)

Cosmology Seminar, Perimeter Institute, April 27, 2010

The **7**-Year *WMAP* Observations: Cosmological Interpretation

Eiichiro Komatsu (Texas Cosmology Center, UT Austin)

Cosmology Seminar, Perimeter Institute, April 27, 2010

The **7**-Year *WMAP* Observations: Cosmological Interpretation

Eiichiro Komatsu (Texas Cosmology Center, UT Austin)

Cosmology Seminar, Perimeter Institute, April 27, 2010

The **7**-Year *WMAP* Observations: Cosmological Interpretation

Eiichiro Komatsu (Texas Cosmology Center, UT Austin)

Cosmology Seminar, Perimeter Institute, April 27, 2010

The **7**-Year *WMAP* Observations: Cosmological Interpretation

Eiichiro Komatsu (Texas Cosmology Center, UT Austin)
Cosmology Seminar, Perimeter Institute, April 27, 2010

WMAP will have collected 9 years of data by August

June 2001:
WMAP launched!

February 2003:
The first-year data release

March 2006:
The three-year data release

March 2008:
The five-year data release

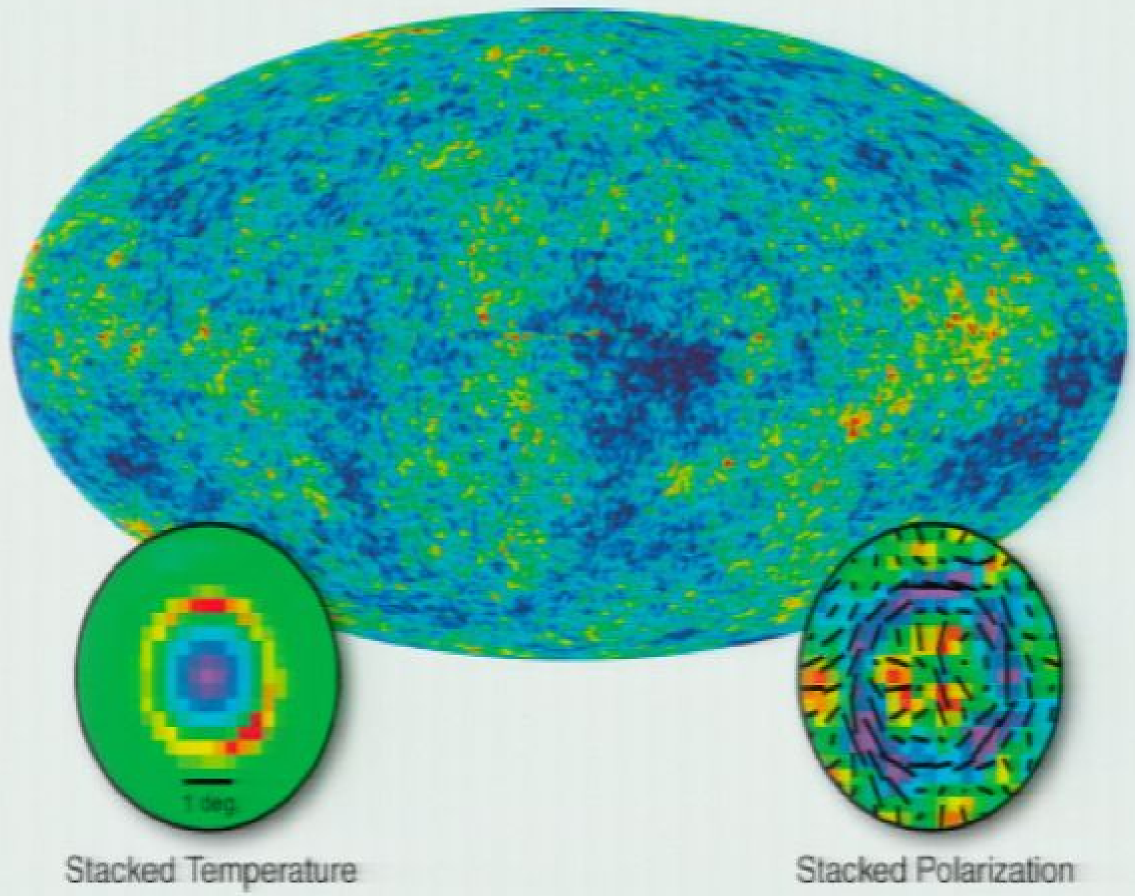

- **January 2010: The seven-year data release**

WMAP 7-Year Papers

- **Jarosik et al.**, "*Sky Maps, Systematic Errors, and Basic Results*" arXiv:1001.4744
- **Gold et al.**, "*Galactic Foreground Emission*" arXiv:1001.4555
- **Weiland et al.**, "*Planets and Celestial Calibration Sources*" arXiv:1001.4731
- **Bennett et al.**, "*Are There CMB Anomalies?*" arXiv:1001.4758
- **Larson et al.**, "*Power Spectra and WMAP-Derived Parameters*" arXiv:1001.4635
- **Komatsu et al.**, "*Cosmological Interpretation*" arXiv:1001.4538

WMAP 7-Year Science Team

- C.L. Bennett
- G. Hinshaw
- N. Jarosik
- S.S. Meyer
- L. Page
- D.N. Spergel
- E.L. Wright
- M.R. Greason
- M. Halpern
- R.S. Hill
- A. Kogut
- M. Limon
- N. Odegard
- G.S. Tucker
- J. L. Weiland
- E. Wollack
- J. Dunkley
- B. Gold
- E. Komatsu
- D. Larson
- M.R. Nolta
- K.M. Smith
- C. Barnes
- R. Bean
- O. Dore
- H.V. Peiris
- L. Verde

7-year Science Highlights

- First detection (>3σ) of the effect of primordial **helium** on the temperature power spectrum.
- The primordial **tilt** is less than one at >3σ:
  - n_s=0.96±0.01 (68%CL)
- Improved limits on **neutrino** parameters:
  - $\sum m_\nu$<0.58eV (95%CL); N_{eff}=4.3±0.9 (68%CL)
- First direct confirmation of the predicted **polarization** pattern around temperature spots.
- Measurement of the SZ effect: *missing* ***pressure***?

5

WMAP 7-Year Science Team

- C.L. Bennett
- G. Hinshaw
- N. Jarosik
- S.S. Meyer
- L. Page
- D.N. Spergel
- E.L. Wright
- M.R. Greason
- M. Halpern
- R.S. Hill
- A. Kogut
- M. Limon
- N. Odegard
- G.S. Tucker
- J. L. Weiland
- E. Wollack
- J. Dunkley
- B. Gold
- E. Komatsu
- D. Larson
- M.R. Nolta
- K.M. Smith
- C. Barnes
- R. Bean
- O. Dore
- H.V. Peiris
- L. Verde

7-year Science Highlights

- First detection (>3σ) of the effect of primordial **helium** on the temperature power spectrum.
- The primordial **tilt** is less than one at >3σ:
  - n_s=0.96±0.01 (68%CL)
- Improved limits on **neutrino** parameters:
  - $\sum m_\nu$<0.58eV (95%CL); N_{eff}=4.3±0.9 (68%CL)
- First direct confirmation of the predicted **polarization** pattern around temperature spots.
- Measurement of the SZ effect: *missing* ***pressure***?

7-year Temperature C_l

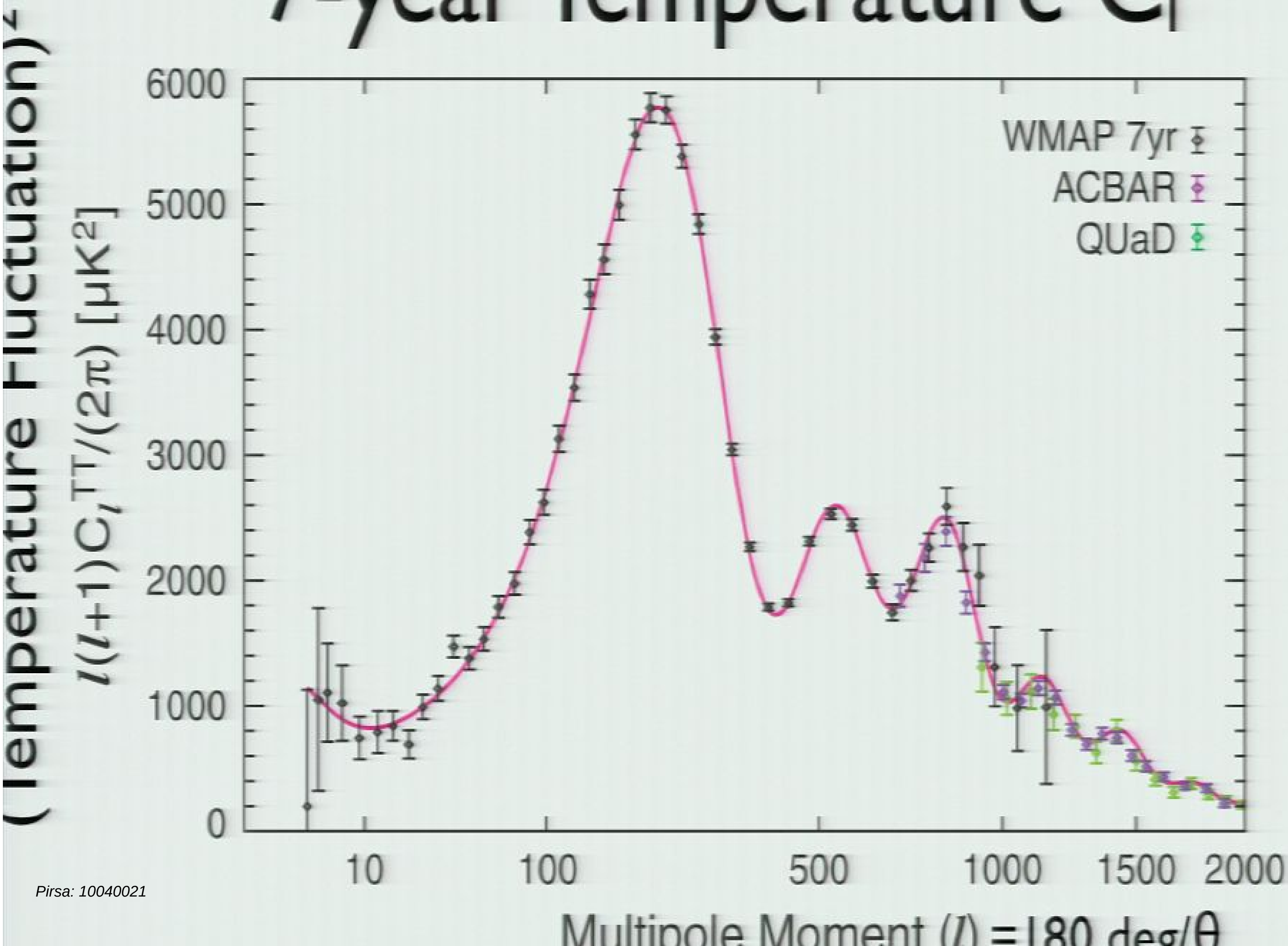

7-year Science Highlights

- First detection (>3σ) of the effect of primordial **helium** on the temperature power spectrum.
- The primordial **tilt** is less than one at >3σ:
  - n_s=0.96±0.01 (68%CL)
- Improved limits on **neutrino** parameters:
  - $\sum m_\nu$<0.58eV (95%CL); N_{eff}=4.3±0.9 (68%CL)
- First direct confirmation of the predicted **polarization** pattern around temperature spots.
- Measurement of the SZ effect: *missing* ***pressure***?

7-year Temperature C$_l$

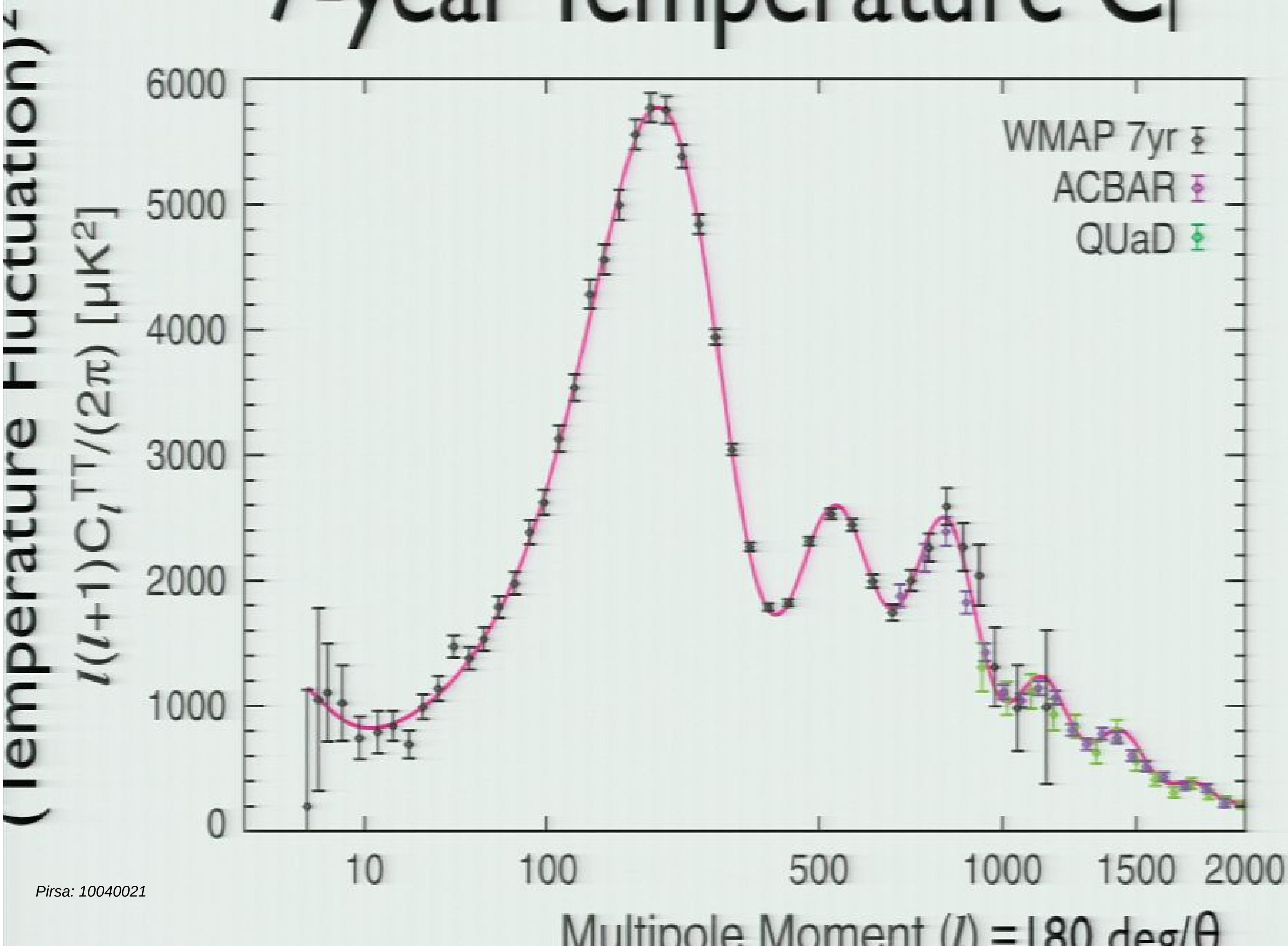

Zooming into the 3rd peak...

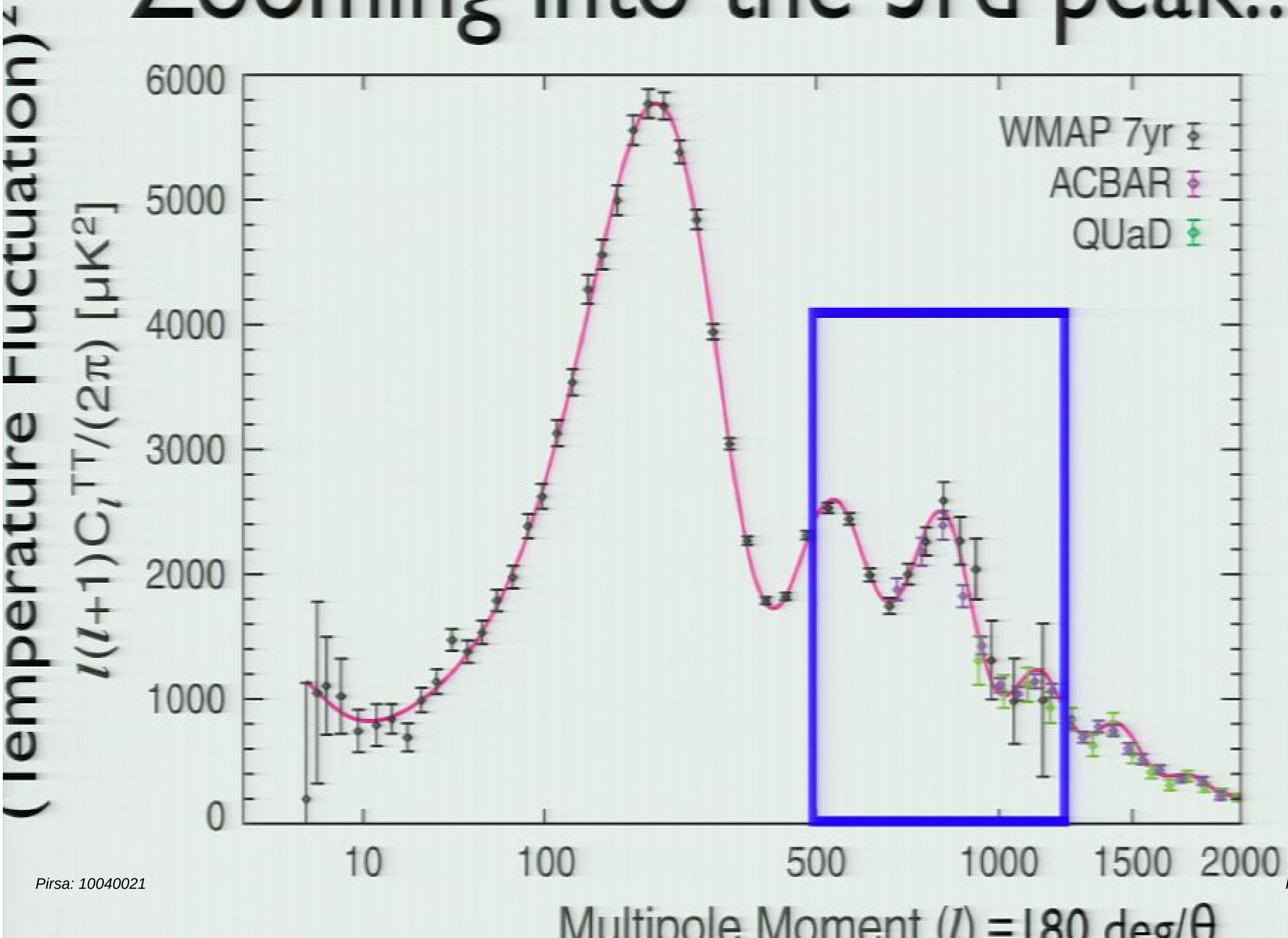

High-l Temperature C_l: Improvement from 5-year

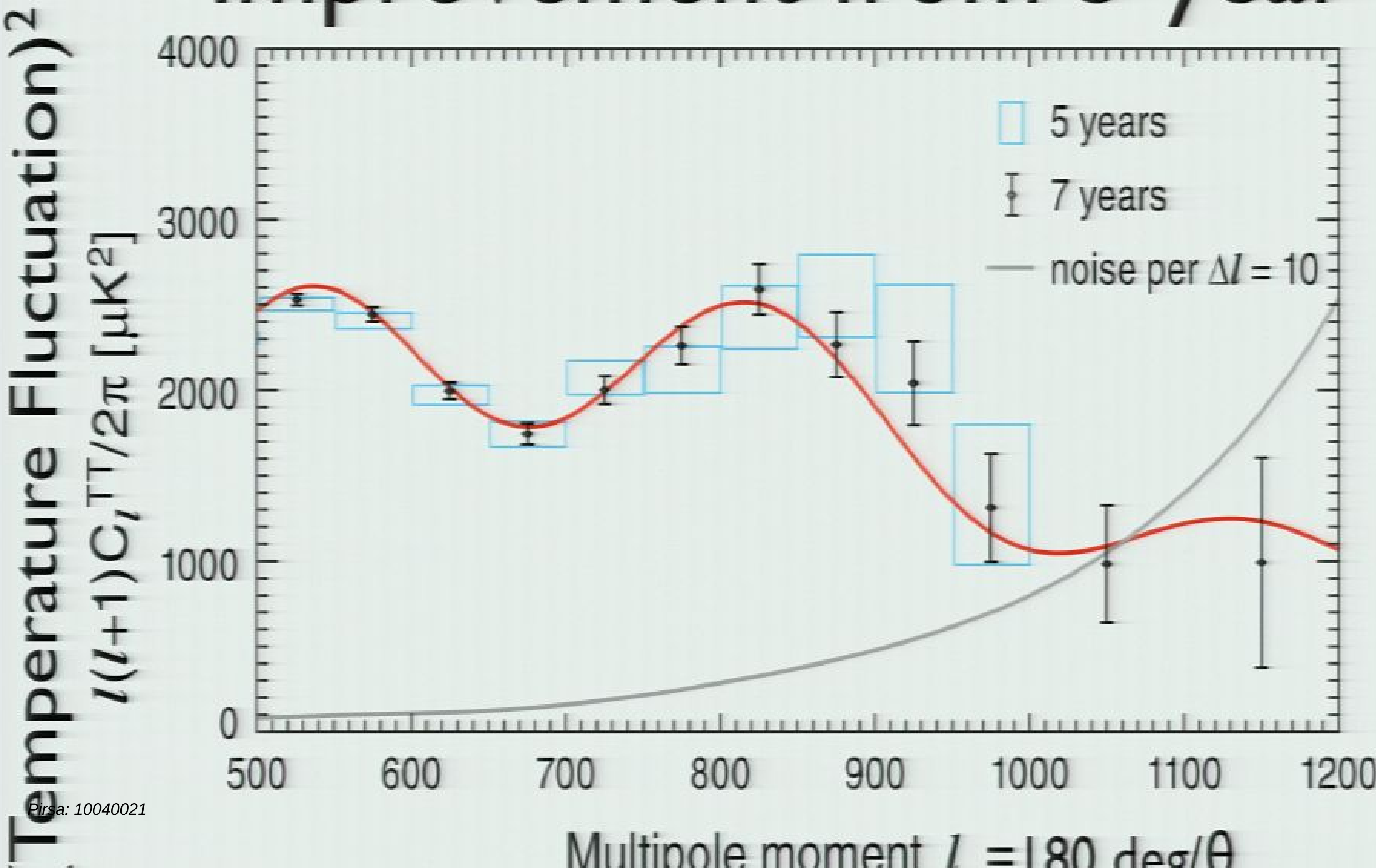

WMAP and ACT

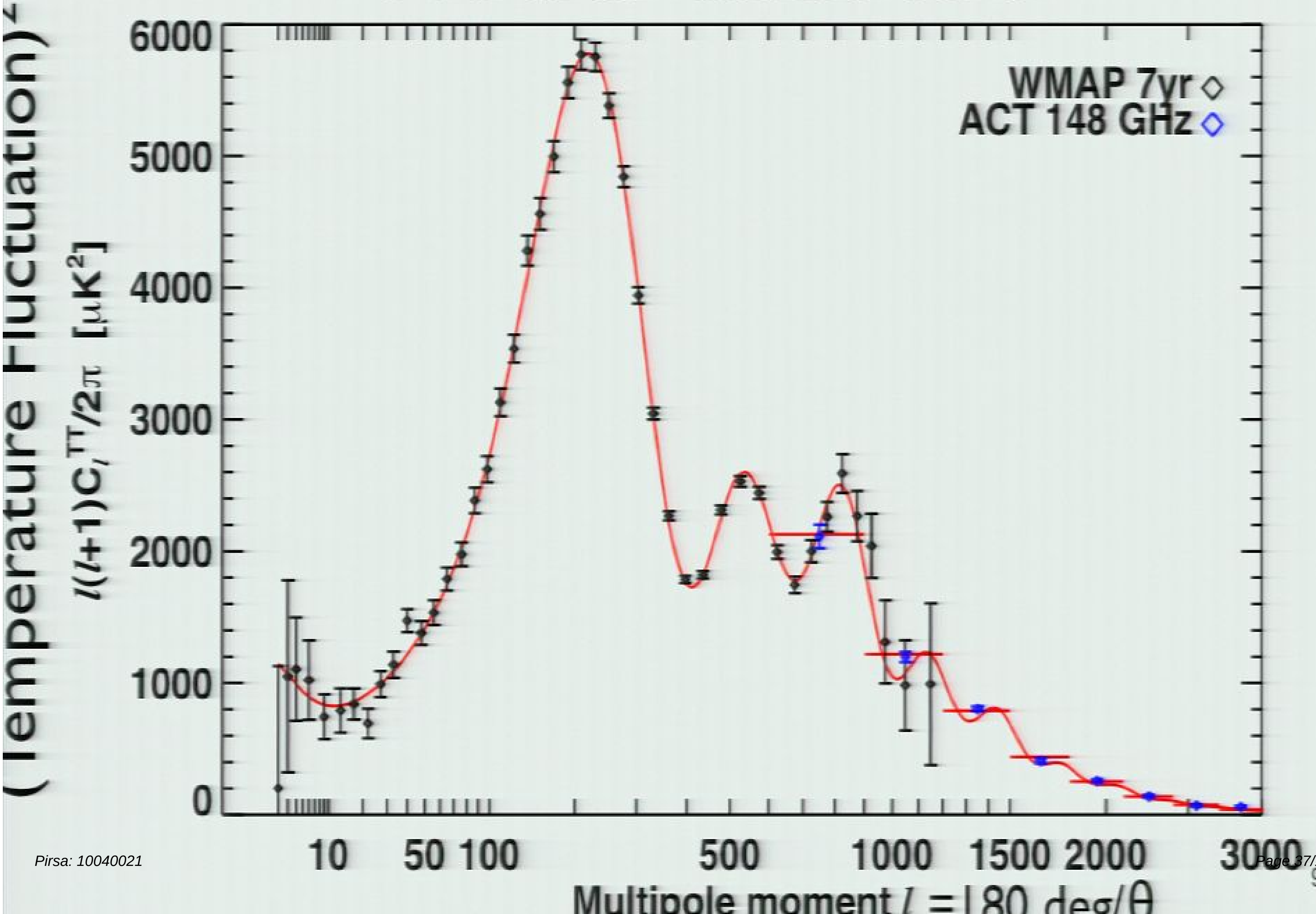

(Temperature Fluctuation)²
$l(l+1)C_l^{TT}/2\pi$ [μK²]
6000
5000
4000
3000
2000
1000
0
WMAP 7yr
ACT 148 GHz
10
50 100
500
1000
1500 2000
3000
Multipole moment l = 180 deg/θ

High-l Temperature C_l: Improvement from 5-year

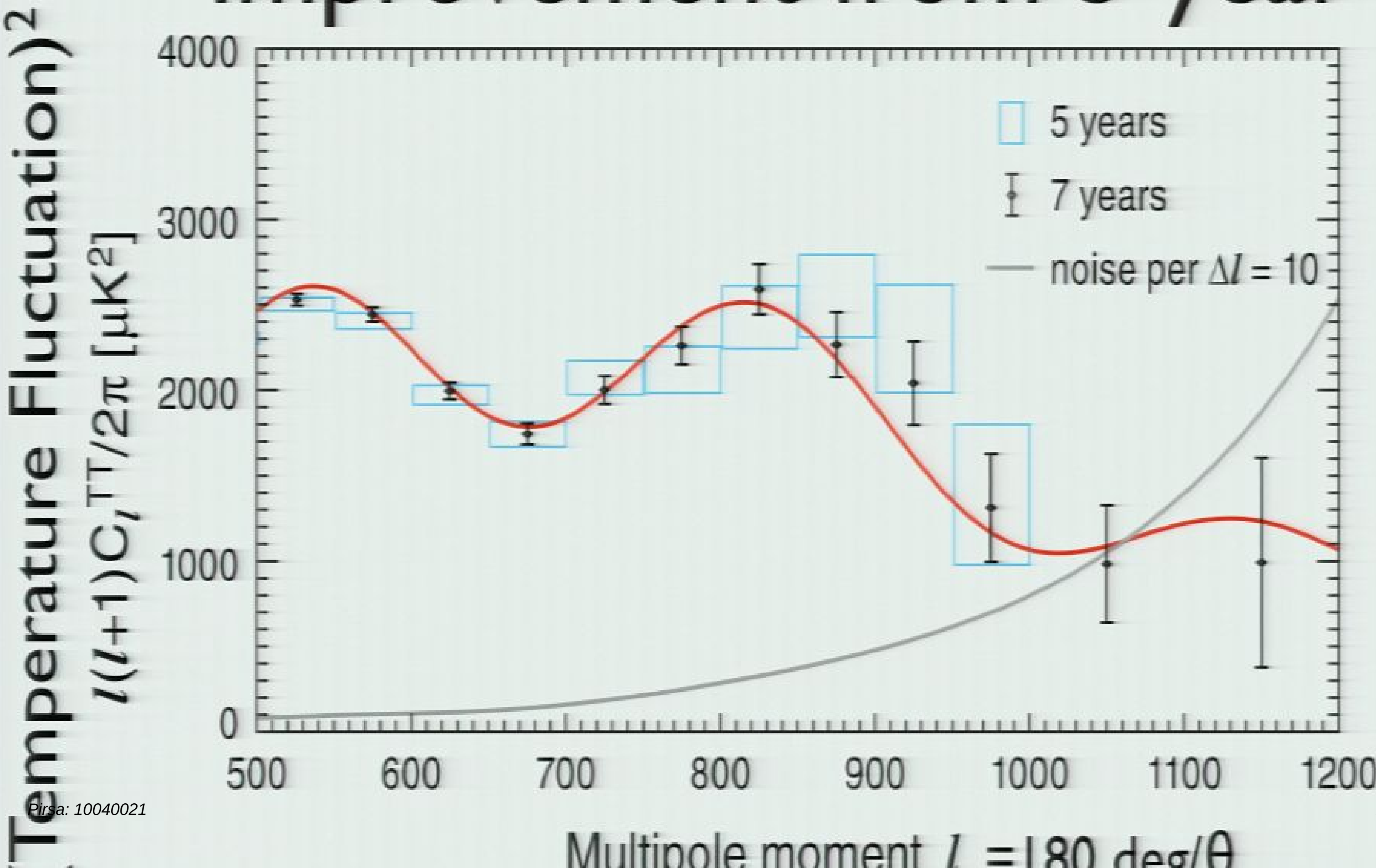

Zooming into the 3rd peak...

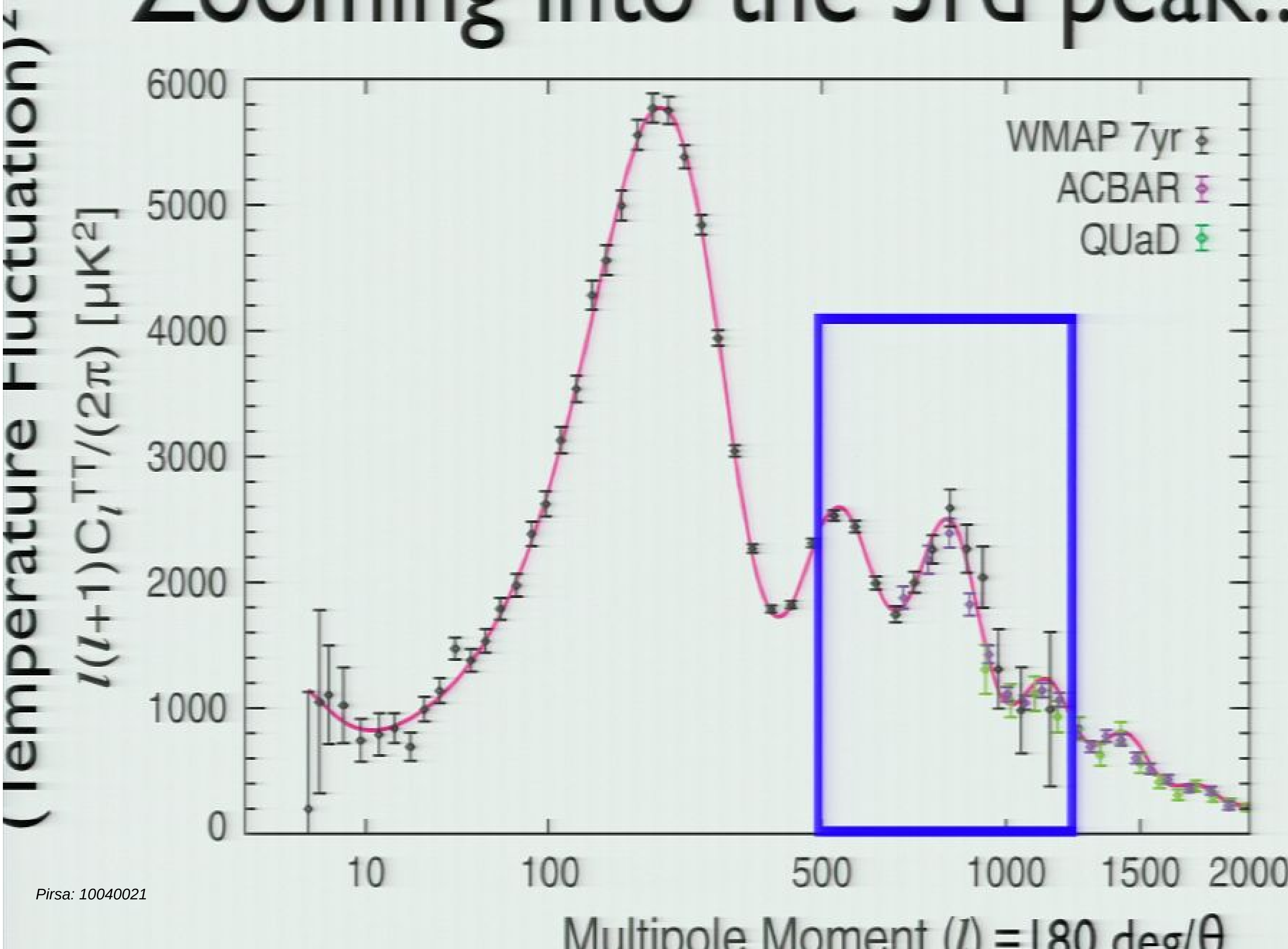

High-l Temperature C_l: Improvement from 5-year

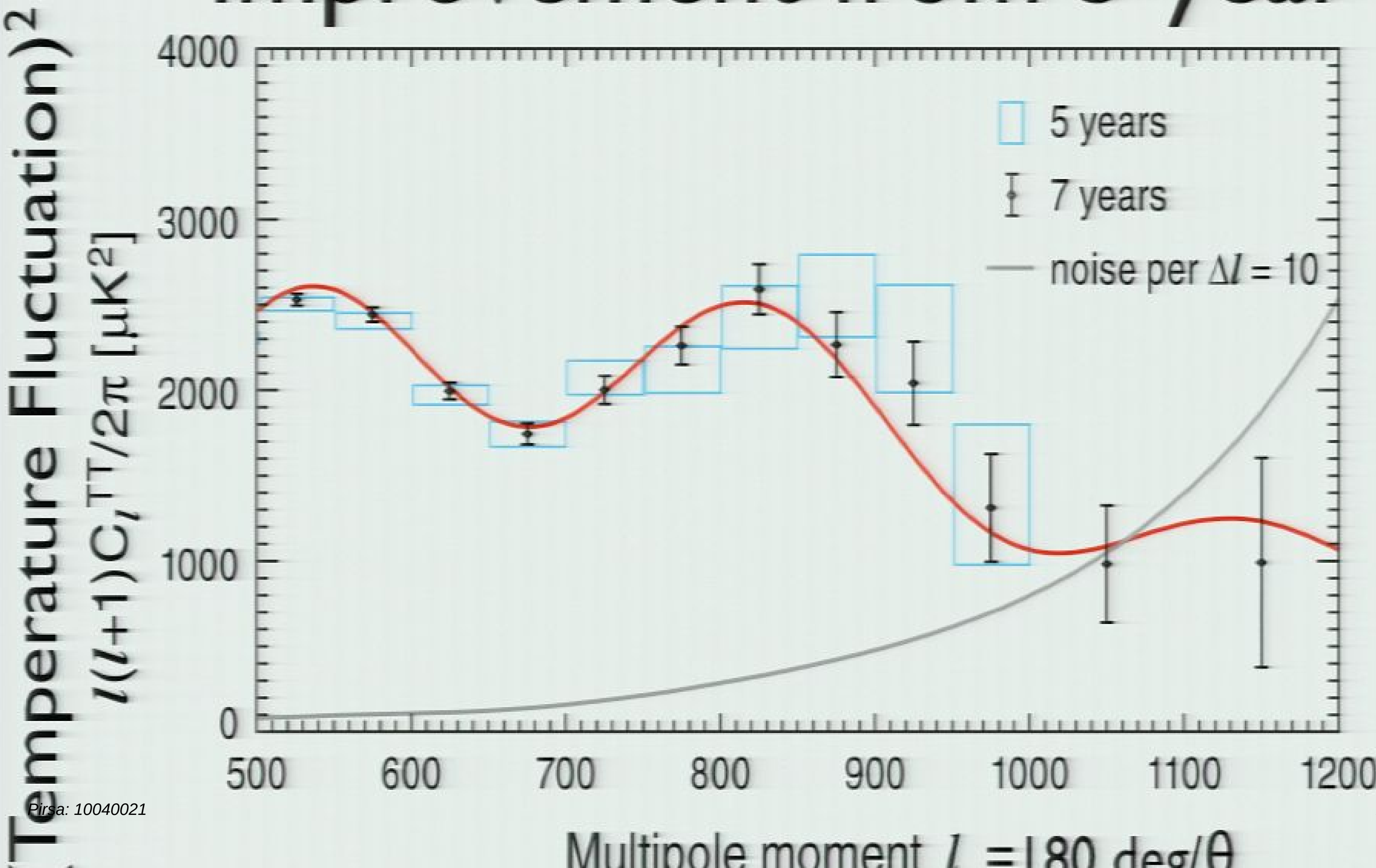

WMAP and ACT

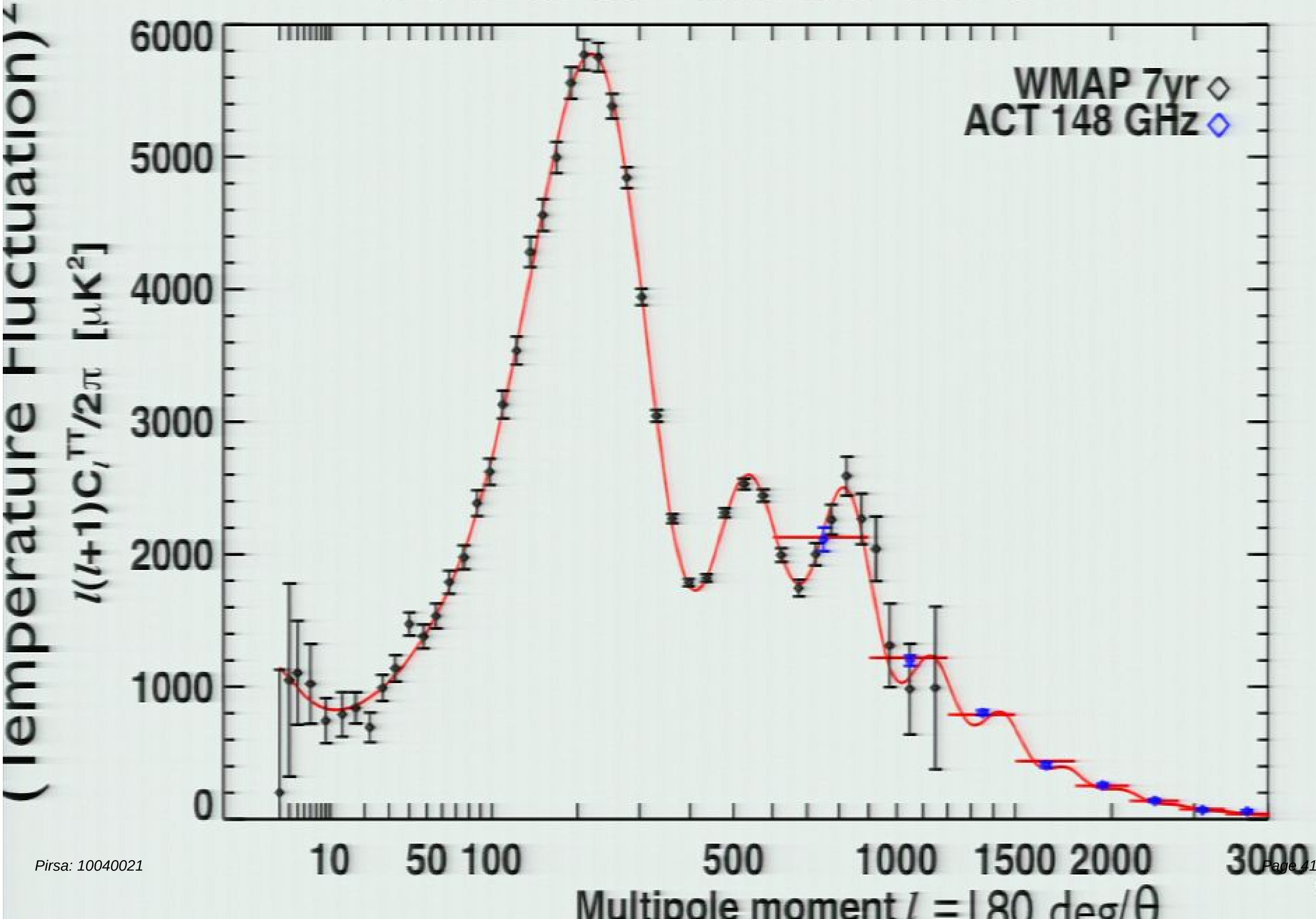

WMAP 7yr
ACT 148 GHz
6000
5000
4000
3000
2000
1000
0
10
50 100
500
1000
1500 2000
3000

Detection of Primordial Helium

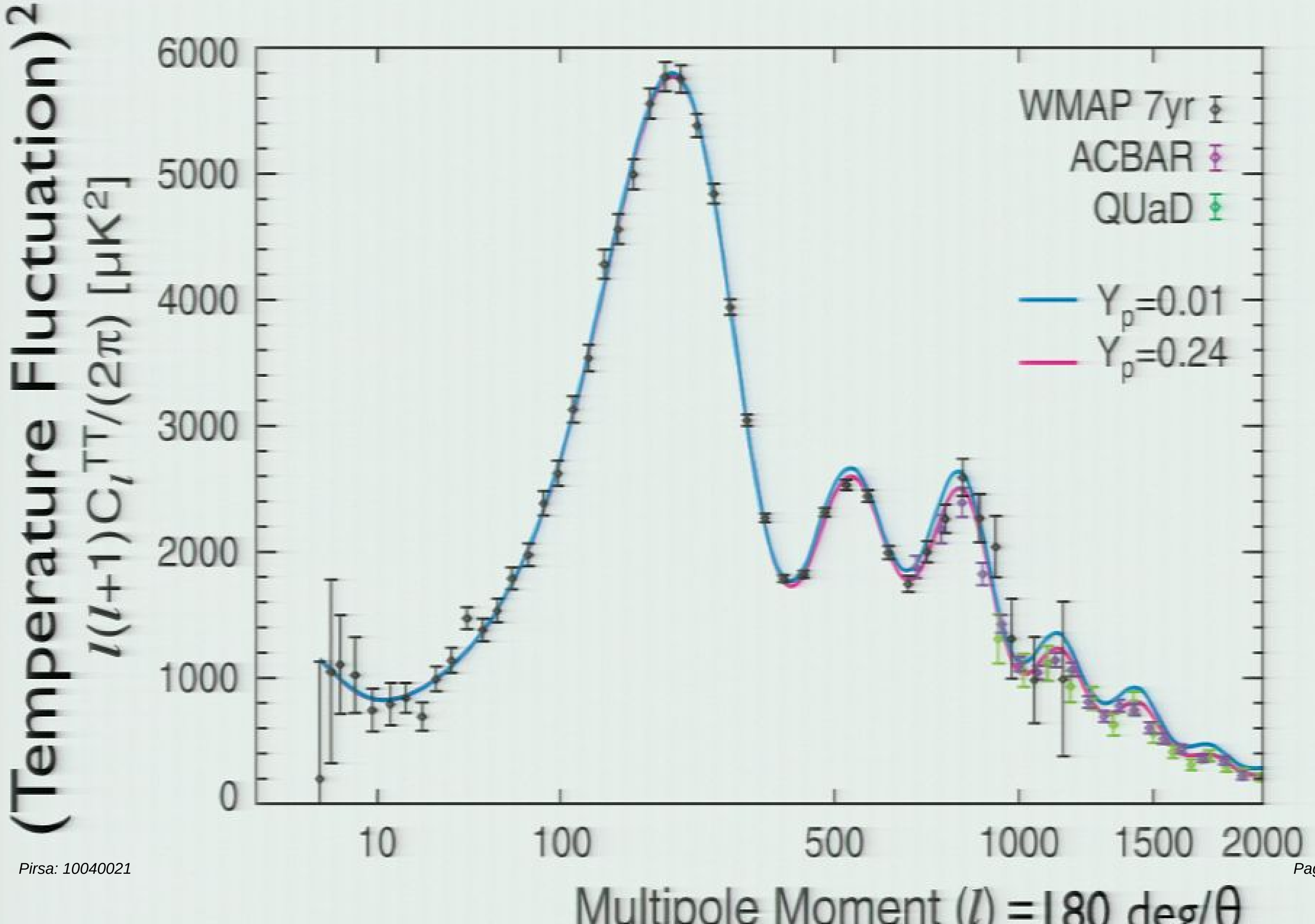

Effect of helium on C_l^{TT}

- We measure the baryon number density, n_b, from the 1st-to-2nd peak ratio.
- As helium recombined at z~1800, there were fewer electrons at the decoupling epoch (z=1090): $n_e=(1-Y_p)n_b$.
- **More helium** = Fewer electrons = Longer photon mean free path $1/(\sigma_T n_e)$ = **Enhanced Silk damping**
- This effect might be degenerate with $\Omega_b h^2$ or n_s...

Detection of Primordial Helium

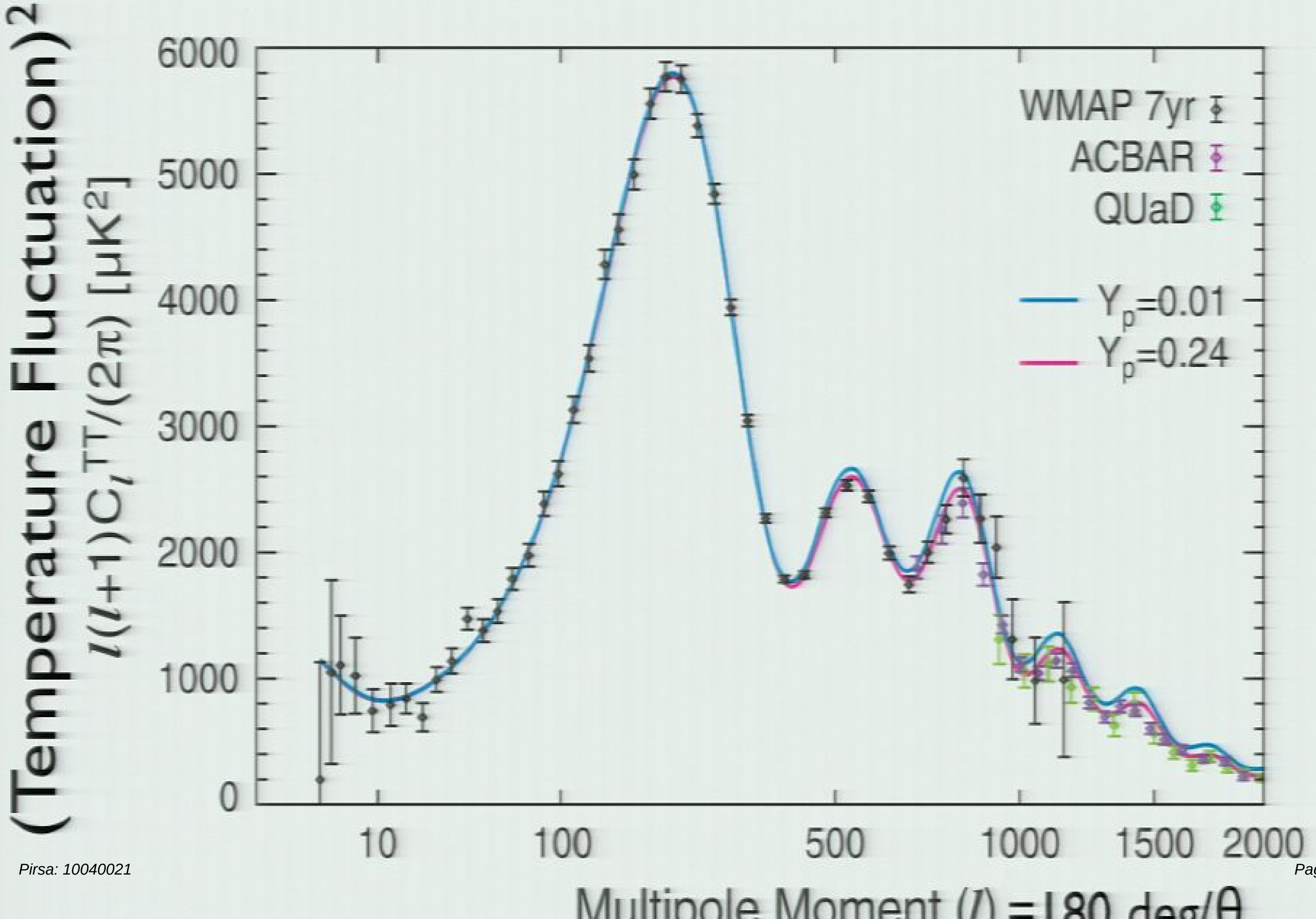

Effect of helium on C_l^{TT}

- We measure the baryon number density, n_b, from the 1st-to-2nd peak ratio.
- As helium recombined at z~1800, there were fewer electrons at the decoupling epoch (z=1090): $n_e=(1-Y_p)n_b$.
- **More helium** = Fewer electrons = Longer photon mean free path $1/(\sigma_T n_e)$ = **Enhanced Silk damping**
- This effect might be degenerate with $\Omega_b h^2$ or n_s...

Detection of Primordial Helium

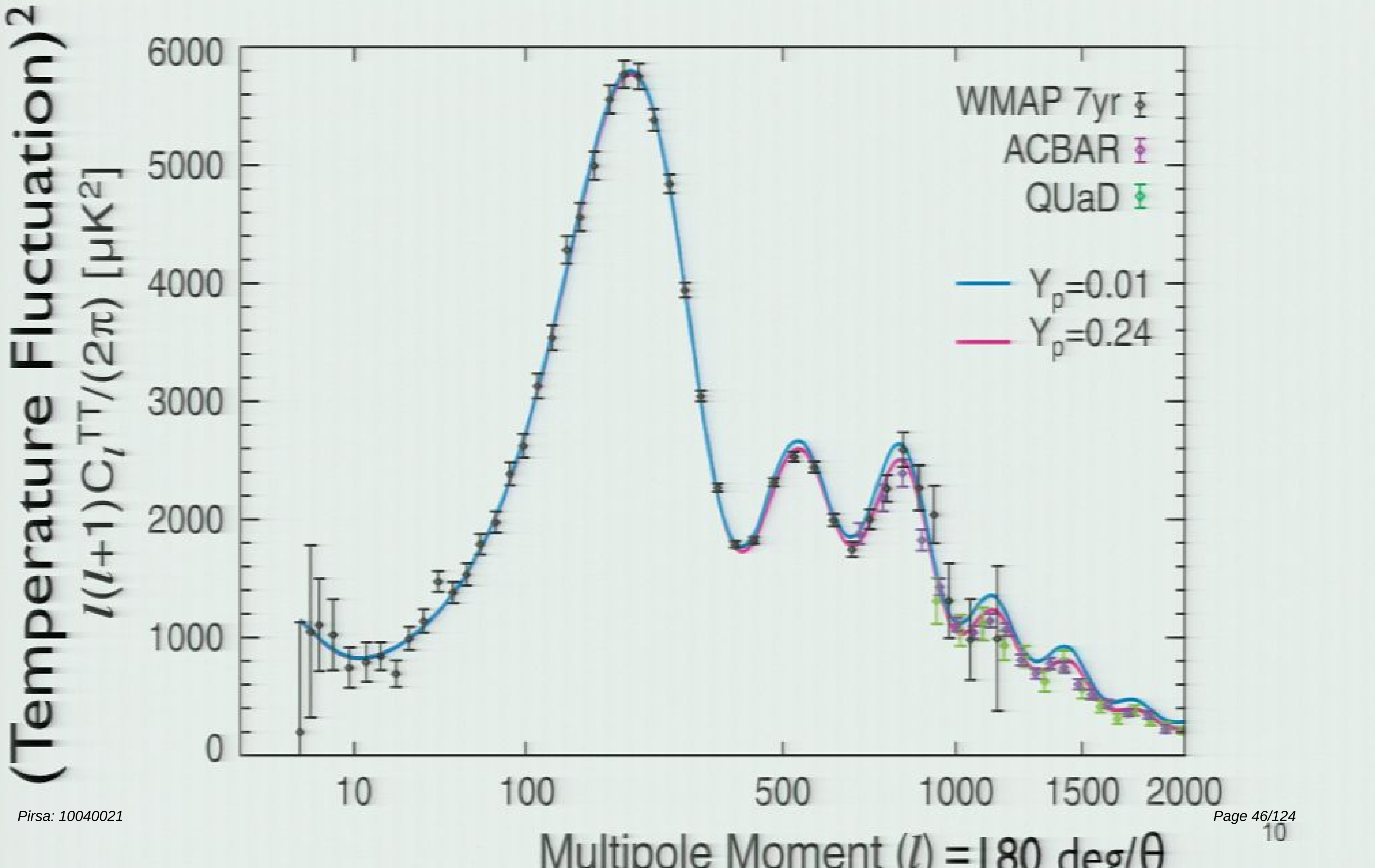

Effect of helium on C_l^{TT}

- We measure the baryon number density, n_b, from the 1st-to-2nd peak ratio.
- As helium recombined at z~1800, there were fewer electrons at the decoupling epoch (z=1090): $n_e=(1-Y_p)n_b$.
- **More helium** = Fewer electrons = Longer photon mean free path $1/(\sigma_T n_e)$ = **Enhanced Silk damping**
- This effect might be degenerate with $\Omega_b h^2$ or n_s...

Detection of Primordial Helium

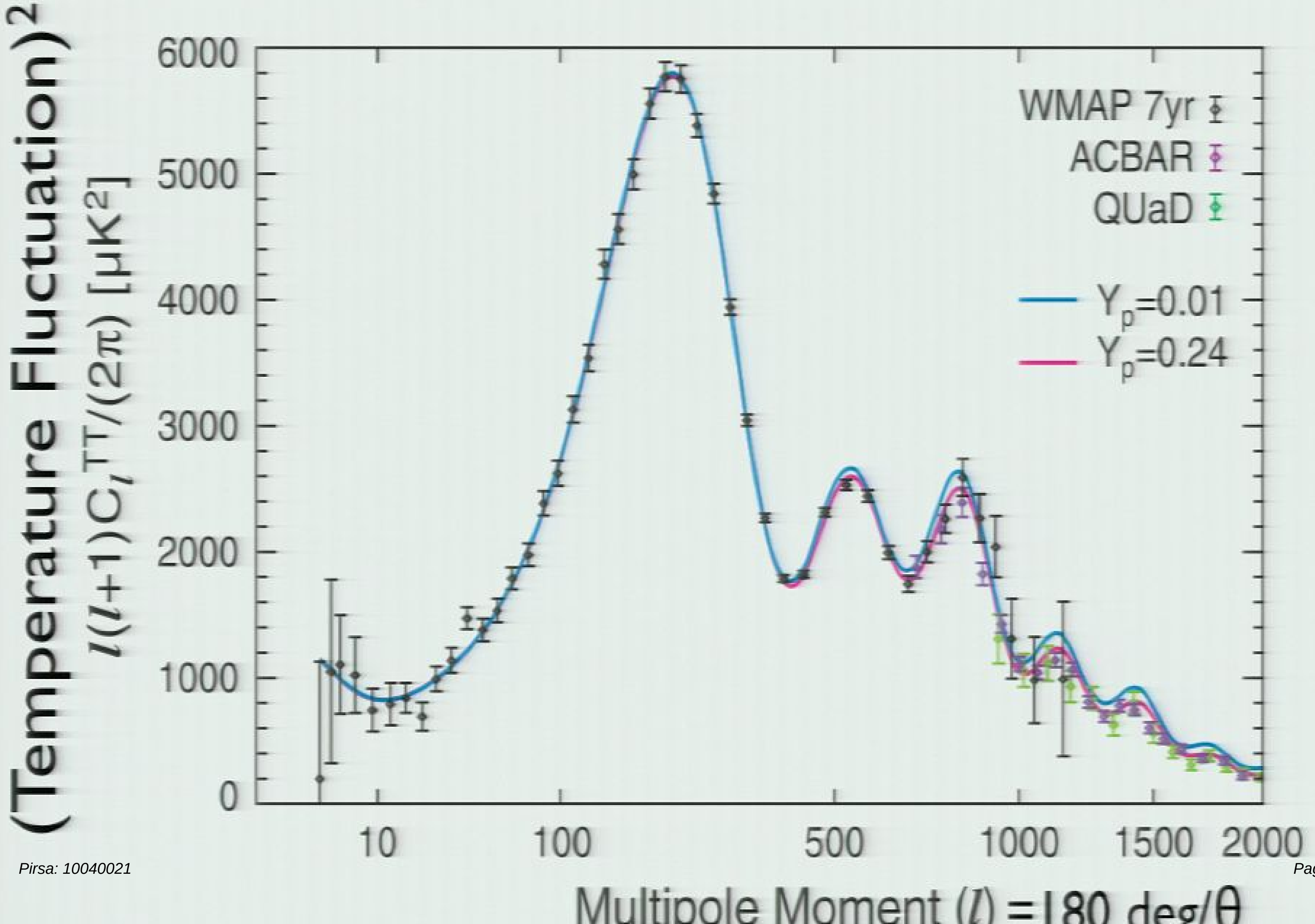

WMAP + higher-l CMB = Detection of Helium

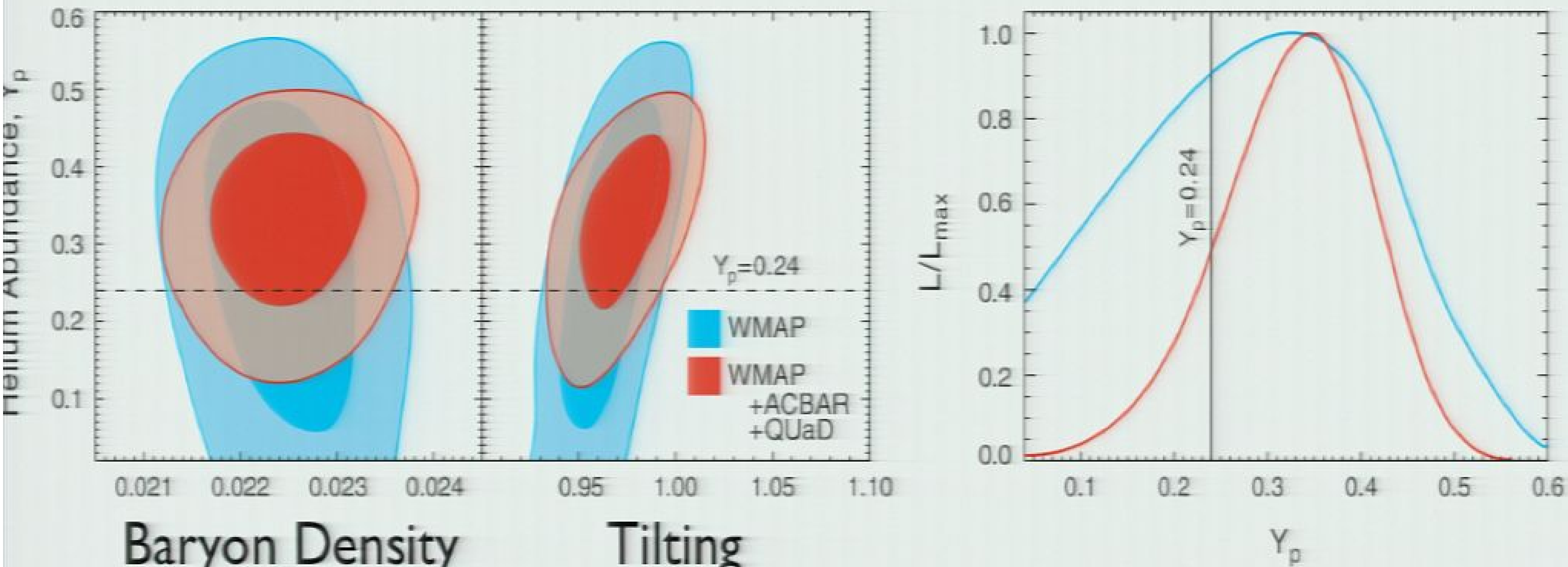

- The combination of WMAP and high-l CMB data (ACBAR and QUaD) is powerful enough to isolate the effect of helium: **Y_p = 0.33 ± 0.08** (68%CL)

Why this can be useful

- The helium abundance has been measured from Sun and ionized regions (HII regions); however, as helium can be produced in the stellar core, one has to extrapolate the measured Y_p to the zero-metallicity values.
- In other words, the traditional methods give a robust **upper limit** on Y_p: $Y_p<0.3$.
- The CMB data give us a robust **lower limit** on Y_p.

$0.23 < Y_p < 0.3$ (68%CL)

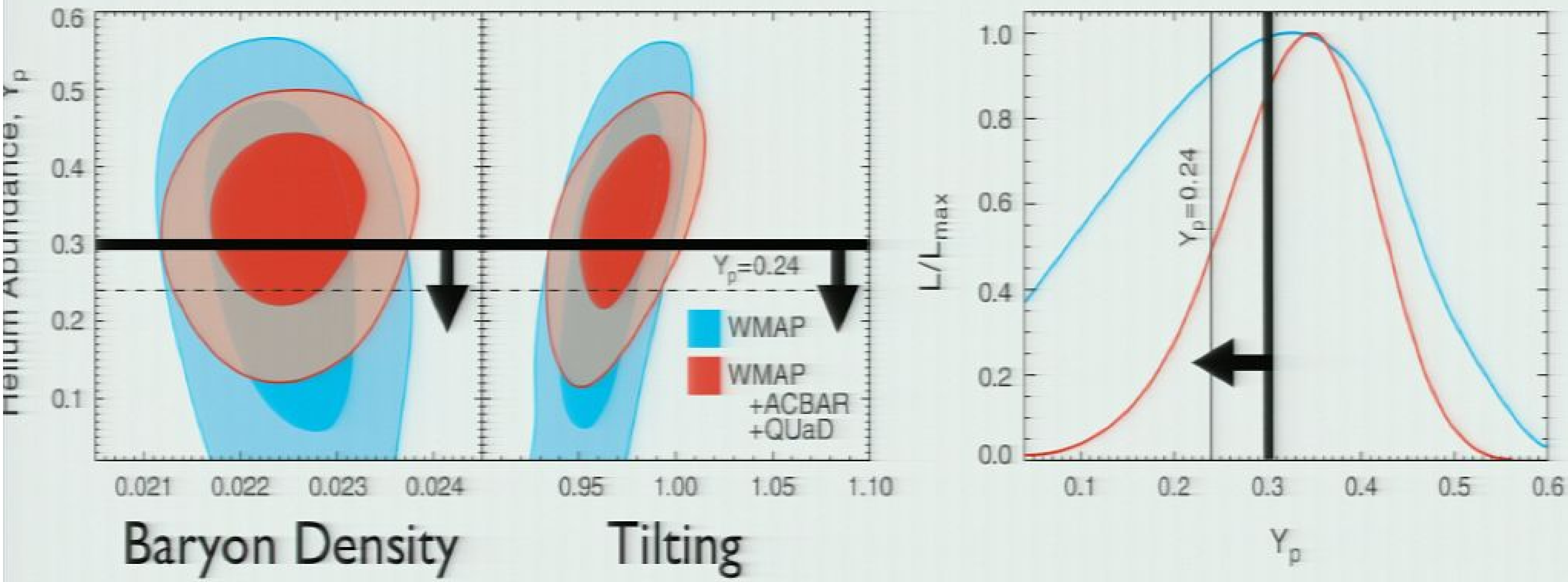

- Planck is expected to yield $\Delta Y_p \sim 0.01$ (68%CL; Ichikawa et al. 2008).

Another "3rd peak science": Number of Relativistic Species

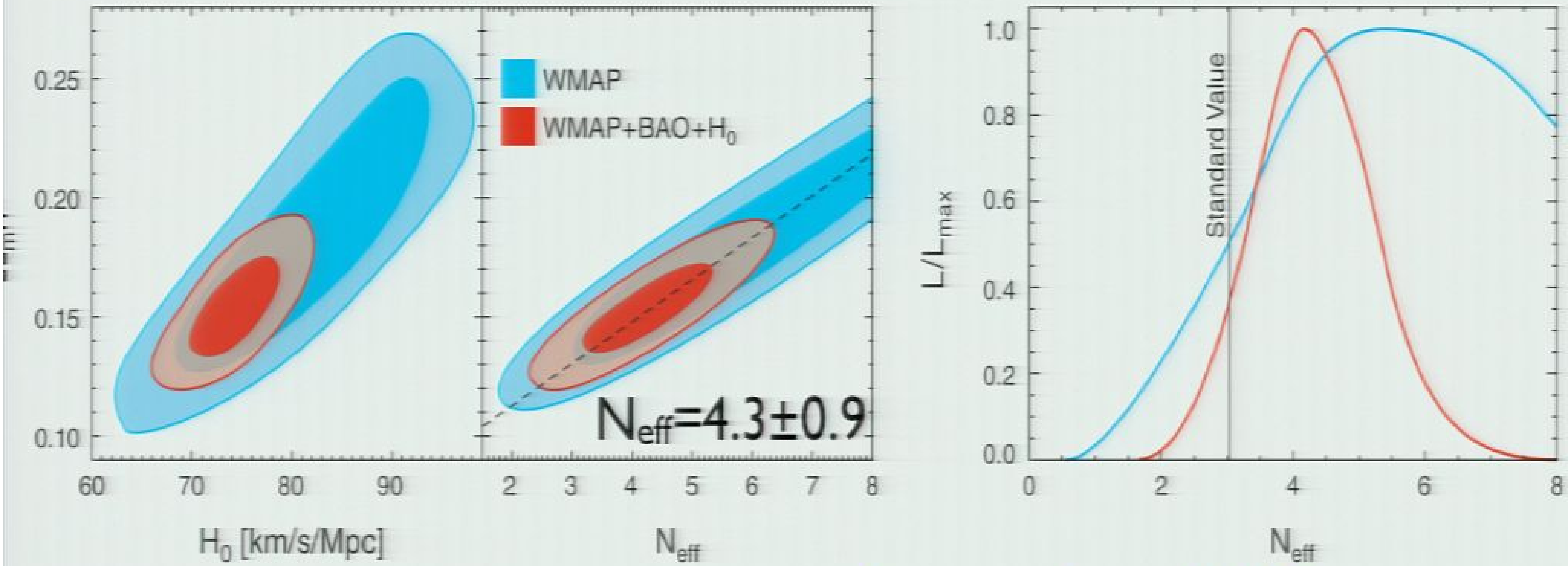

from external data

$$N_{\rm eff} = 3.04 + 7.44\left(\frac{\Omega_m h^2}{0.1308}\frac{3139}{1+z_{\rm eq}} - 1\right)$$

from 3rd peak

15

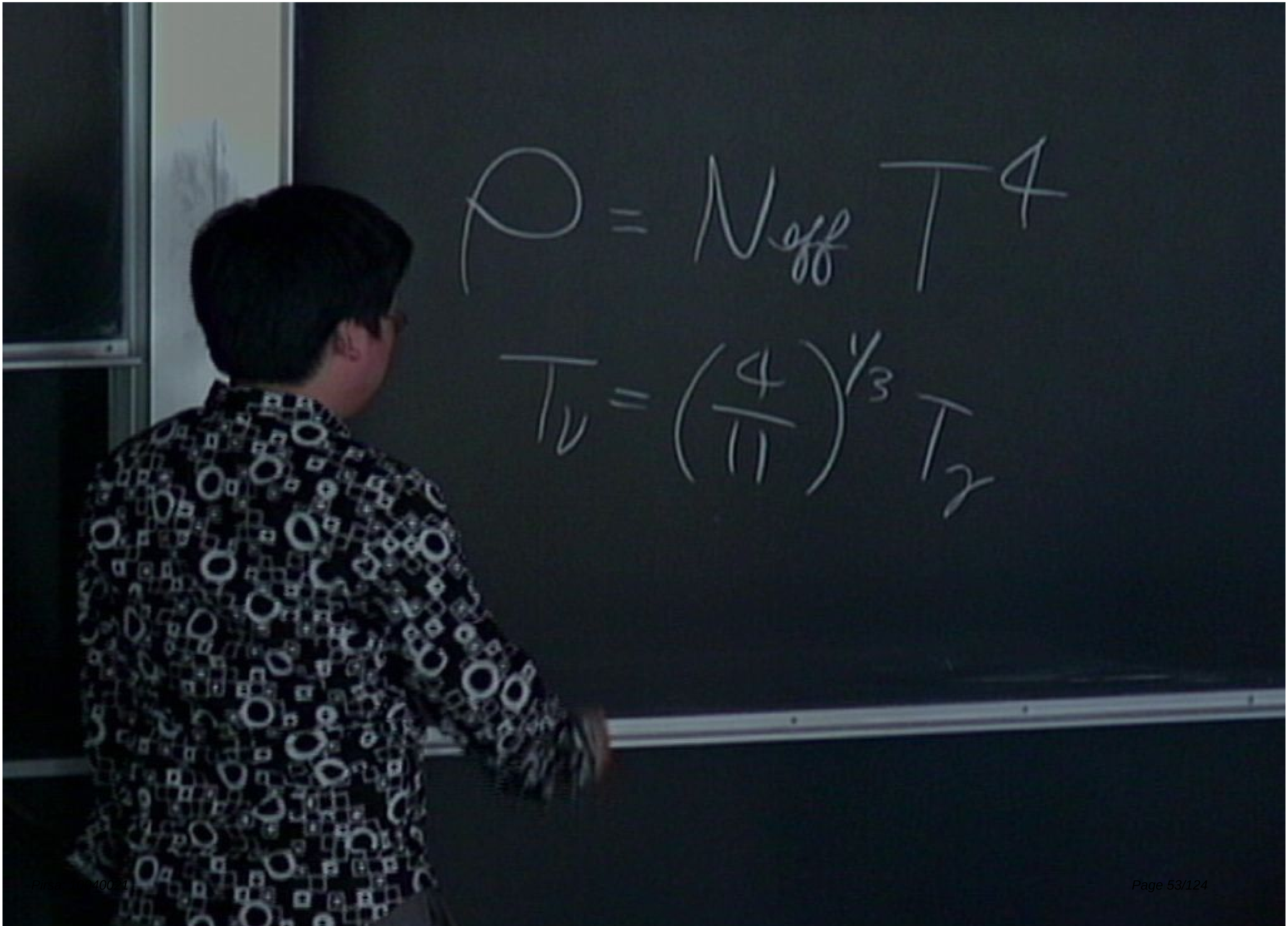
$\rho = N_{eff} T^4$
$T_\nu = \left(\frac{4}{11}\right)^{1/3} T_\gamma$

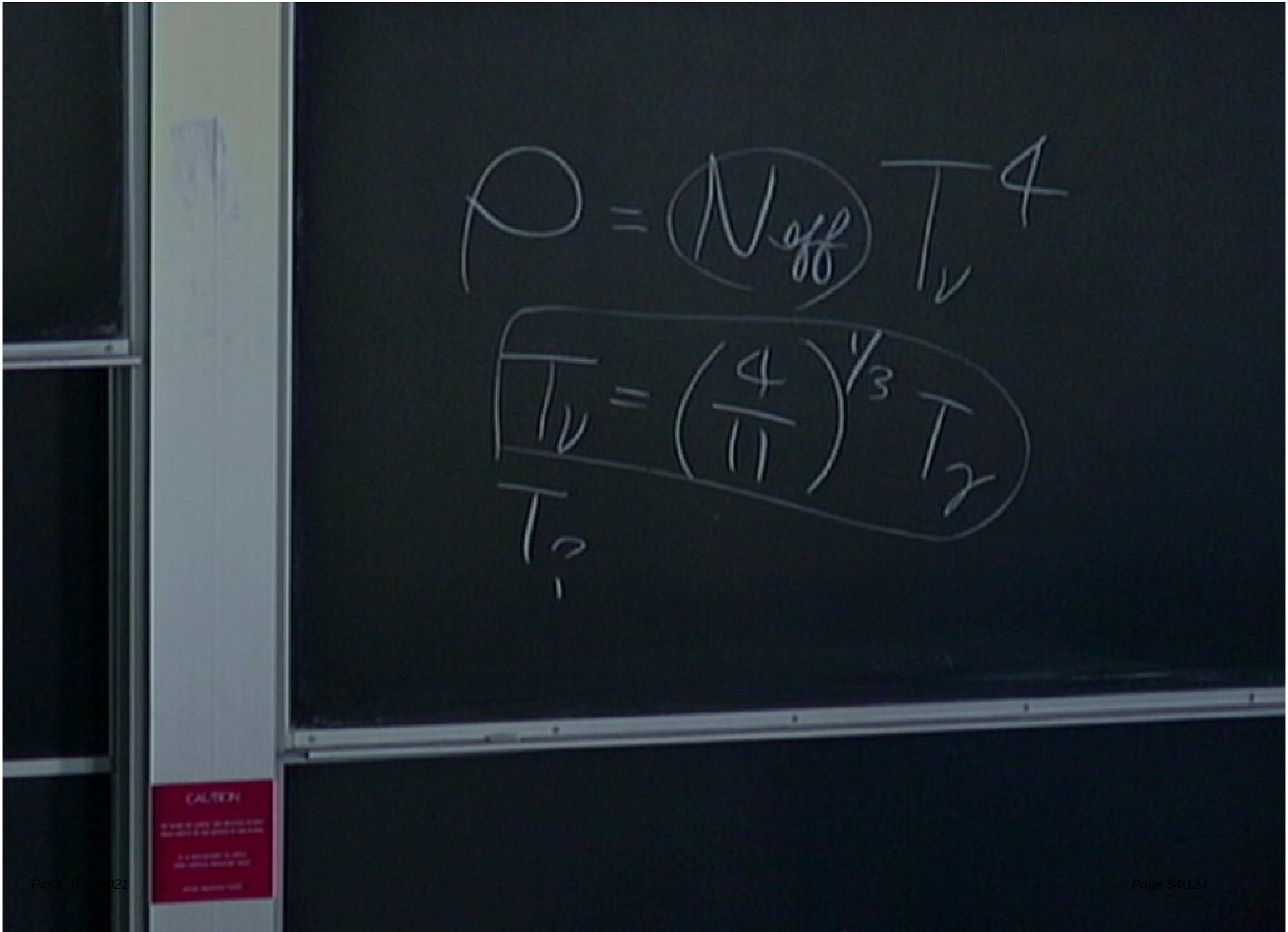
ρ = Neff Tν4
Tν = (4/11)1/3 Tγ
T?
CAUTION

7-year TE Correlation

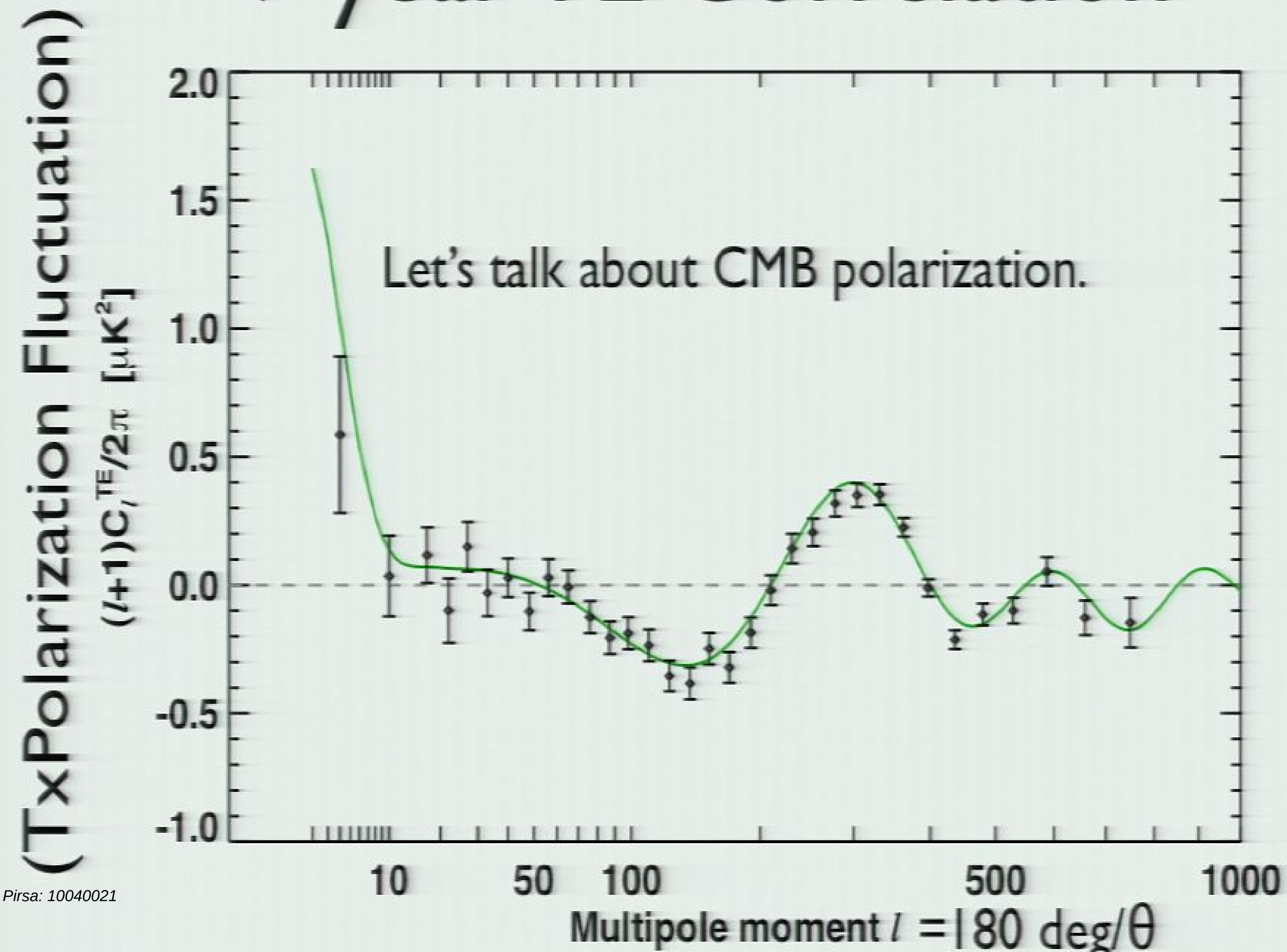

Improvements from 5-year

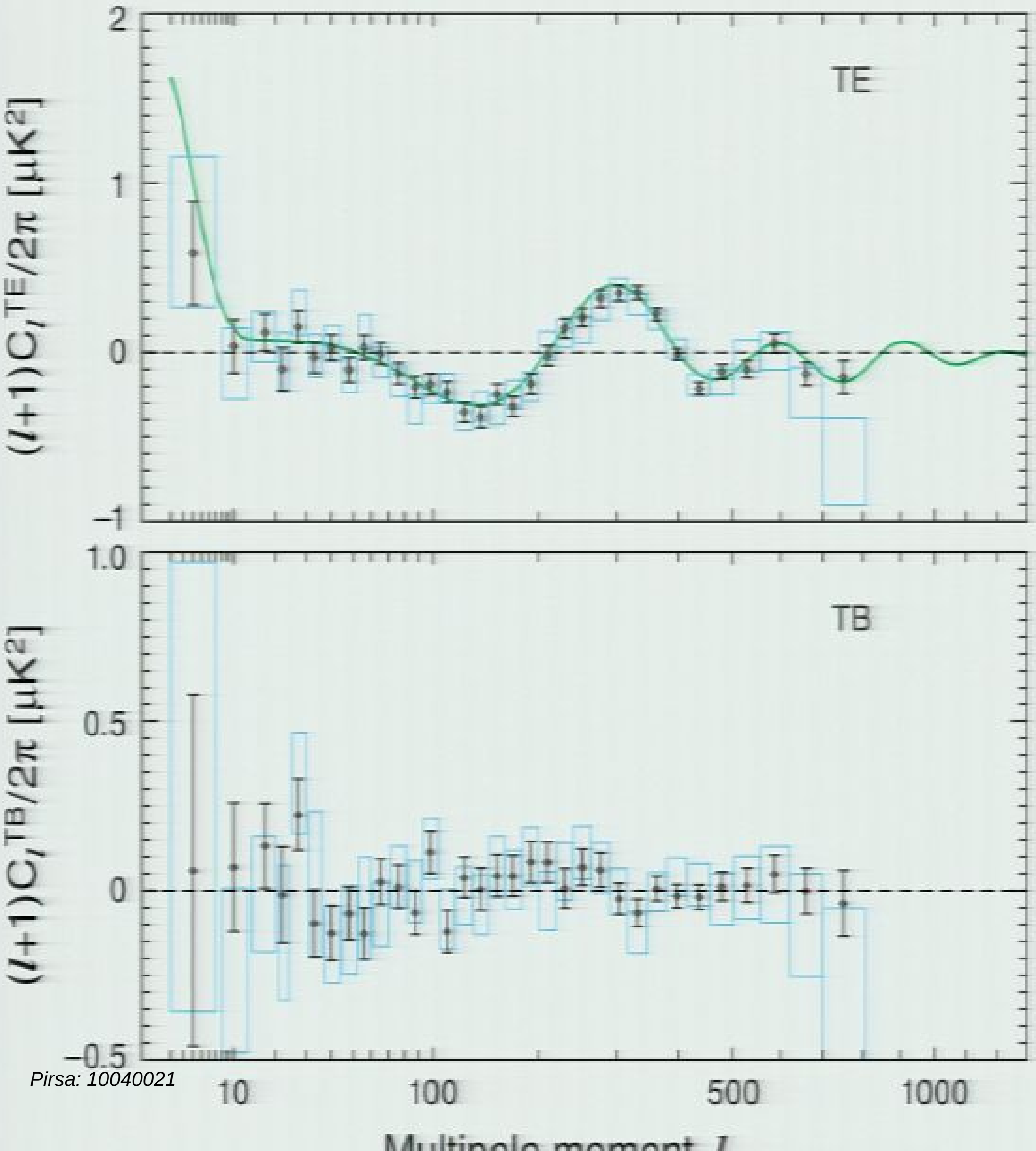

- For 5-year, we used Q and V bands to measure the high-l TE and TB. For 7-year, we also include the W-band data.
- **TE: 21σ detection!** (It was 13σ in 5 year.)
- TB is expected to vanish in a parity-conserving universe, and it is consistent with zero.

17

What Are We Seeing Here?

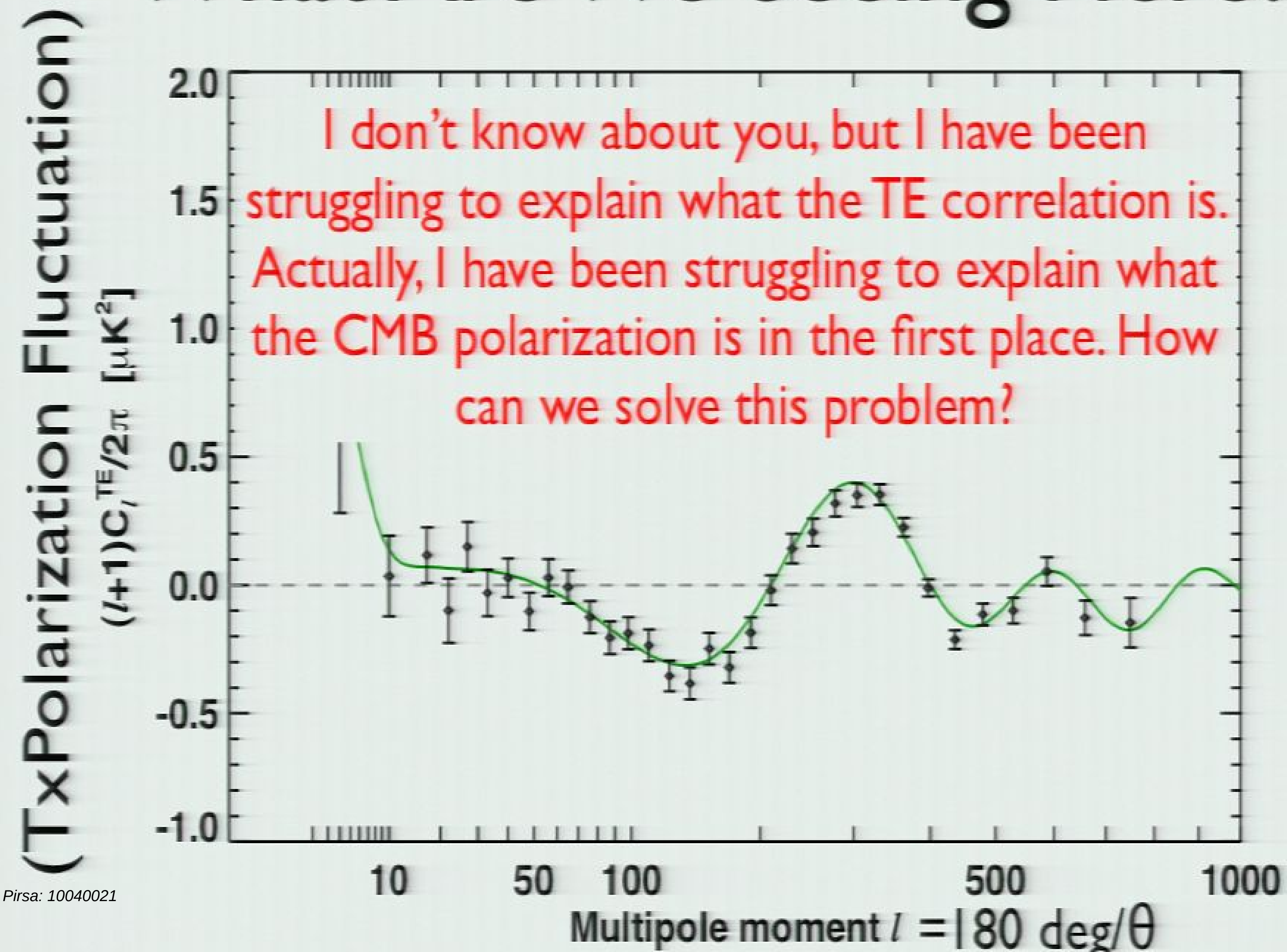

CMB Polarization On the Sky

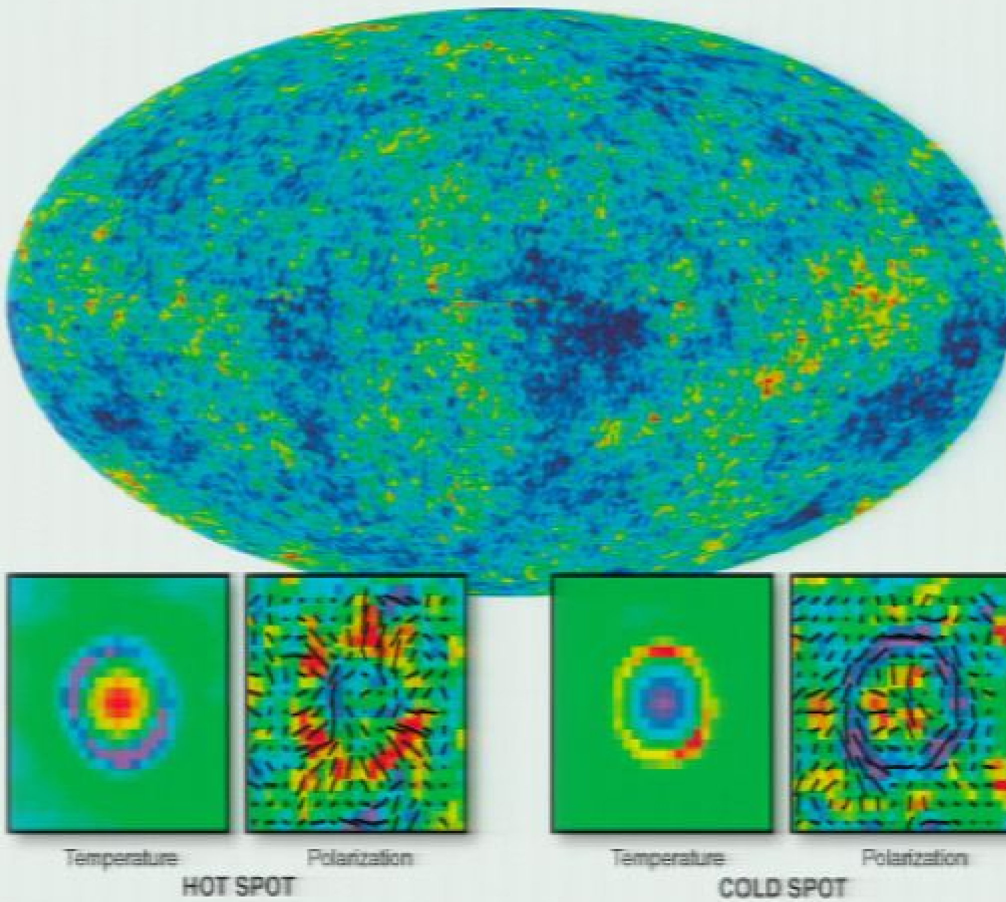

- *Solution*: Leave Fourier space.
  Go back to real space.

CMB Polarization is a Real-space Stuff

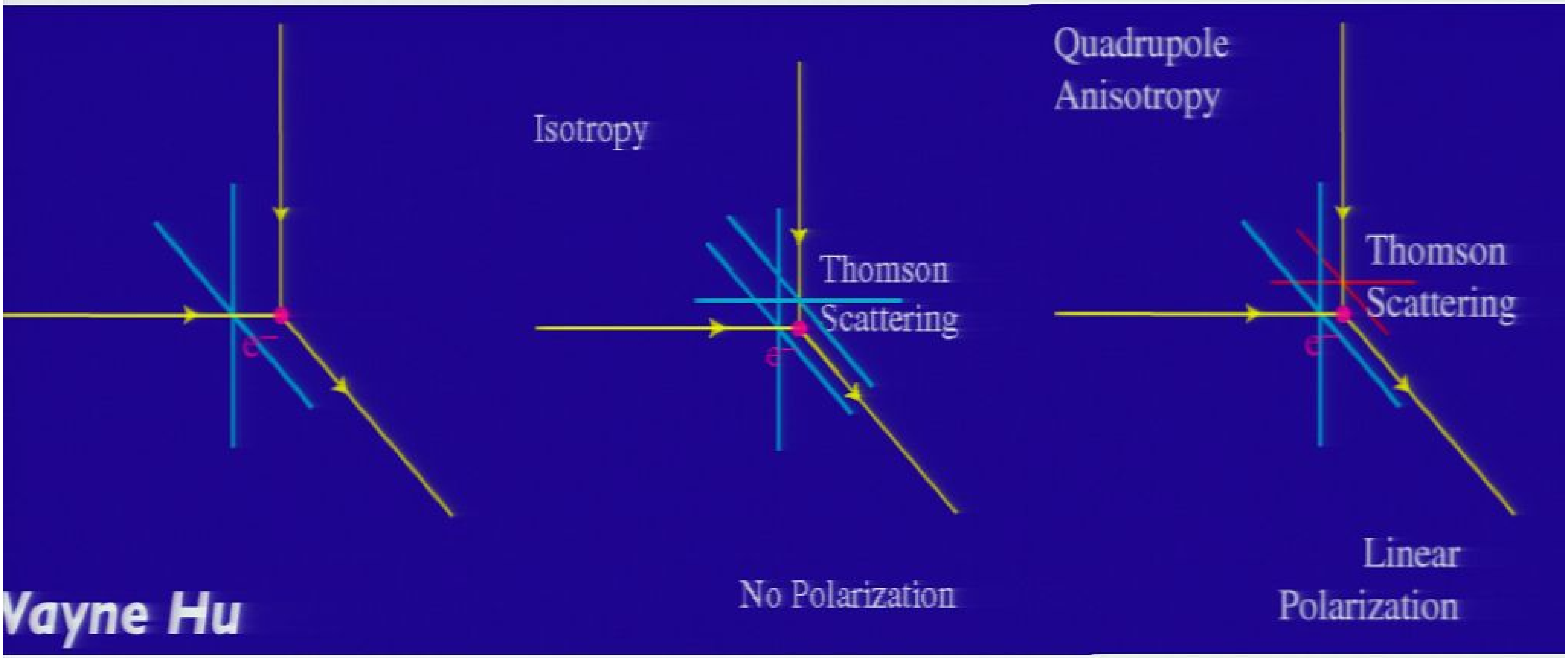

- CMB Polarization is created by a local temperature **quadrupole** anisotropy.

CMB Polarization on Large Angular Scales (>2 deg)

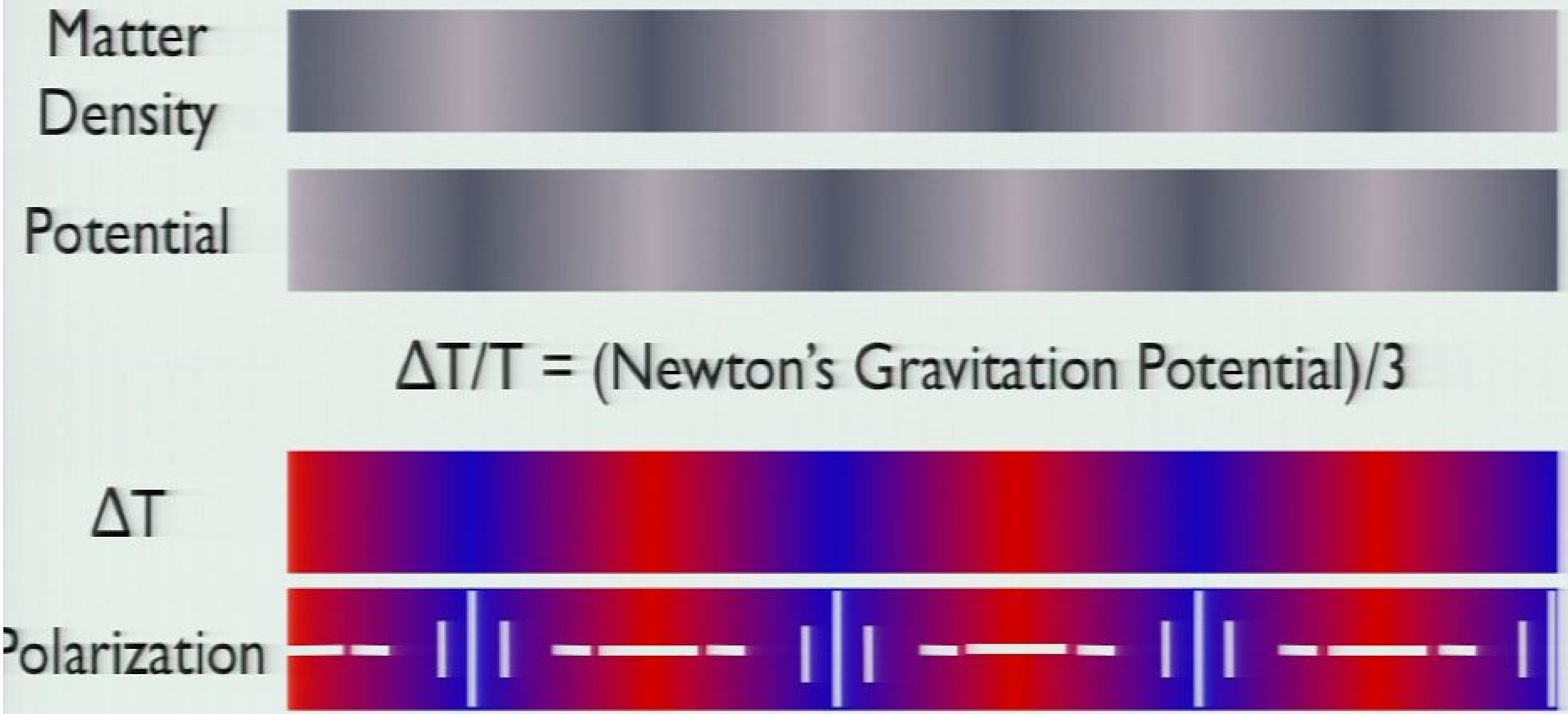

- How does the photon-baryon plasma move?

CMB Polarization on Large Angular Scales (>2 deg)

$\Delta T/T$ = (Newton's Gravitation Potential)/3

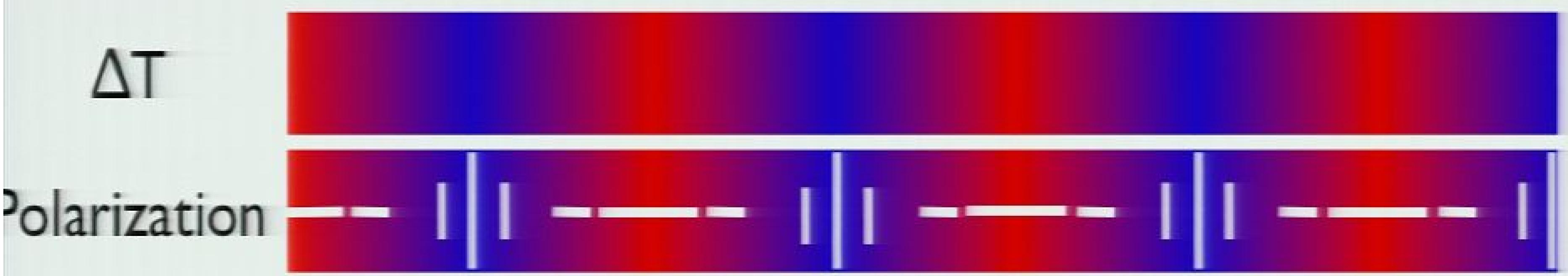

- How does the photon-baryon plasma move?

23

CMB Polarization Tells Us How Plasma Moves at z=1090

Zaldarriaga & Harari (1995)

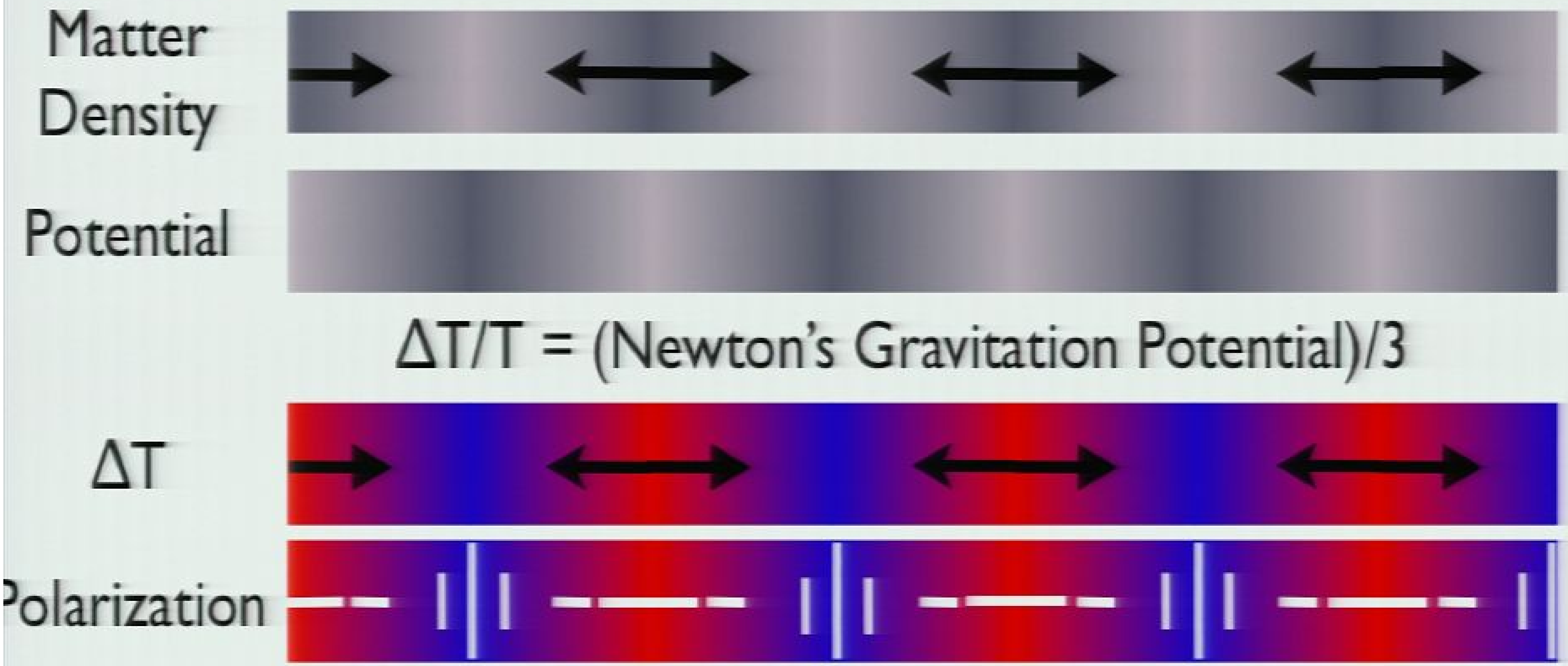

- Plasma **falling into** the gravitational potential well = **Radial** polarization pattern

Quadrupole From Velocity Gradient (Large Scale)

ΔT — Sachs-Wolfe: $\Delta T/T=\Phi/3$

Potential Φ — Stuff flowing *in*

Acceleration $a=-\partial\Phi$

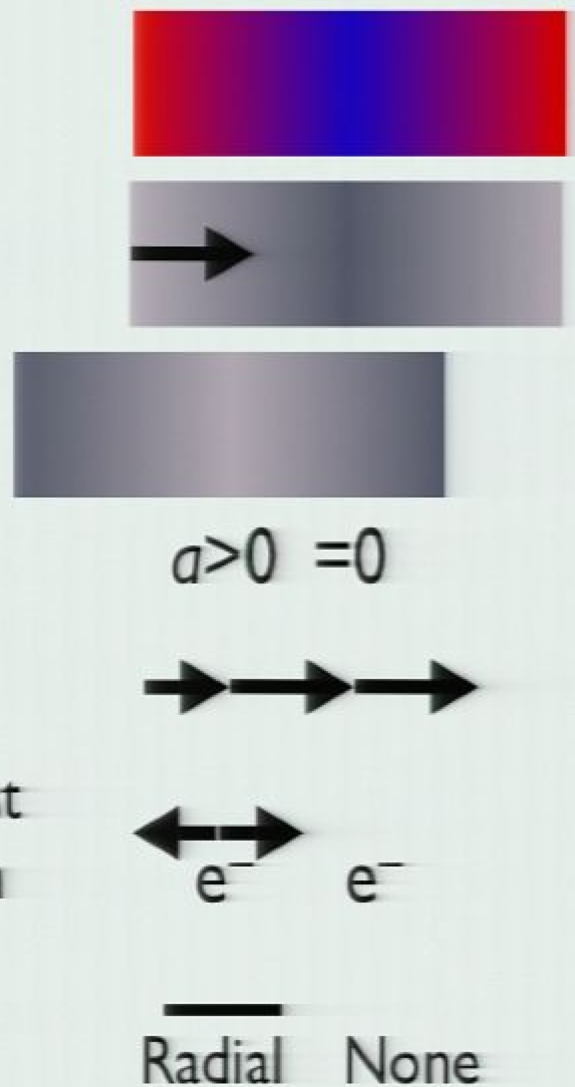

Velocity — Velocity gradient

Velocity in the rest frame of electron — The left electron sees colder photons along the plane wave

Polarization

Quadrupole From Velocity Gradient (Small Scale)

ΔT — Compression increases temperature

Potential Φ — Stuff flowing *in*

Acceleration $a = -\partial\Phi - \partial P$ — Pressure gradient slows down the flow

Velocity — Velocity gradient

Velocity in the rest frame of electron

Polarization

Hence, TE Correlation (Coulson et al. 1994)

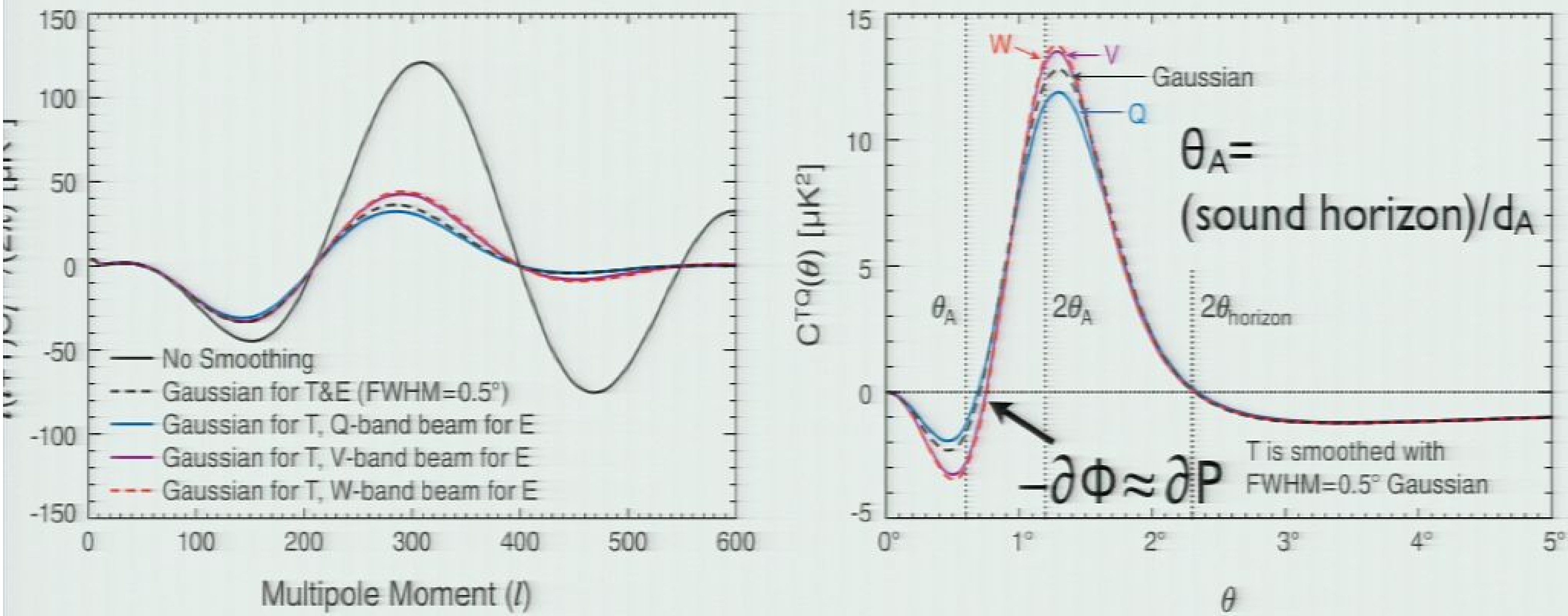

- $C^{TQr}(\theta) = -\int d\ln l\ [l^2 C_l^{TE}/(2\pi)]\ J_2(l\theta)$

Quadrupole From Velocity Gradient (Small Scale)

ΔT — Compression increases temperature

Potential Φ — Stuff flowing *in*

Acceleration $a = -\partial\Phi - \partial P$ — Pressure gradient slows down the flow

Velocity — Velocity gradient

Velocity in the rest frame of electron

Polarization

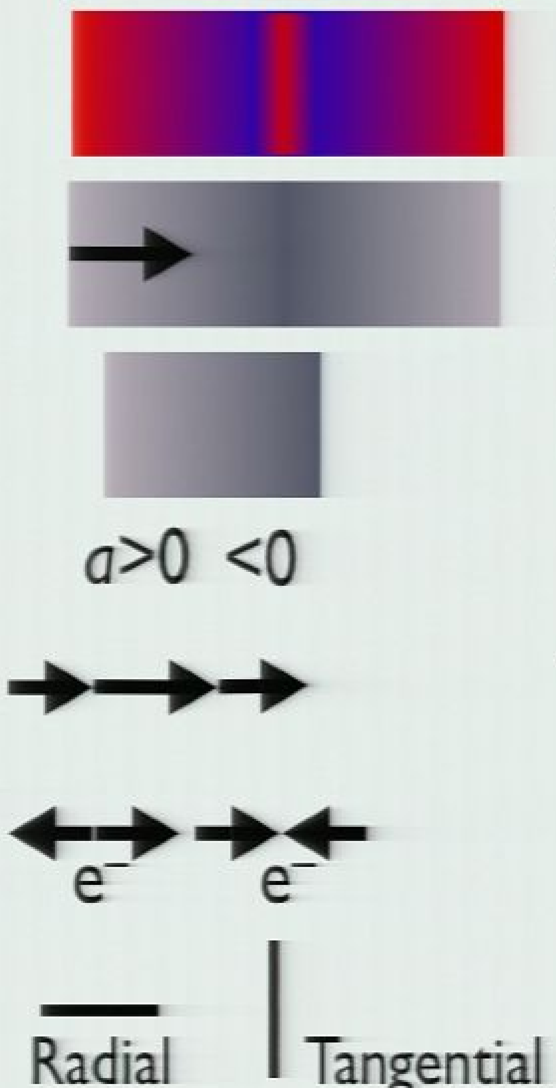

Hence, TE Correlation (Coulson et al. 1994)

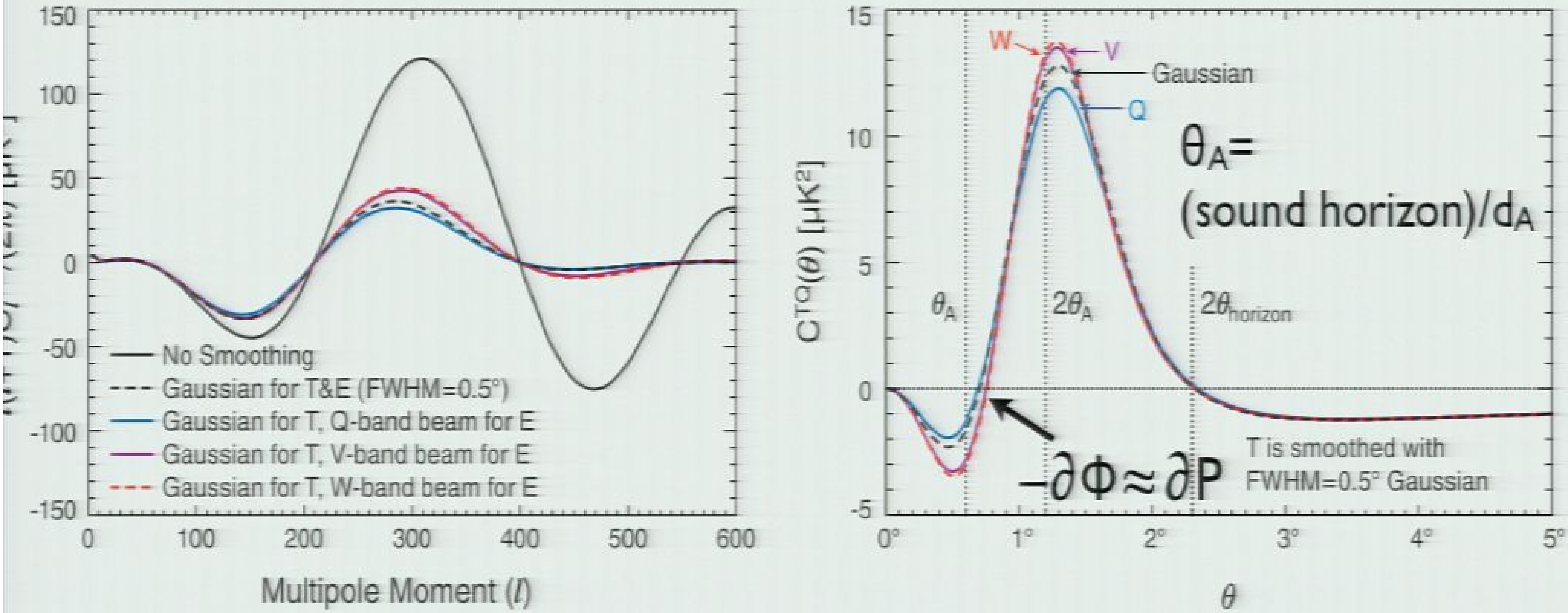

- $C^{TQr}(\theta) = -\int d\ln l\, [l^2 C_l^{TE}/(2\pi)]\, J_2(l\theta)$

Peak Theory and Stacking Analysis

- Stack polarization images around temperature hot and cold spots.

- Outside of the Galaxy mask (not shown), there are **12387 hot spots** and **12628 cold spots**.

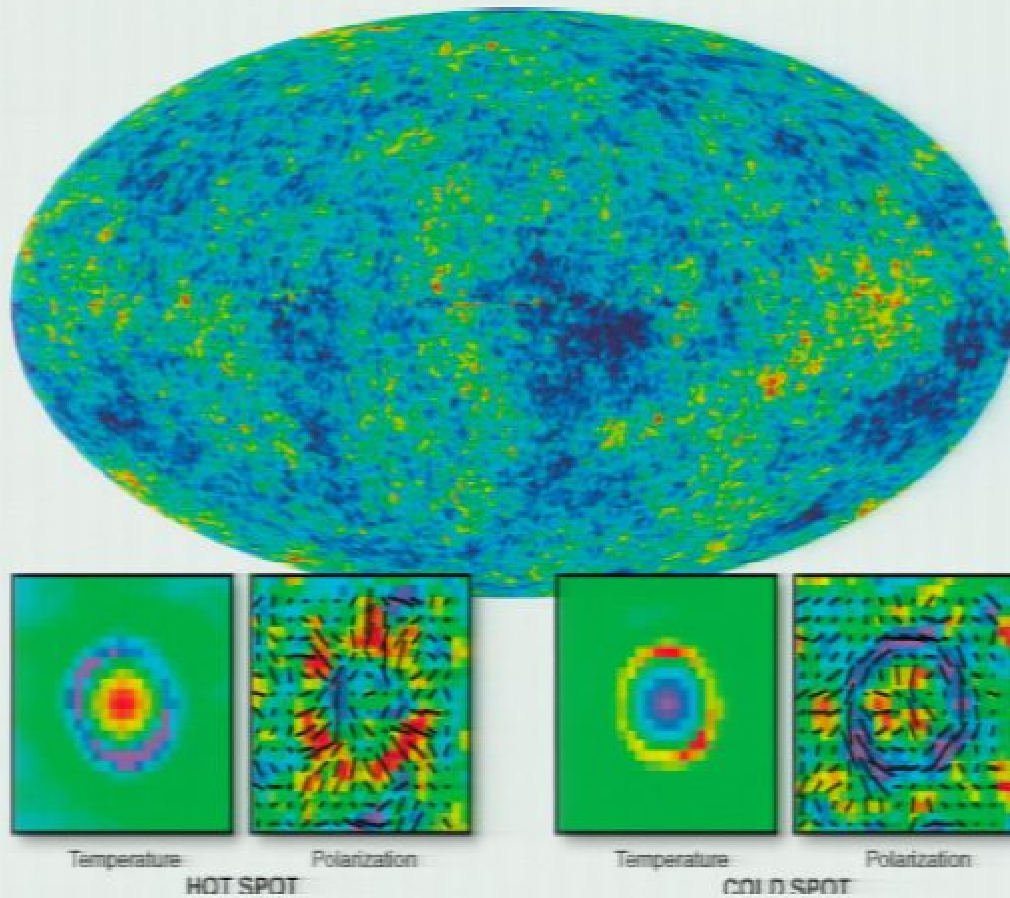

- Peak theory gives:

$$\langle Q_r \rangle(\theta) = -\int \frac{l dl}{2\pi} W_l^T W_l^P (\bar{b}_\nu + \bar{b}_\zeta l^2) C_l^{\rm TE} J_2(l\theta),$$

[Note the l^2 term! (Desjacques 2008)]

$$\langle U_r \rangle(\theta) = -\int \frac{l dl}{2\pi} W_l^T W_l^P (\bar{b}_\nu + \bar{b}_\zeta l^2) C_l^{\rm TB} J_2(l\theta),$$

Analogy to Weak Lensing

- If you are familiar with weak lensing, this statistic is equivalent to the *tangential shear:* $\langle \bar{\gamma}_t^h \rangle (R, z_L) = \frac{\Delta\Sigma(R, z_L)}{\Sigma_c(z_L)}$

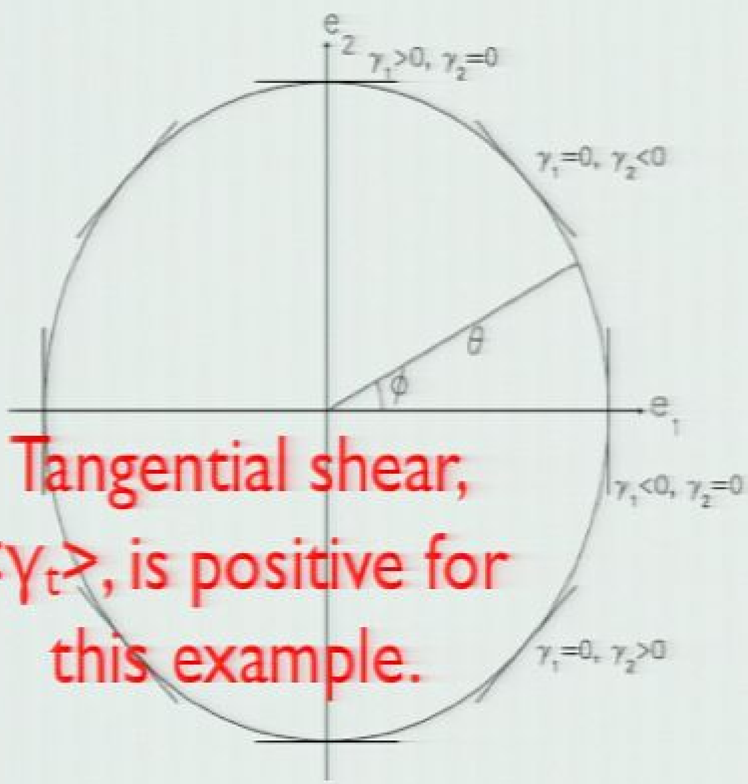

Tangential shear, $\langle\gamma_t\rangle$, is positive for this example.

$$\Delta\Sigma(R, z_L) = \rho_0 b_1 \int \frac{kdk}{2\pi} P_m(k, z_L) J_2(kR)$$

However, all the formulae given in the literature use a scale-independent bias, b_1. This formula must be modified to include the k^2 term.

$$\gamma_t(\boldsymbol{\theta}) = -\gamma_1(\boldsymbol{\theta})\cos(2\phi) - \gamma_2(\boldsymbol{\theta})\sin(2\phi)$$

emperature hot spots are stacked

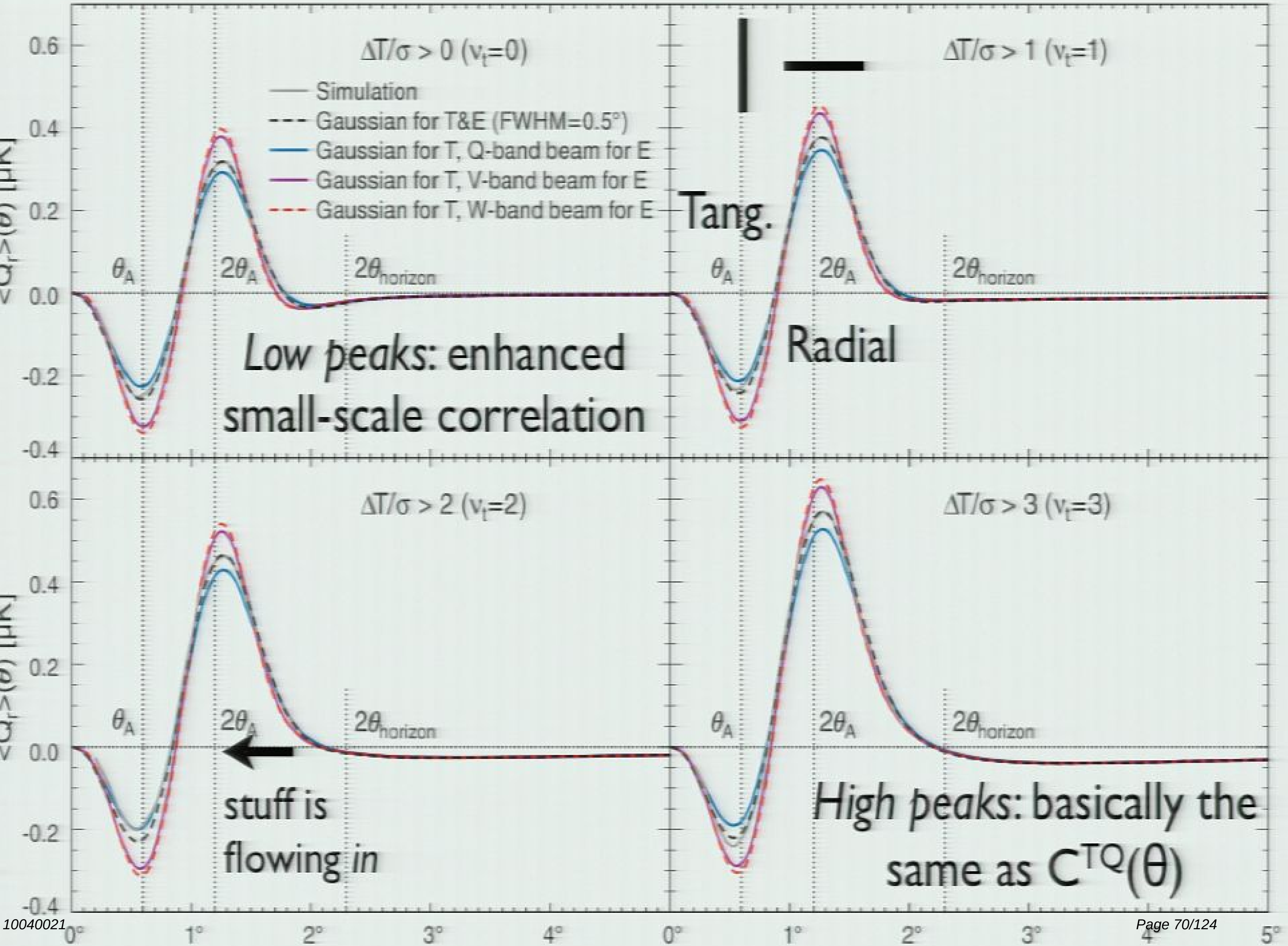

Analogy to Weak Lensing

- If you are familiar with weak lensing, this statistic is equivalent to the *tangential shear:* $\langle\overline{\gamma}_t^h\rangle(R, z_L) = \dfrac{\Delta\Sigma(R, z_L)}{\Sigma_c(z_L)}$

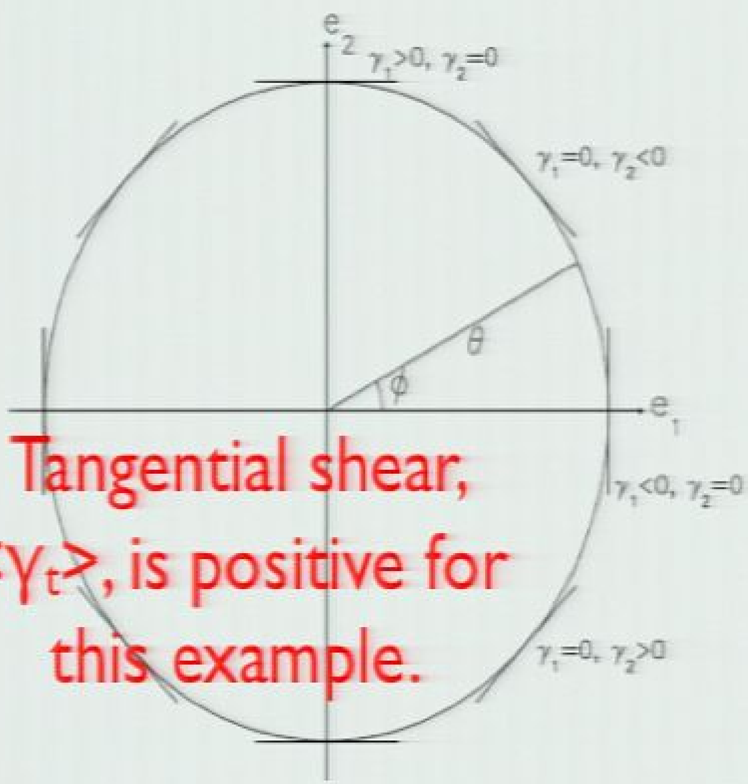

Tangential shear, $\langle\gamma_t\rangle$, is positive for this example.

$$\Delta\Sigma(R, z_L) = \rho_0 b_1 \int \frac{kdk}{2\pi} P_m(k, z_L) J_2(kR)$$

However, all the formulae given in the literature use a scale-independent bias, b_1. This formula must be modified to include the k^2 term.

$$\gamma_t(\boldsymbol{\theta}) = -\gamma_1(\boldsymbol{\theta})\cos(2\phi) - \gamma_2(\boldsymbol{\theta})\sin(2\phi)$$

Peak Theory and Stacking Analysis

- Stack polarization images around temperature hot and cold spots.

- Outside of the Galaxy mask (not shown), there are **12387 hot spots** and **12628 cold spots**.

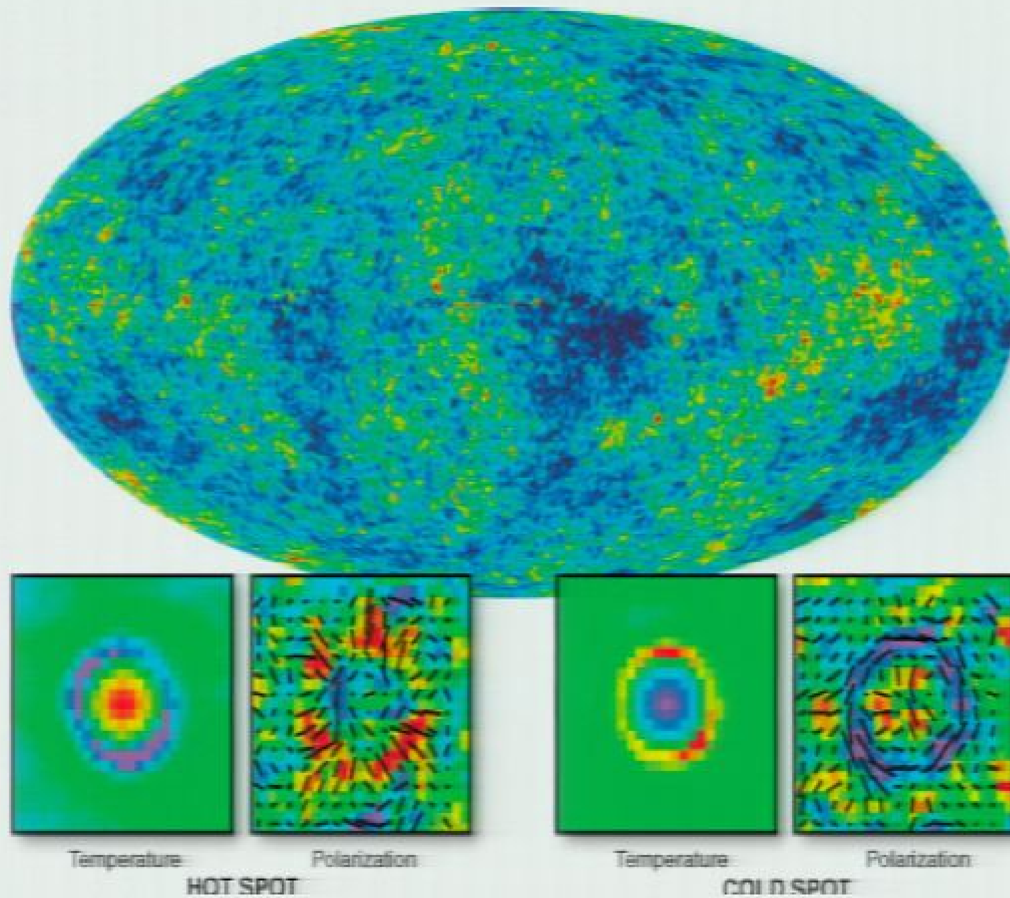

- Peak theory gives:

  [Note the l^2 term! (Desjacques 2008)]

$$\langle Q_r\rangle(\theta) = -\int \frac{l\,dl}{2\pi} W_l^T W_l^P (\bar{b}_\nu + \bar{b}_\zeta l^2) C_l^{\mathrm{TE}} J_2(l\theta),$$

$$\langle U_r\rangle(\theta) = -\int \frac{l\,dl}{2\pi} W_l^T W_l^P (\bar{b}_\nu + \bar{b}_\zeta l^2) C_l^{\mathrm{TB}} J_2(l\theta),$$

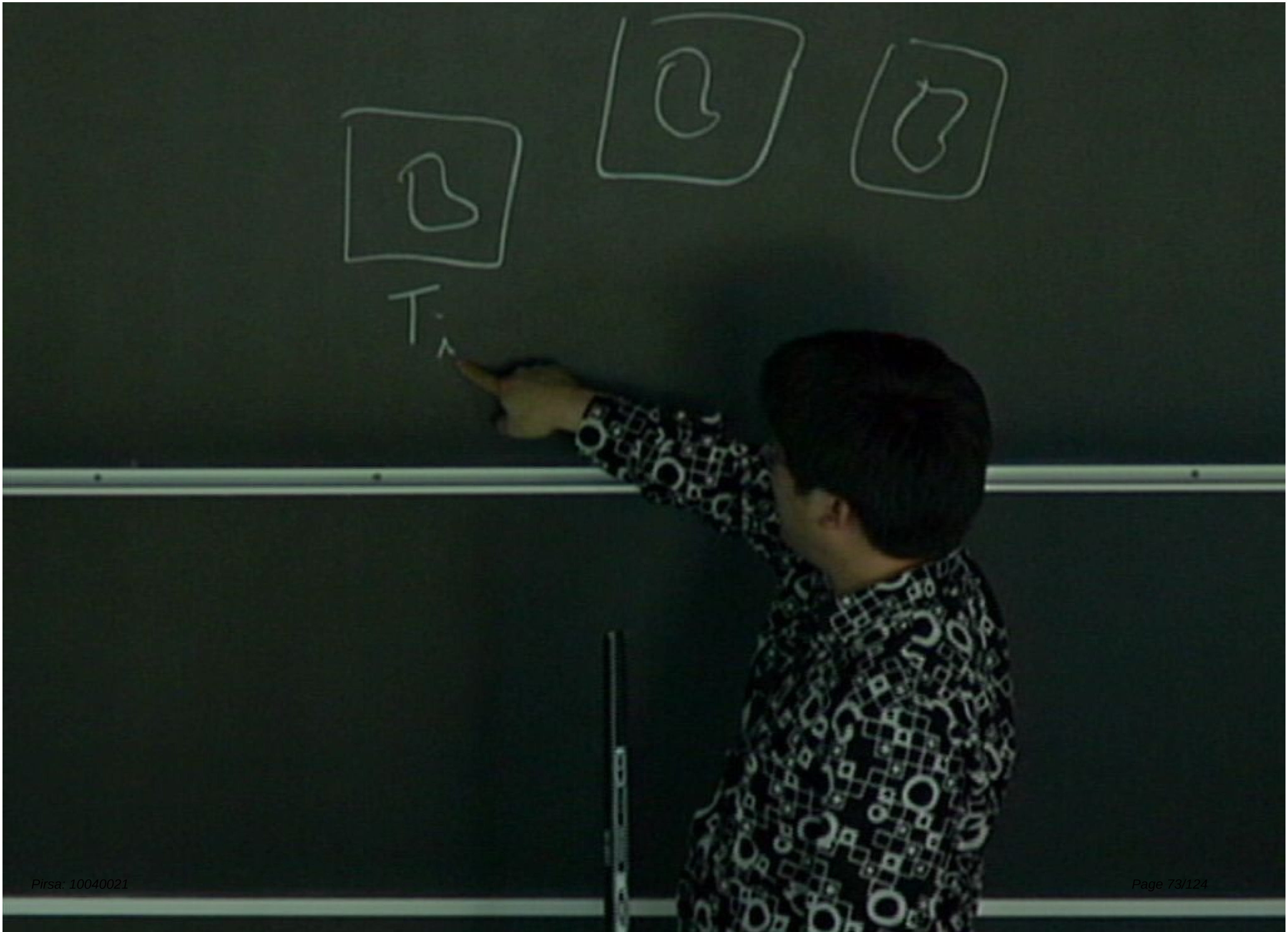

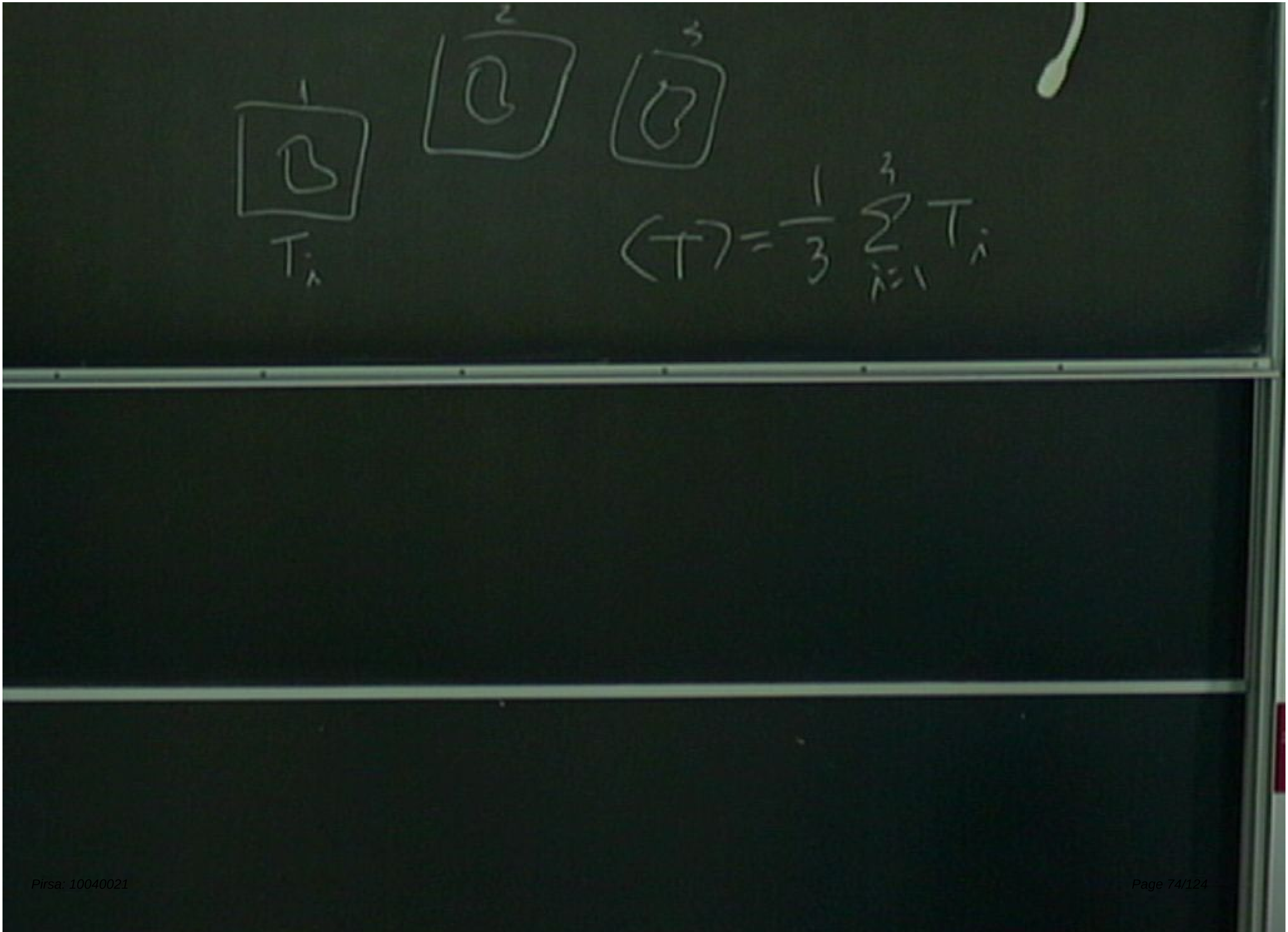

1
2
3
T_i
<T> = 1/3 Σ_{i=1}^{3} T_i

Peak Theory and Stacking Analysis

- Stack polarization images around temperature hot and cold spots.

- Outside of the Galaxy mask (not shown), there are **12387 hot spots** and **12628 cold spots**.

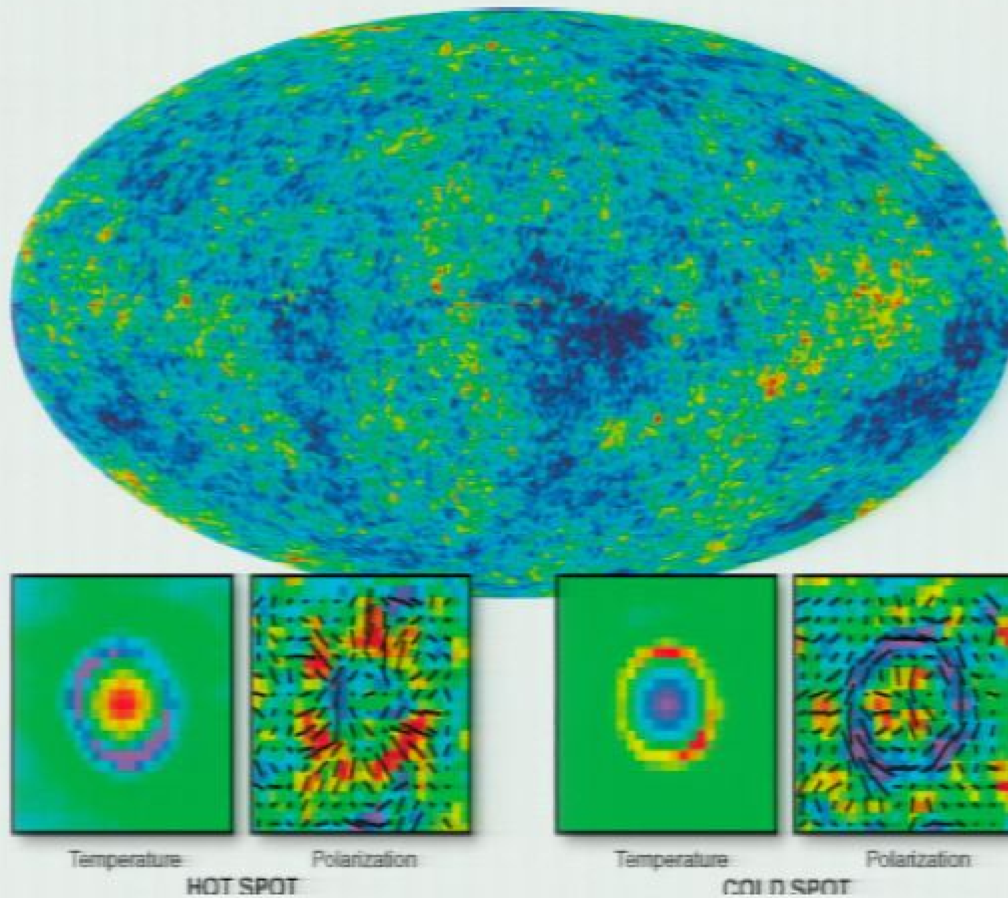

- Peak theory gives:

$$\langle Q_r\rangle(\theta) = -\int \frac{l\,dl}{2\pi} W_l^T W_l^P (\bar{b}_\nu + \bar{b}_\zeta l^2) C_l^{\rm TE} J_2(l\theta),$$

$$\langle U_r\rangle(\theta) = -\int \frac{l\,dl}{2\pi} W_l^T W_l^P (\bar{b}_\nu + \bar{b}_\zeta l^2) C_l^{\rm TE} J_2(l\theta),$$

[Note the l^2 term! (Desjacques 2008)]

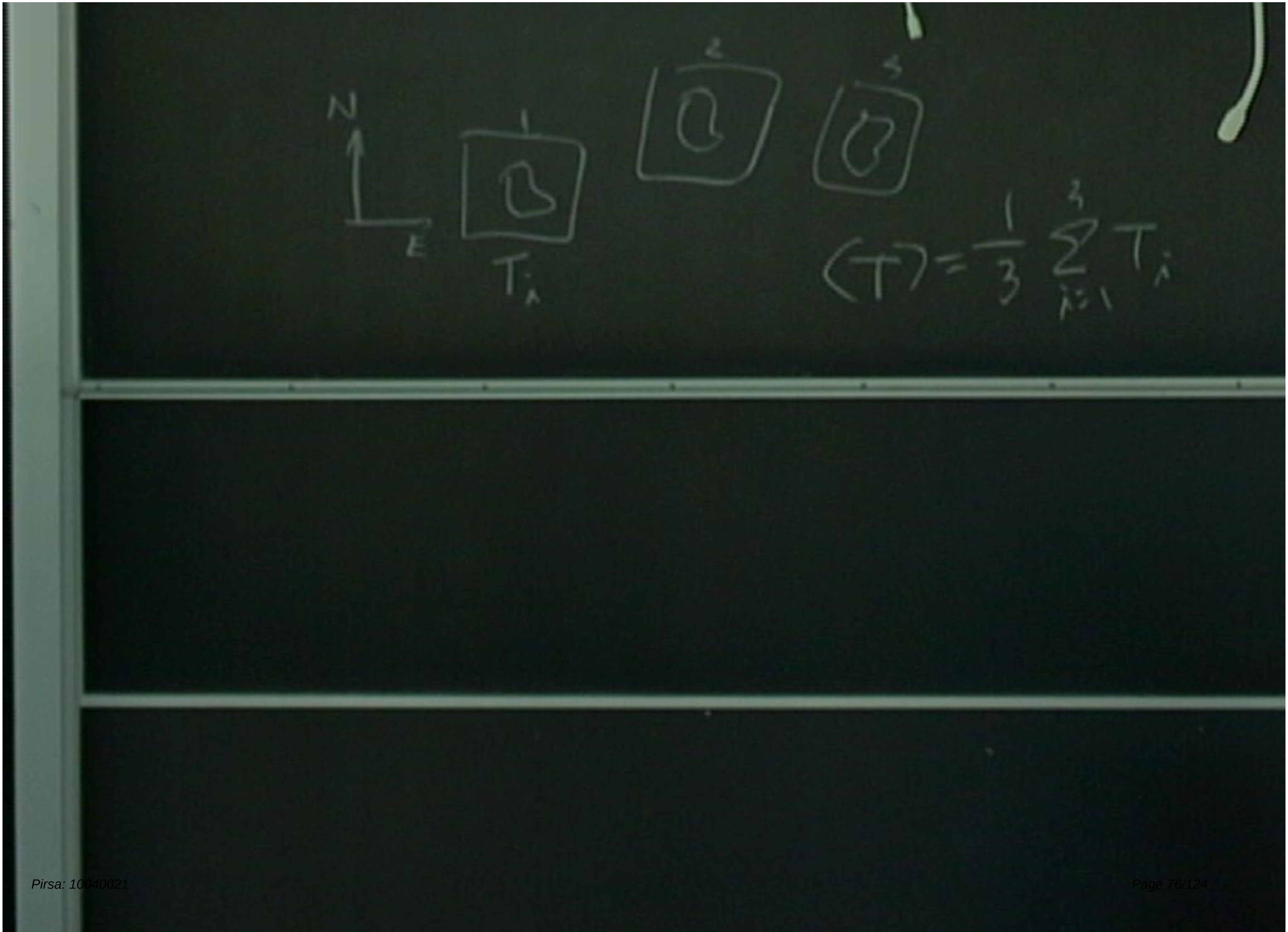
N
E
1
2
3
T_i
$\langle T \rangle = \frac{1}{3} \sum_{i=1}^{3} T_i$

Peak Theory and Stacking Analysis

- Stack polarization images around temperature hot and cold spots.

- Outside of the Galaxy mask (not shown), there are **12387 hot spots** and **12628 cold spots**.

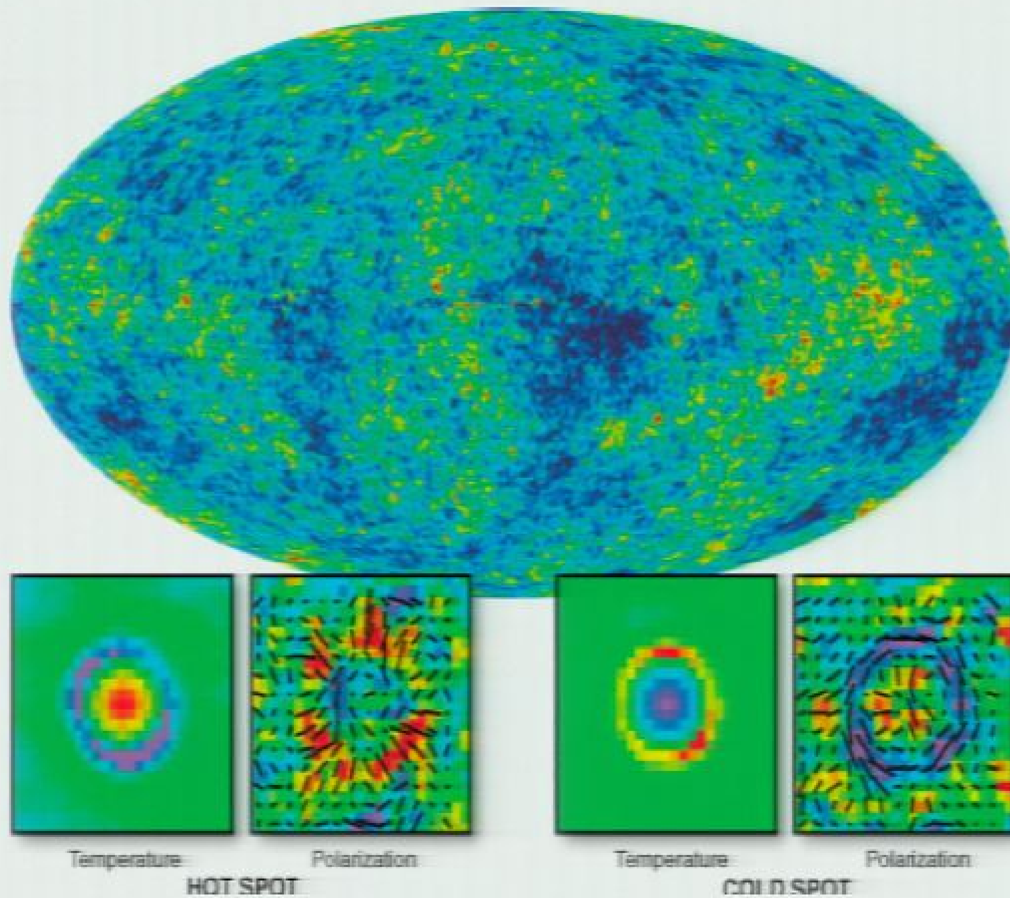

- Peak theory gives:

$$\langle Q_r \rangle(\theta) = -\int \frac{l dl}{2\pi} W_l^T W_l^P (\bar{b}_\nu + \bar{b}_\zeta l^2) C_l^{\mathrm{TE}} J_2(l\theta),$$

$$\langle U_r \rangle(\theta) = -\int \frac{l dl}{2\pi} W_l^T W_l^P (\bar{b}_\nu + \bar{b}_\zeta l^2) C_l^{\mathrm{TB}} J_2(l\theta),$$

[Note the l^2 term! (Desjacques 2008)]

Analogy to Weak Lensing

- If you are familiar with weak lensing, this statistic is equivalent to the *tangential shear:* $\langle \overline{\gamma}_t^h \rangle (R, z_L) = \frac{\Delta\Sigma(R, z_L)}{\Sigma_c(z_L)}$

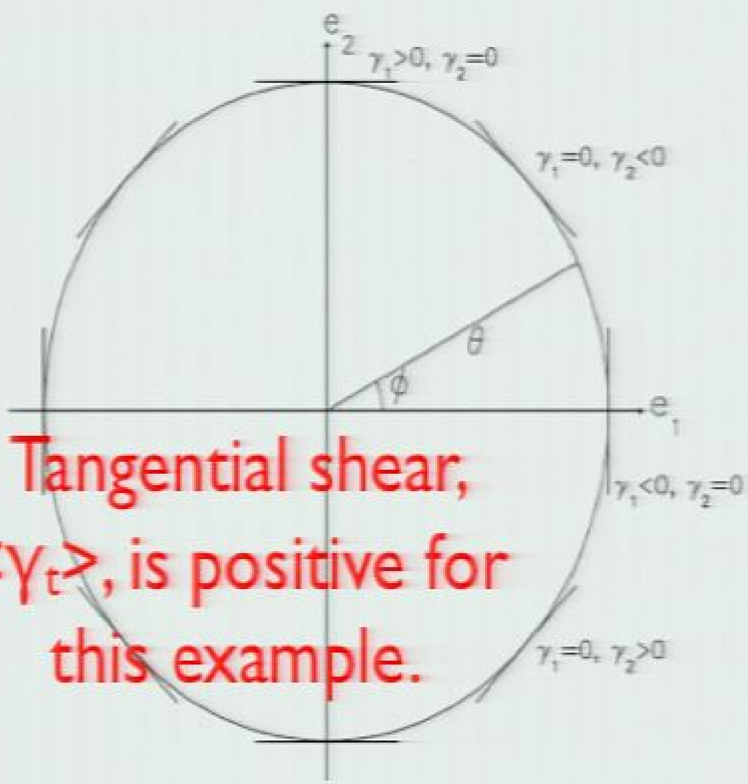

Tangential shear, $\langle\gamma_t\rangle$, is positive for this example.

$$\Delta\Sigma(R, z_L) = \rho_0 b_1 \int \frac{k dk}{2\pi} P_m(k, z_L) J_2(kR)$$

However, all the formulae given in the literature use a scale-independent bias, b_1. This formula must be modified to include the k^2 term.

$$\gamma_t(\boldsymbol{\theta}) = -\gamma_1(\boldsymbol{\theta}) \cos(2\phi) - \gamma_2(\boldsymbol{\theta}) \sin(2\phi)$$

Hence, TE Correlation (Coulson et al. 1994)

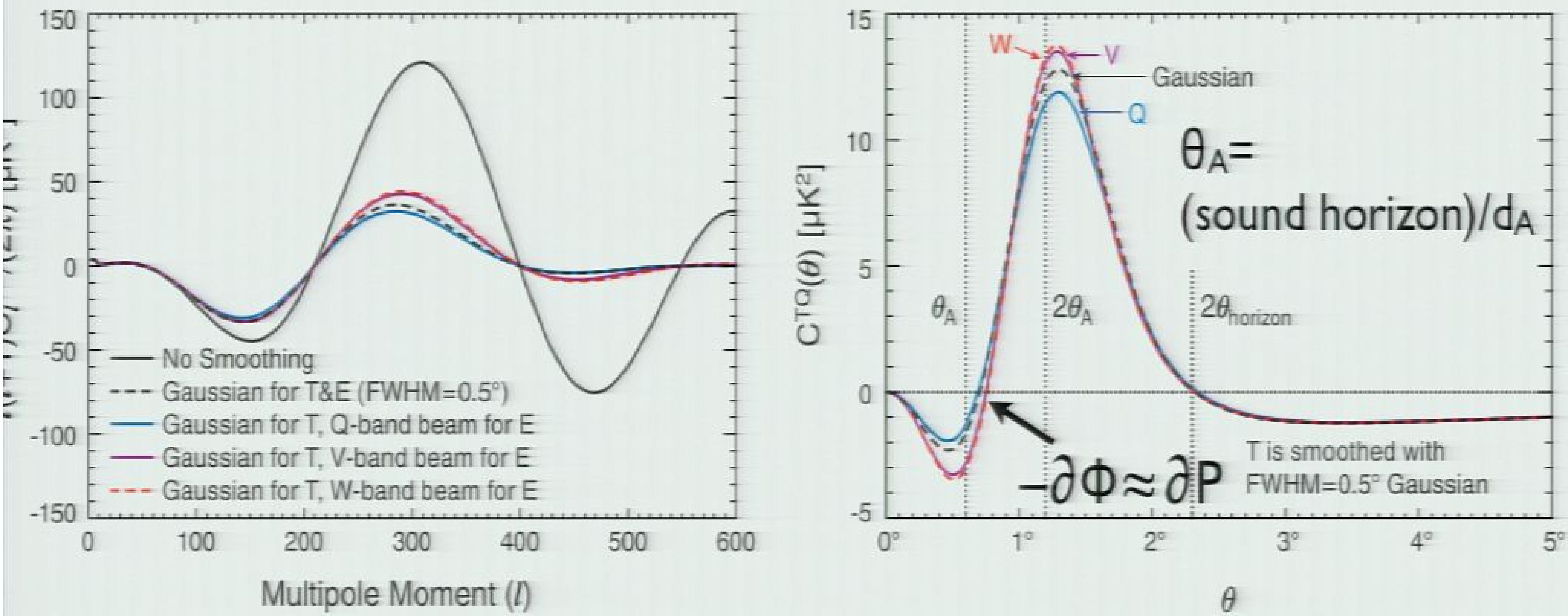

- $C^{TQr}(\theta) = -\int d\ln l\ [l^2 C_l^{TE}/(2\pi)]\ J_2(l\theta)$

Peak Theory and Stacking Analysis

- Stack polarization images around temperature hot and cold spots.

- Outside of the Galaxy mask (not shown), there are **12387 hot spots** and **12628 cold spots**.

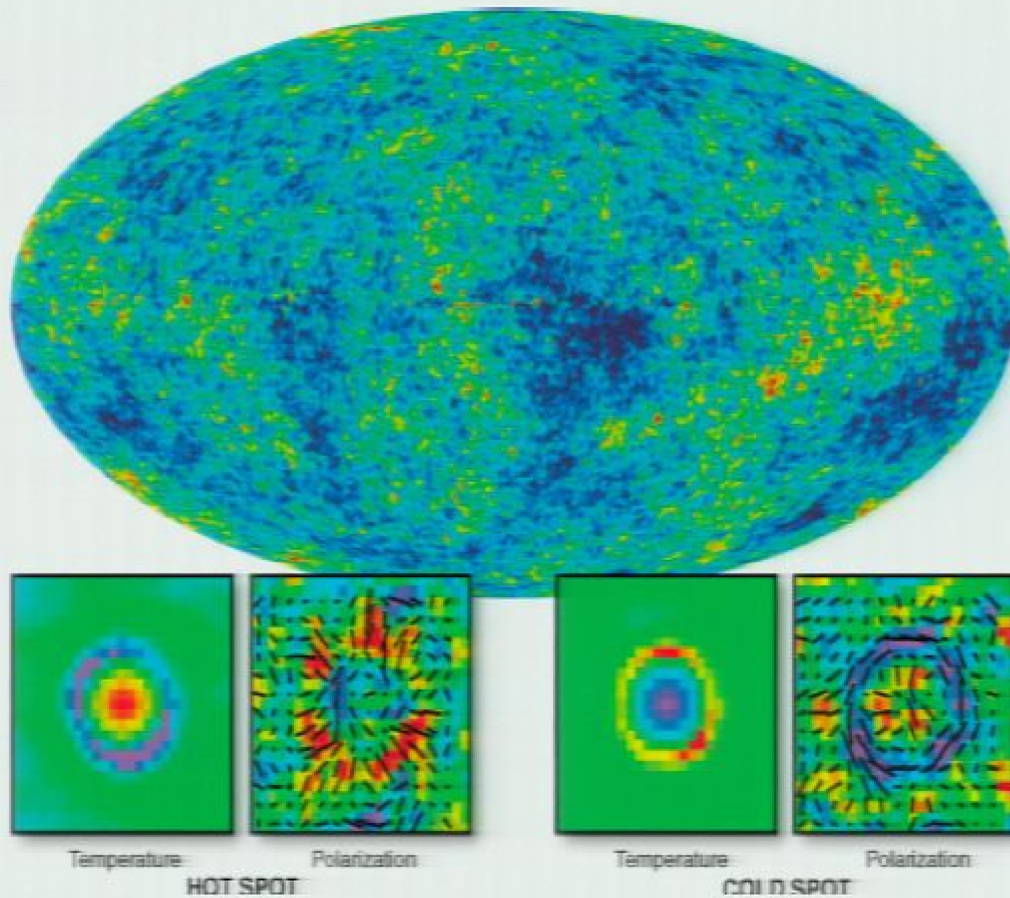

- Peak theory gives:

$$\langle Q_r\rangle(\theta) = -\int \frac{ldl}{2\pi} W_l^T W_l^P (\bar{b}_\nu + \bar{b}_\zeta l^2) C_l^{\mathrm{TE}} J_2(l\theta),$$

$$\langle U_r\rangle(\theta) = -\int \frac{ldl}{2\pi} W_l^T W_l^P (\bar{b}_\nu + \bar{b}_\zeta l^2) C_l^{\mathrm{TB}} J_2(l\theta),$$

[Note the l^2 term! (Desjacques 2008)]

28

Analogy to Weak Lensing

- If you are familiar with weak lensing, this statistic is equivalent to the *tangential shear:* $\langle \overline{\gamma}_t^h \rangle (R, z_L) = \frac{\Delta\Sigma(R, z_L)}{\Sigma_c(z_L)}$

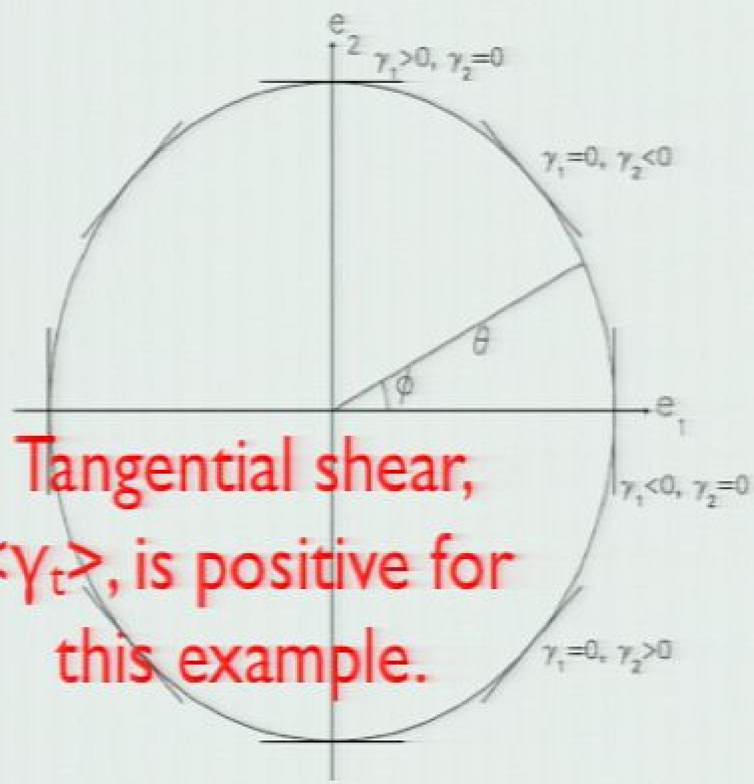

Tangential shear, $\langle\gamma_t\rangle$, is positive for this example.

$$\Delta\Sigma(R, z_L) = \rho_0 b_1 \int \frac{kdk}{2\pi} P_m(k, z_L) J_2(kR)$$

However, all the formulae given in the literature use a scale-independent bias, b_1. This formula must be modified to include the k^2 term.

$$\gamma_t(\boldsymbol{\theta}) = -\gamma_1(\boldsymbol{\theta}) \cos(2\phi) - \gamma_2(\boldsymbol{\theta}) \sin(2\phi)$$

Peak Theory and Stacking Analysis

- Stack polarization images around temperature hot and cold spots.

- Outside of the Galaxy mask (not shown), there are **12387 hot spots** and **12628 cold spots**.

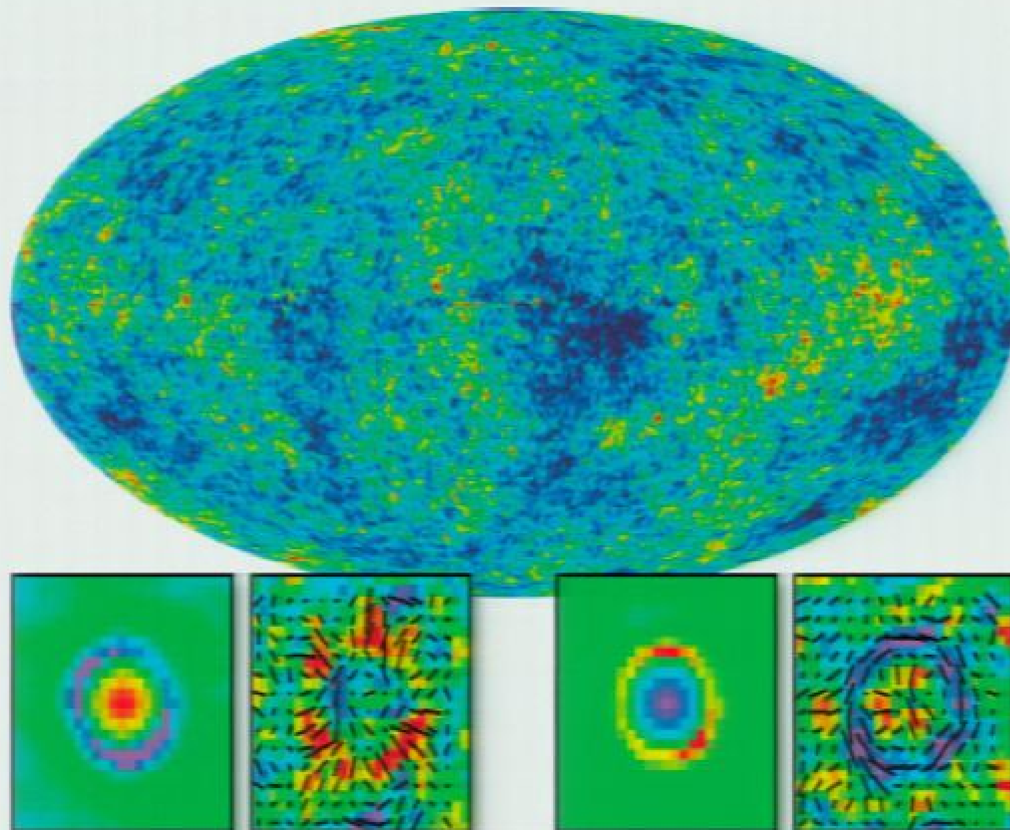

- Peak theory gives:

  [Note the l^2 term! (Desjacques 2008)]

$$\langle Q_r\rangle(\theta) = -\int \frac{ldl}{2\pi} W_l^T W_l^P (\bar{b}_\nu + \bar{b}_\zeta l^2) C_l^{\rm TE} J_2(l\theta),$$

$$\langle U_r\rangle(\theta) = -\int \frac{ldl}{2\pi} W_l^T W_l^P (\bar{b}_\nu + \bar{b}_\zeta l^2) C_l^{\rm TB} J_2(l\theta),$$

Analogy to Weak Lensing

- If you are familiar with weak lensing, this statistic is equivalent to the *tangential shear:* $\langle\bar{\gamma}_t^h\rangle(R, z_L) = \frac{\Delta\Sigma(R, z_L)}{\Sigma_c(z_L)}$

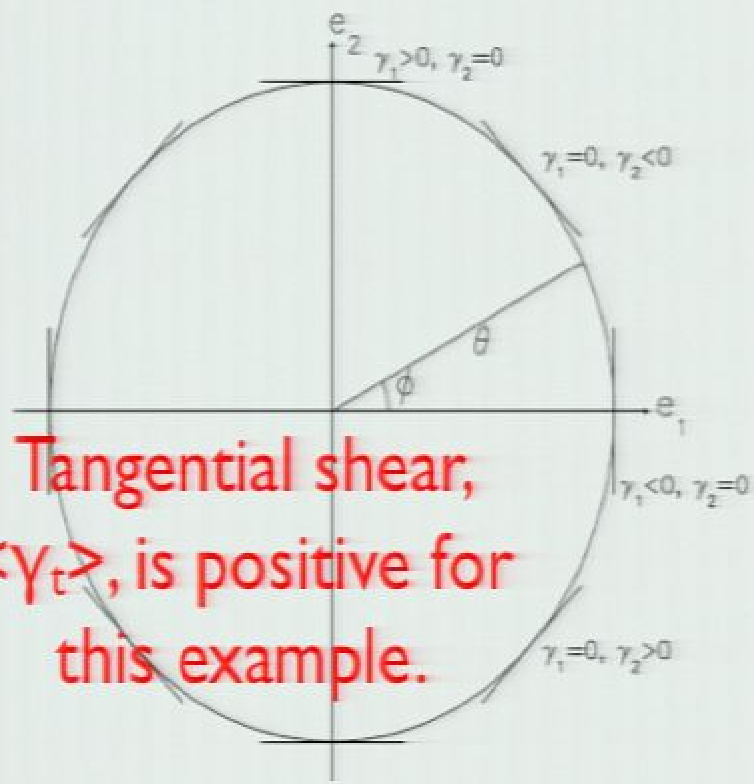

Tangential shear, $\langle\gamma_t\rangle$, is positive for this example.

$$\Delta\Sigma(R, z_L) = \rho_0 b_1 \int \frac{kdk}{2\pi} P_m(k, z_L) J_2(kR)$$

However, all the formulae given in the literature use a scale-independent bias, b_1. This formula must be modified to include the k^2 term.

$$\gamma_t(\boldsymbol{\theta}) = -\gamma_1(\boldsymbol{\theta})\cos(2\phi) - \gamma_2(\boldsymbol{\theta})\sin(2\phi)$$

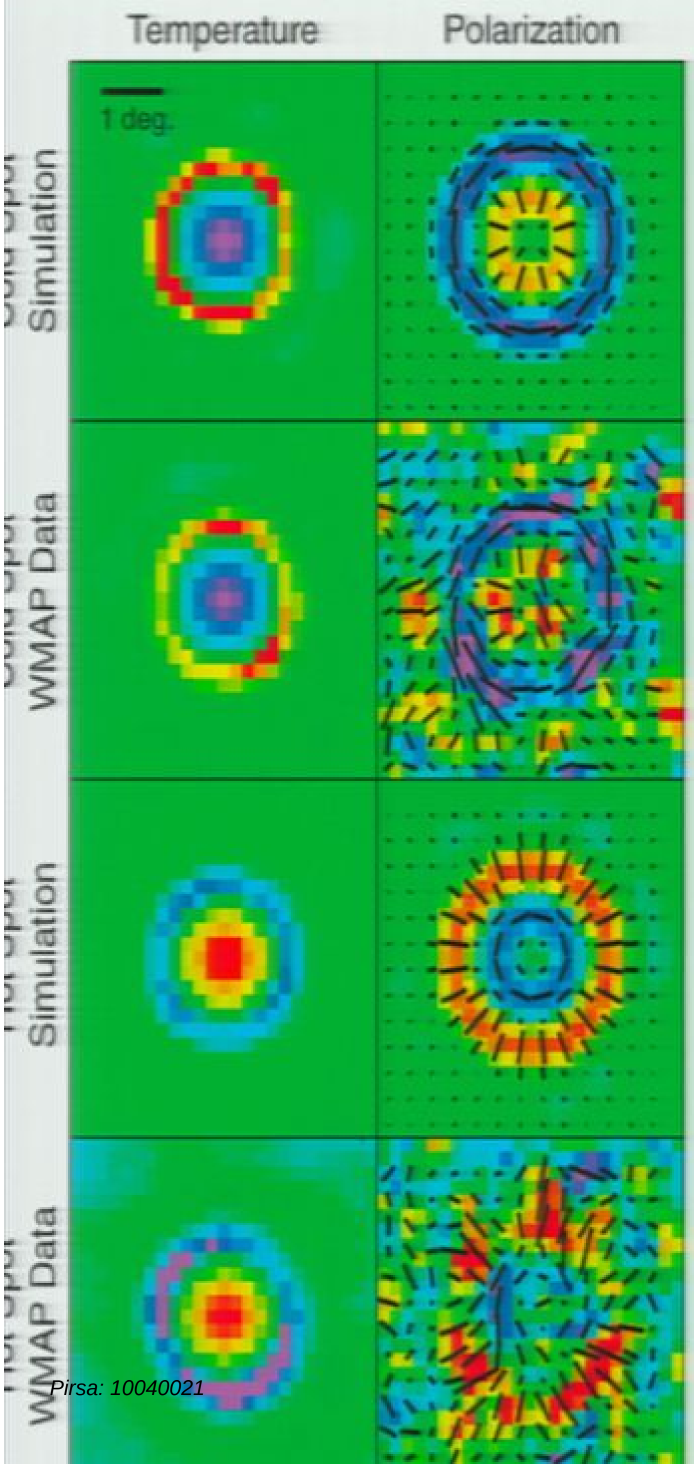

Two-dimensional View

- All hot and cold spots are stacked (the threshold peak height, $\Delta T/\sigma$, is zero)
- "Compression phase" at θ=1.2 deg and "slow-down phase" at θ=0.6 deg are predicted to be there and we observe them!
  - The overall significance level: 8σ
- Striking confirmation of the physics of CMB and the dominance of **adiabatic** & **scalar** perturbation.

How About U_r?

- U_r is produced by the TB correlation, which is expected to vanish in a parity-conserving universe.

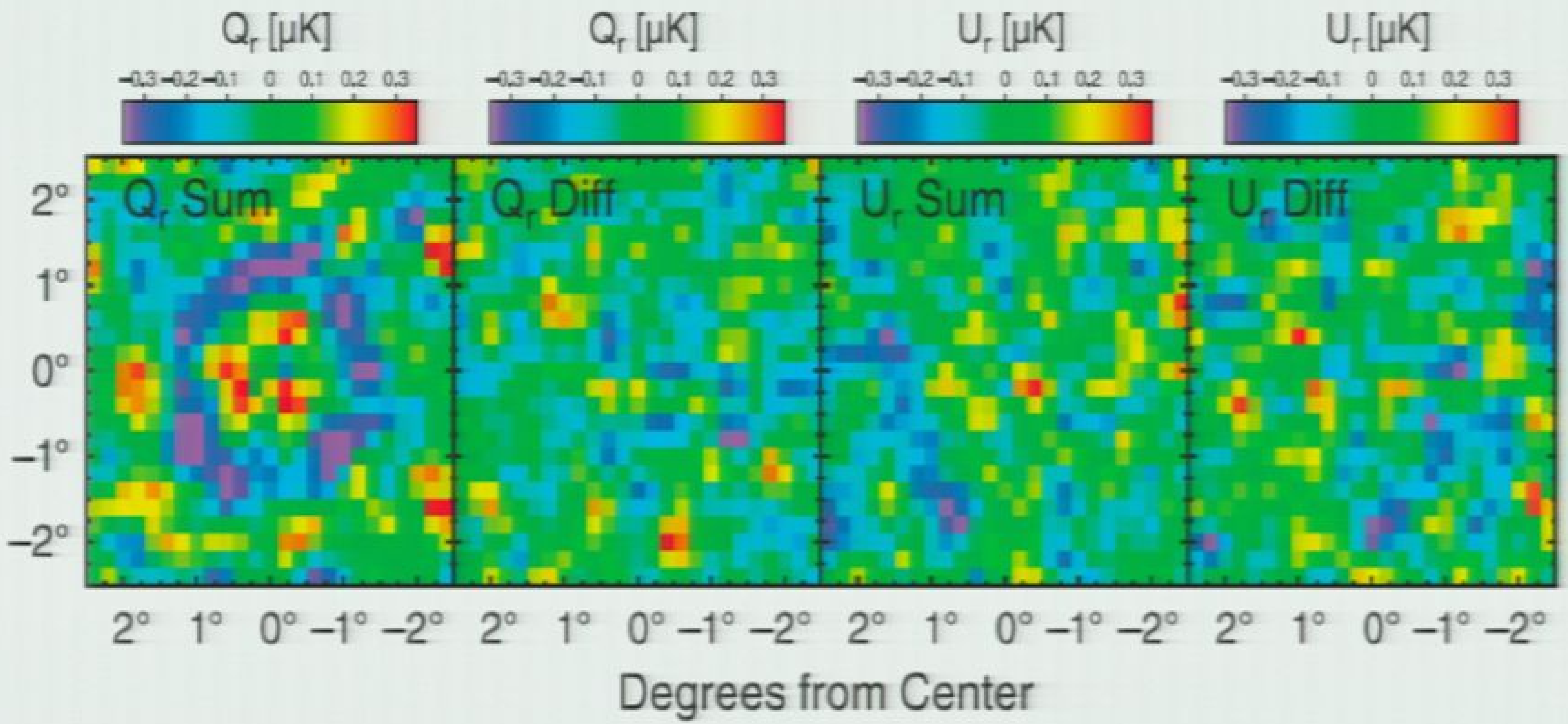

- The U_r map is consistent with noise.

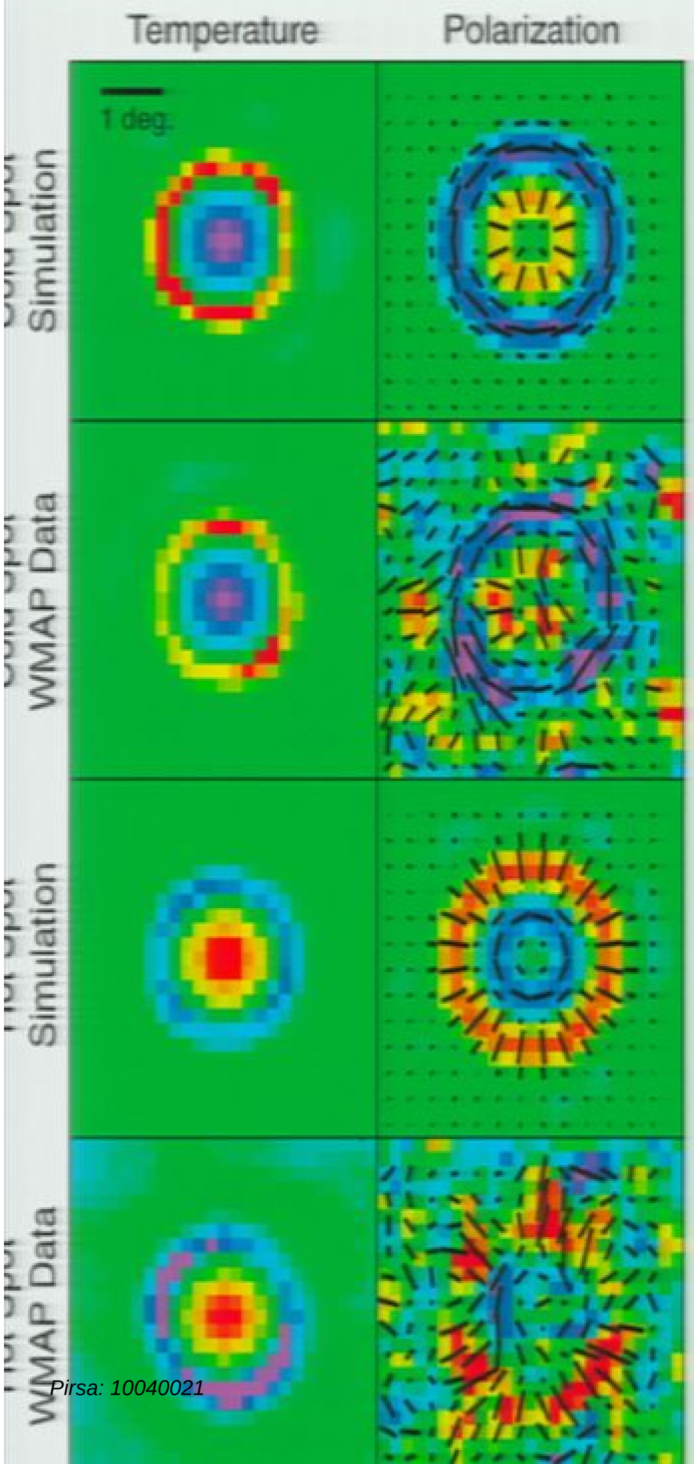

Two-dimensional View

- All hot and cold spots are stacked (the threshold peak height, $\Delta T/\sigma$, is zero)
- "Compression phase" at θ=1.2 deg and "slow-down phase" at θ=0.6 deg are predicted to be there and we observe them!
  - The overall significance level: 8σ
- Striking confirmation of the physics of CMB and the dominance of **adiabatic** & **scalar** perturbation.

How About U_r?

- U_r is produced by the TB correlation, which is expected to vanish in a parity-conserving universe.

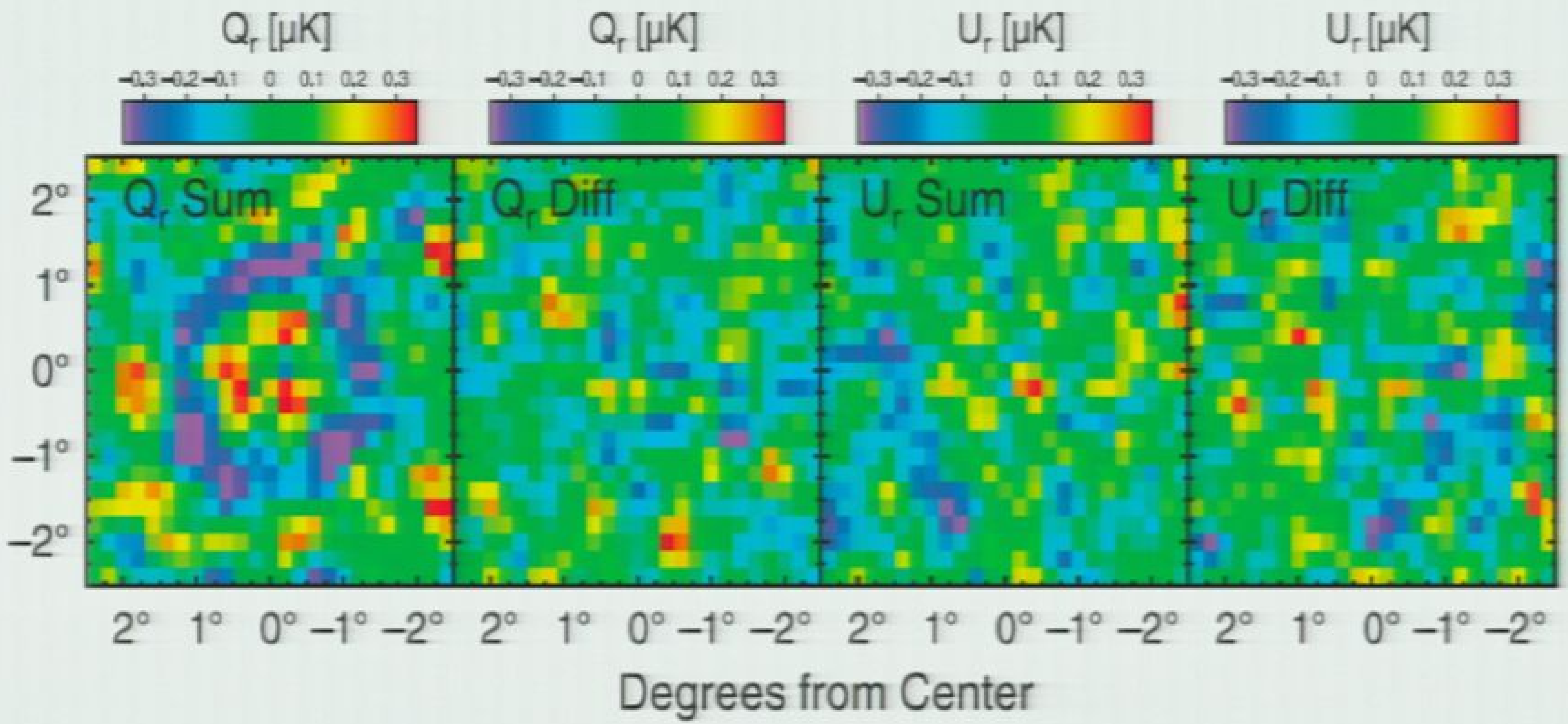

- The U_r map is consistent with noise.

Probing Parity Violation

- Cosmological parity violation ("birefringence," Carroll 1998; Lue et al. 1999) may rotate the polarization plane by an angle $\Delta\alpha$, and convert E modes to B modes:

$$C_l^{\mathrm{TB,obs}} = C_l^{\mathrm{TE}} \sin(2\Delta\alpha)$$

- Non-detection of U_r gives $\Delta\alpha$=1±3 deg (68%CL)
- The full analysis using C_l^{TB} (as well as C_l^{EB}) gives
  - $\Delta\alpha = -1.1 \pm 1.3$(statistical) $\pm$ 1.5(systematic) deg.

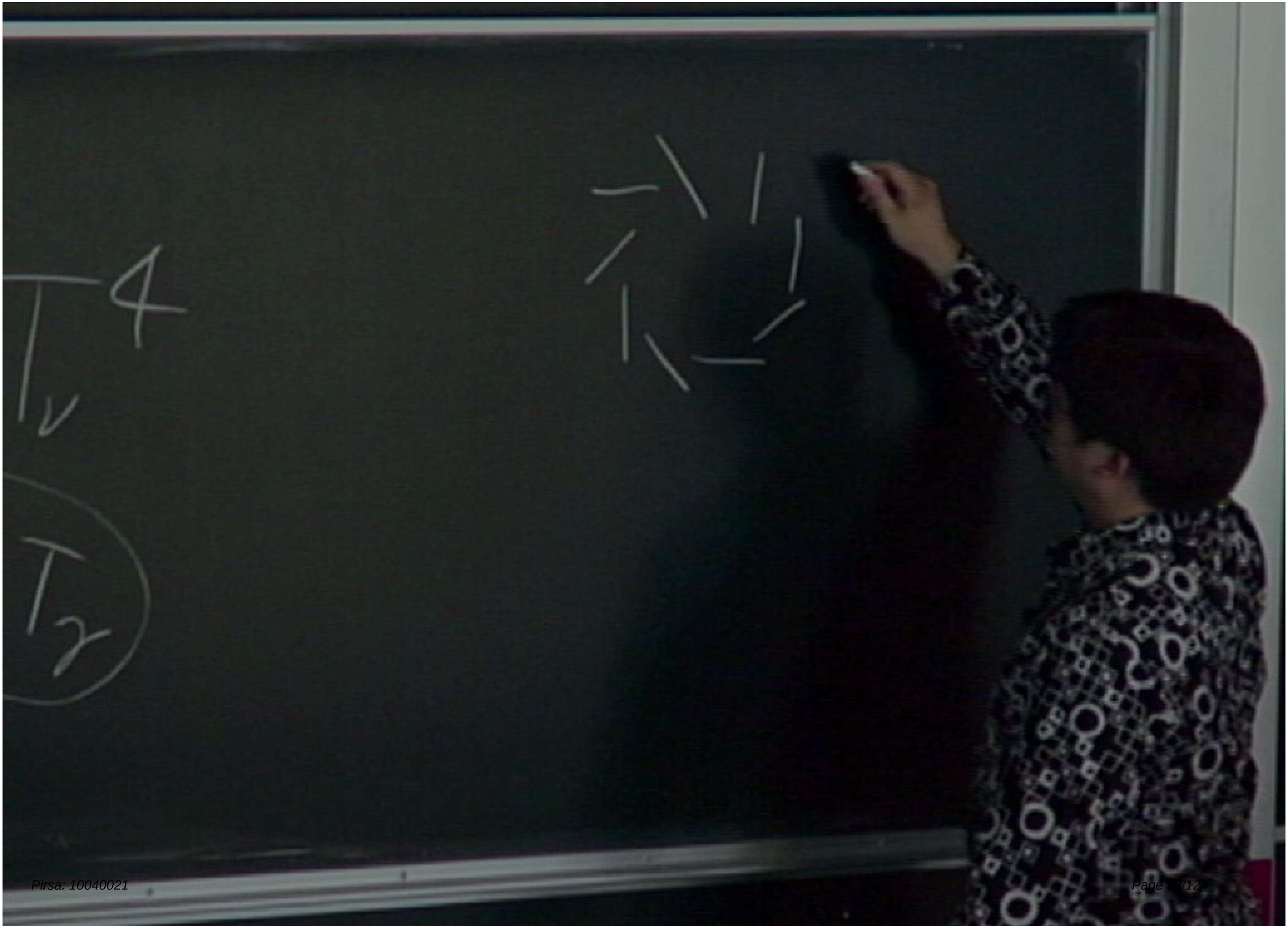

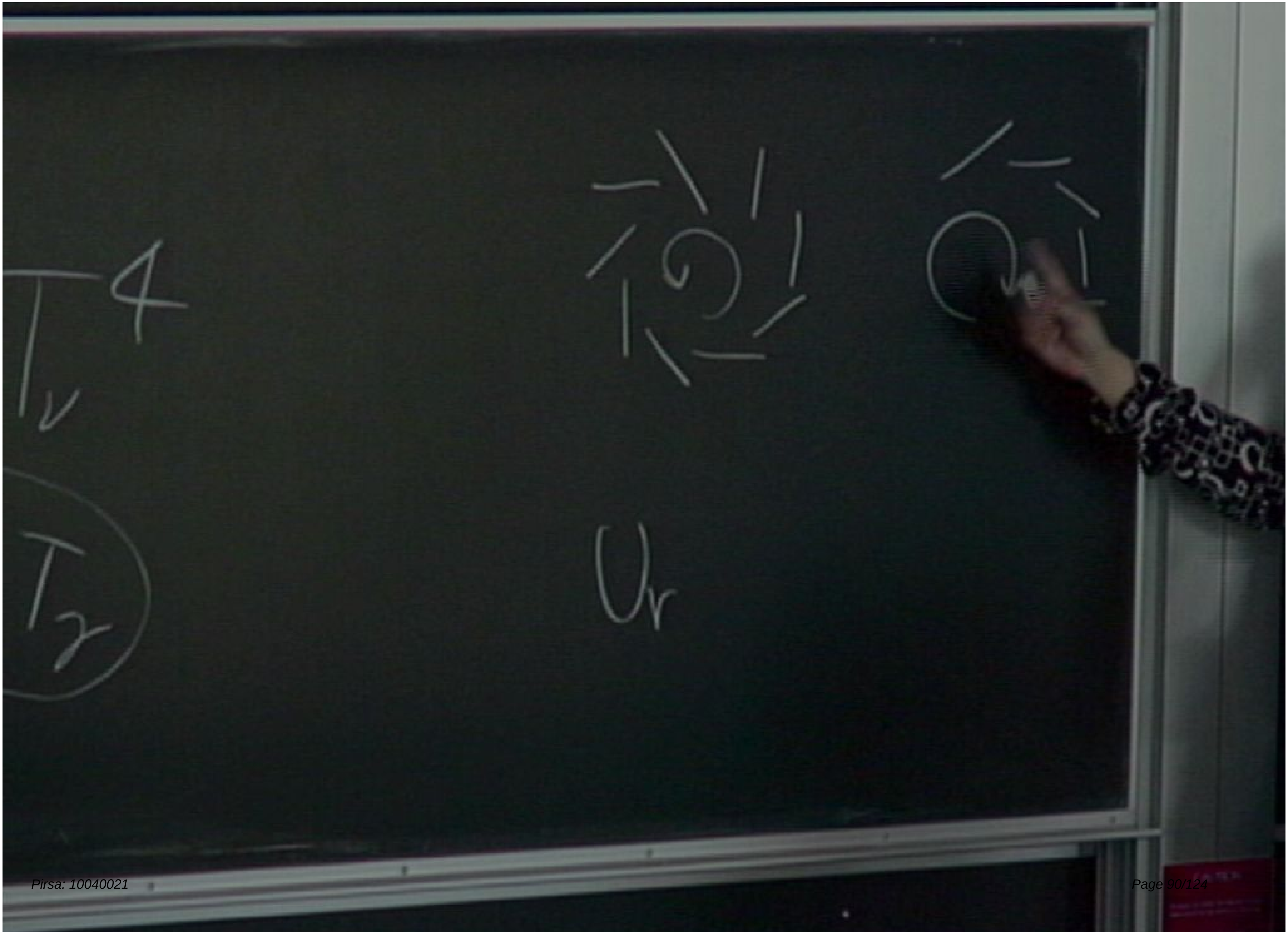
T_ν^4
T_γ
U_r

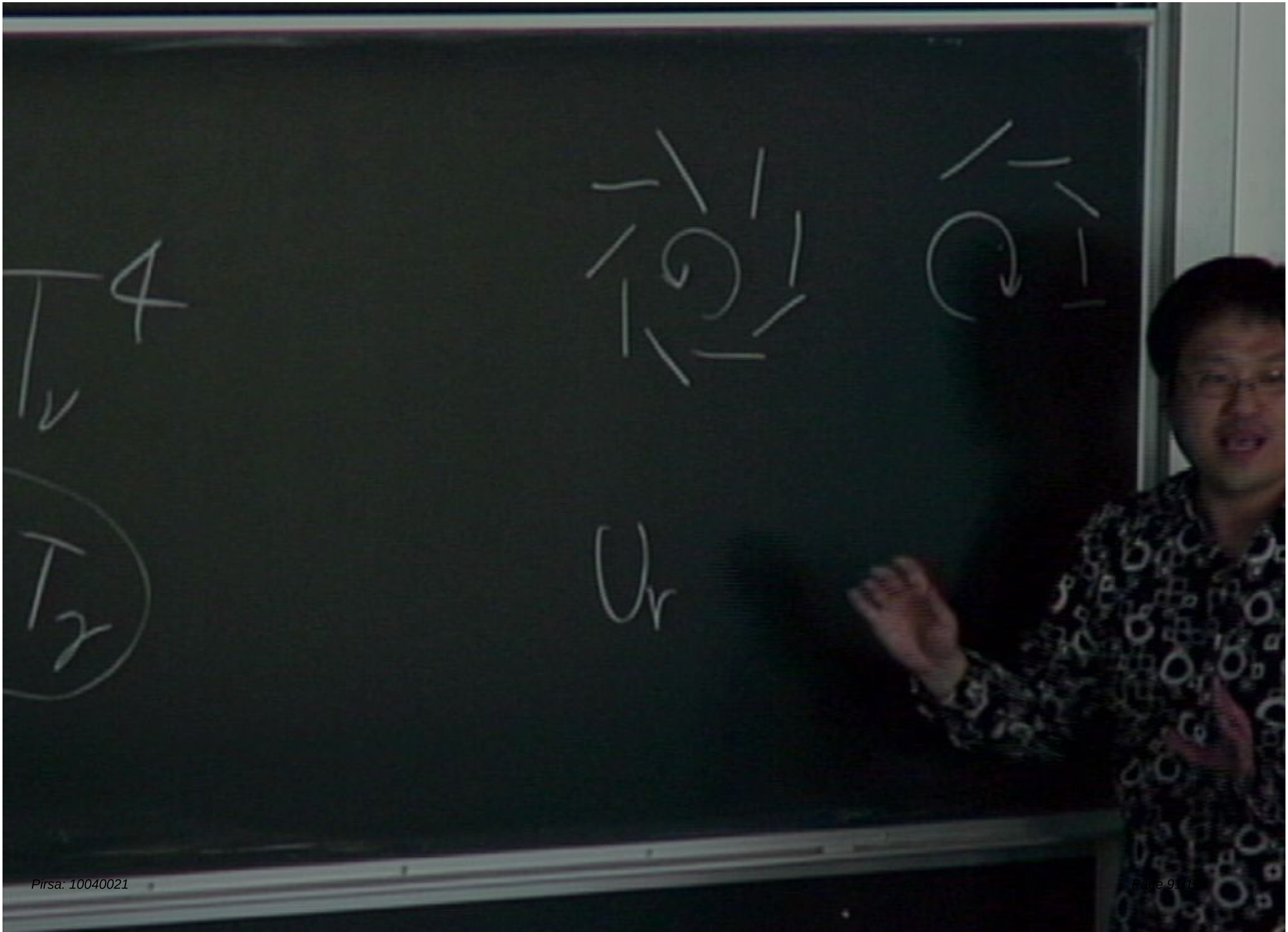
T_ν^4
T_γ
U_r

Probing Parity Violation

- Cosmological parity violation ("birefringence," Carroll 1998; Lue et al. 1999) may rotate the polarization plane by an angle $\Delta\alpha$, and convert E modes to B modes:

$$C_l^{\mathrm{TB,obs}} = C_l^{\mathrm{TE}} \sin(2\Delta\alpha)$$

- Non-detection of U_r gives $\Delta\alpha = 1 \pm 3$ deg (68%CL)
- The full analysis using C_l^{TB} (as well as C_l^{EB}) gives
  - $\Delta\alpha = -1.1 \pm 1.3$(statistical) $\pm$ 1.5(systematic) deg.

Probing Inflation (Power Spectrum)

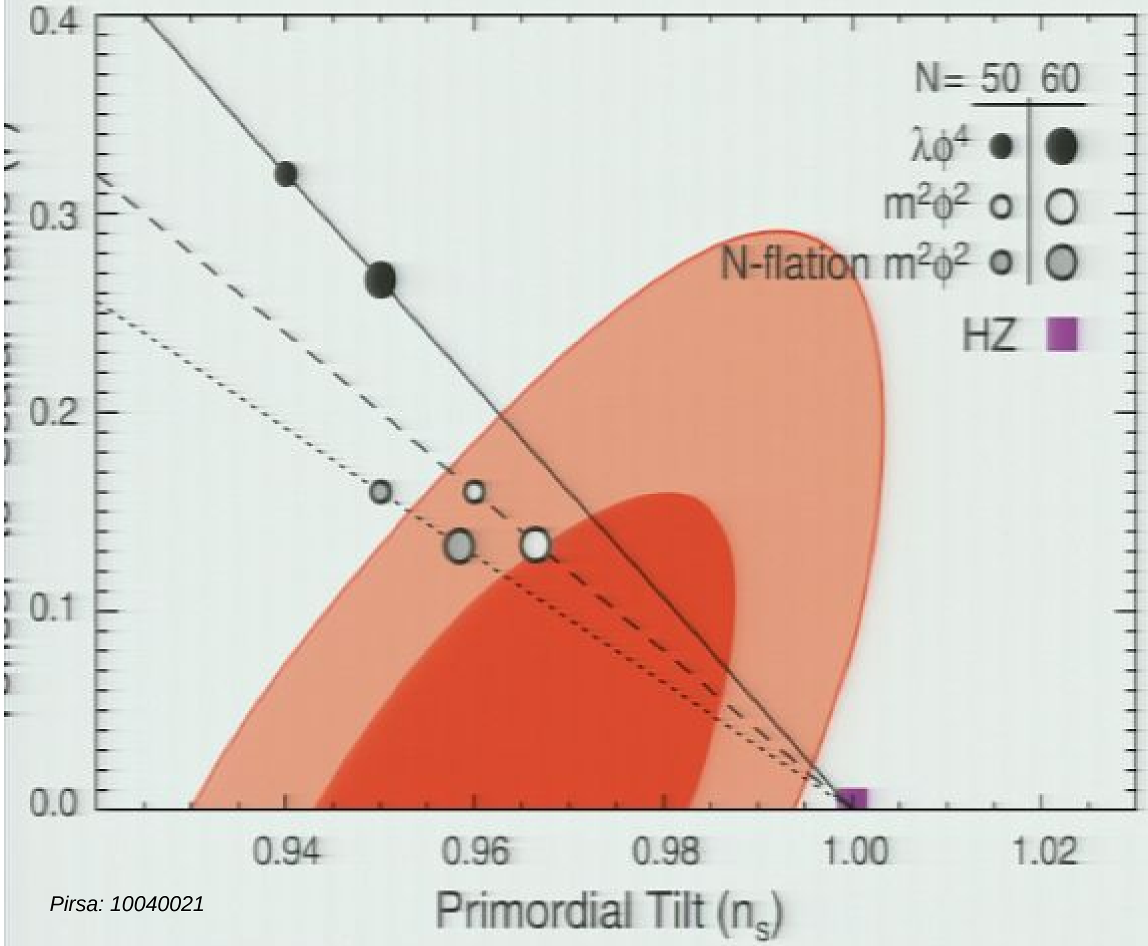

- Joint constraint on the primordial tilt, n_s, and the tensor-to-scalar ratio, r.
  - Not so different from the 5-year limit.
  - $r < 0.24$ (95%CL; w/o SN)
  - $r < 0.20$ (95%CL; w/ SN)

Probing Inflation (Bispectrum)

- No detection of 3-point functions of primordial curvature perturbations. The 95% CL limits are:
  - $-10 < f_{NL}^{local} < 74$
  - $-214 < f_{NL}^{equilateral} < 266$
  - $-410 < f_{NL}^{orthogonal} < 6$
- The WMAP data are consistent with the prediction of **simple single-inflation inflation** models:
  - $1-n_s \approx r \approx f_{NL}^{local}$, $f_{NL}^{equilateral} = 0 = f_{NL}^{orthogonal}$.

Zel'dovich & Sunyaev (1969); Sunyaev & Zel'dovich (1972)

Sunyaev–Zel'dovich Effect

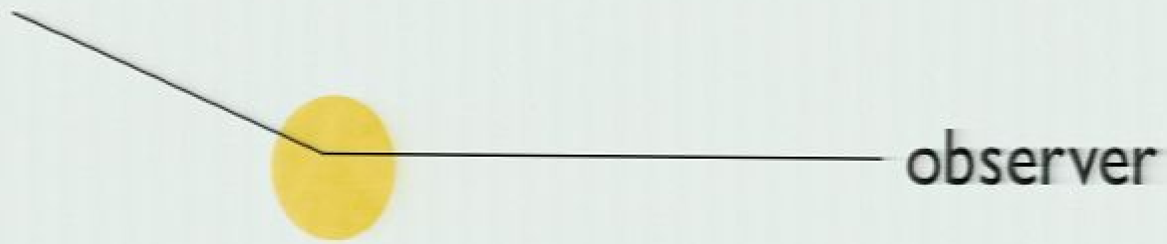

Hot gas with the
electron temperature of $T_e >> T_{cmb}$

- $\Delta T/T_{cmb} = g_\nu$ **y**

$$y = (\text{optical depth of gas})\, k_B T_e/(m_e c^2)$$
$$= [\sigma_T/(m_e c^2)] \int n_e k_B T_e \, d(\text{los})$$
$$= [\sigma_T/(m_e c^2)] \int (\text{electron pressure}) d(\text{los})$$

$g_\nu = -2$ (ν=0); −1.91, −1.81 and −1.56 at ν=41, 61 and 94 GHz

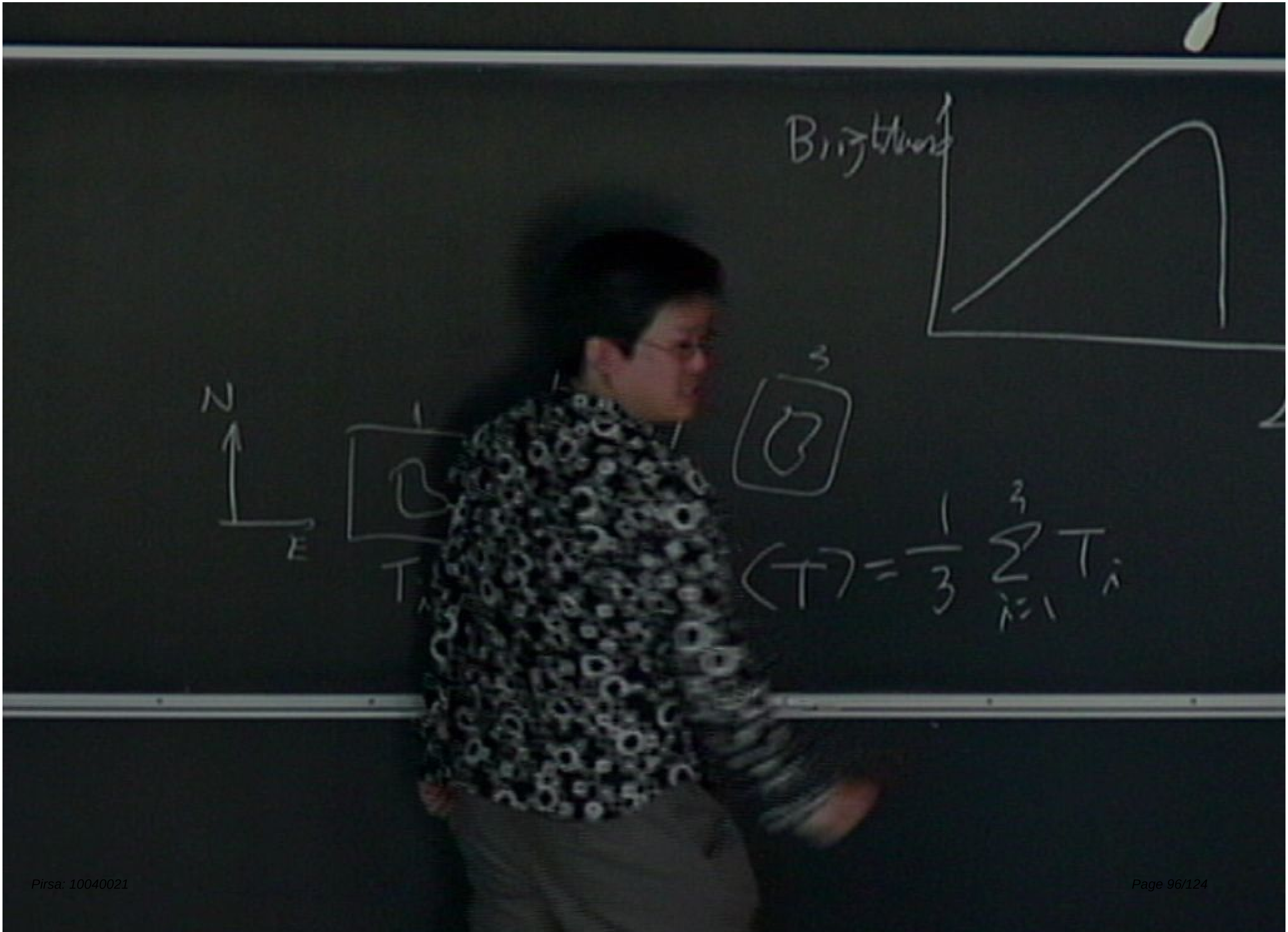
N
E
3
$\langle T \rangle = \frac{1}{3}\sum_{i=1}^{3} T_i$

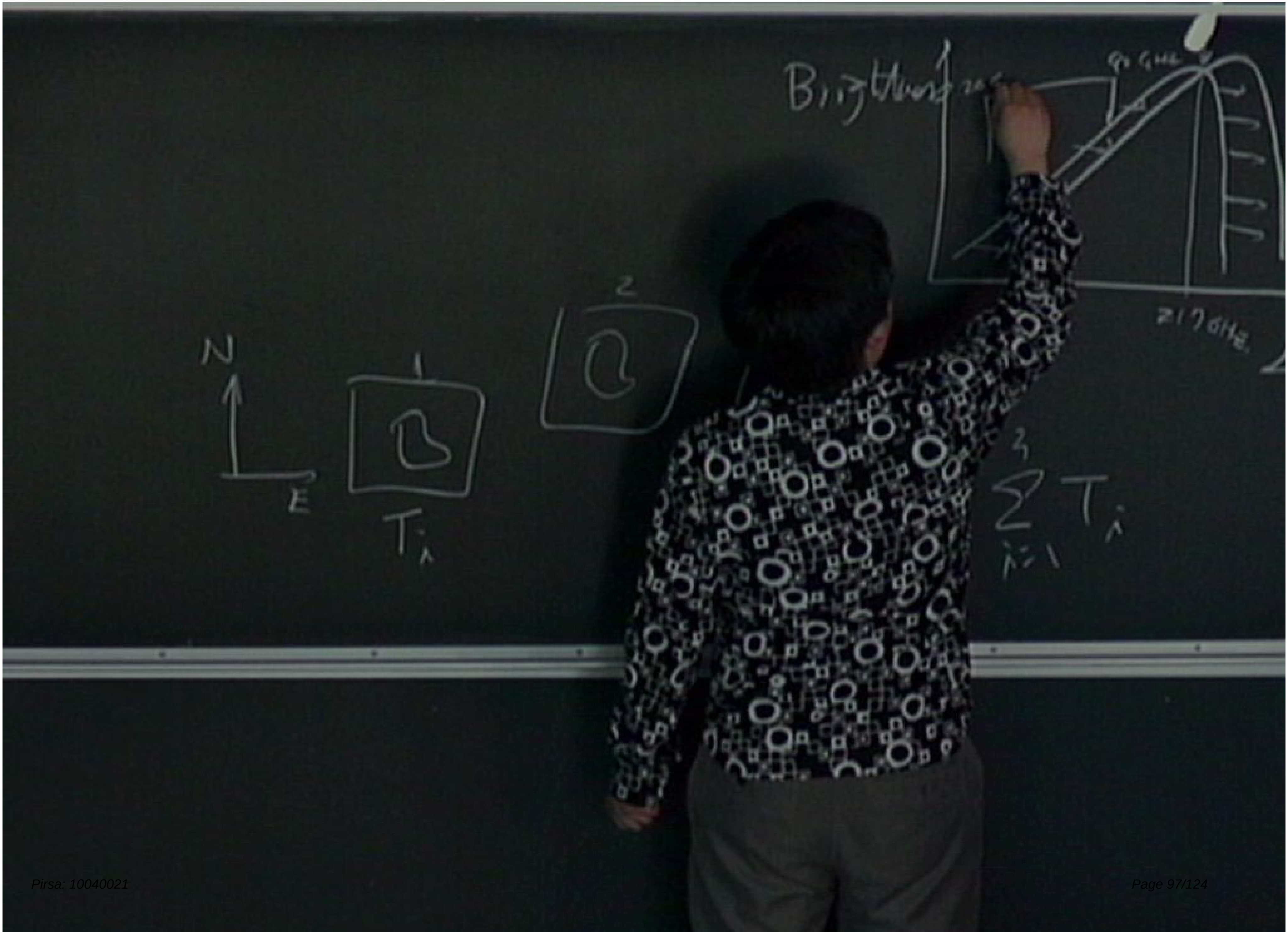
Brightness
N
E
1
2
217 GHz

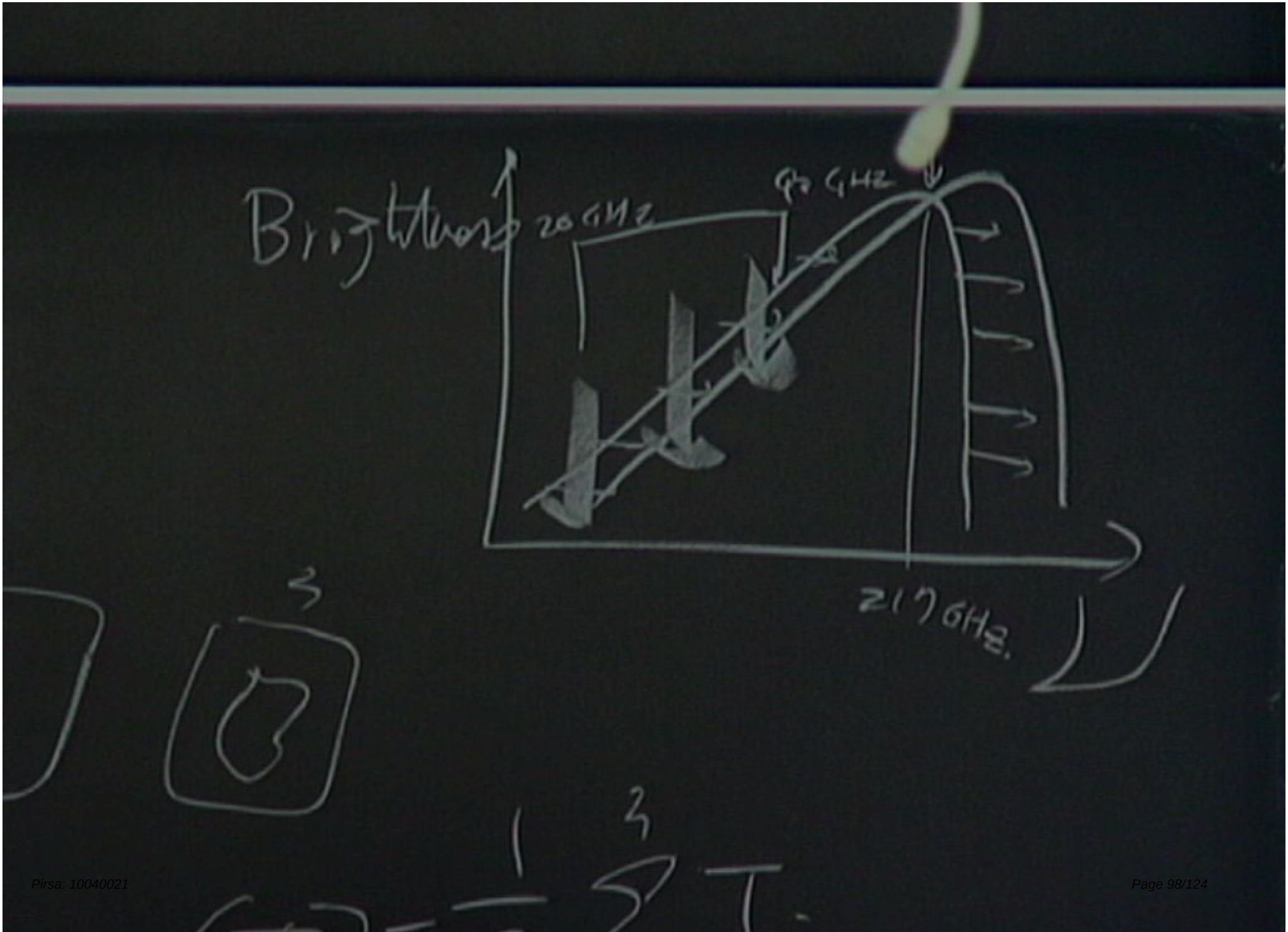
Brightness
20 GHz
90 GHz
217 GHz.

Coma Cluster (z=0.023)

We find that the CMB fluctuation in the direction of Coma is ≈ –100uK. (This is a new result!)

$y_{coma}(0)=(7\pm2)\times10^{-5}$ (68%CL)

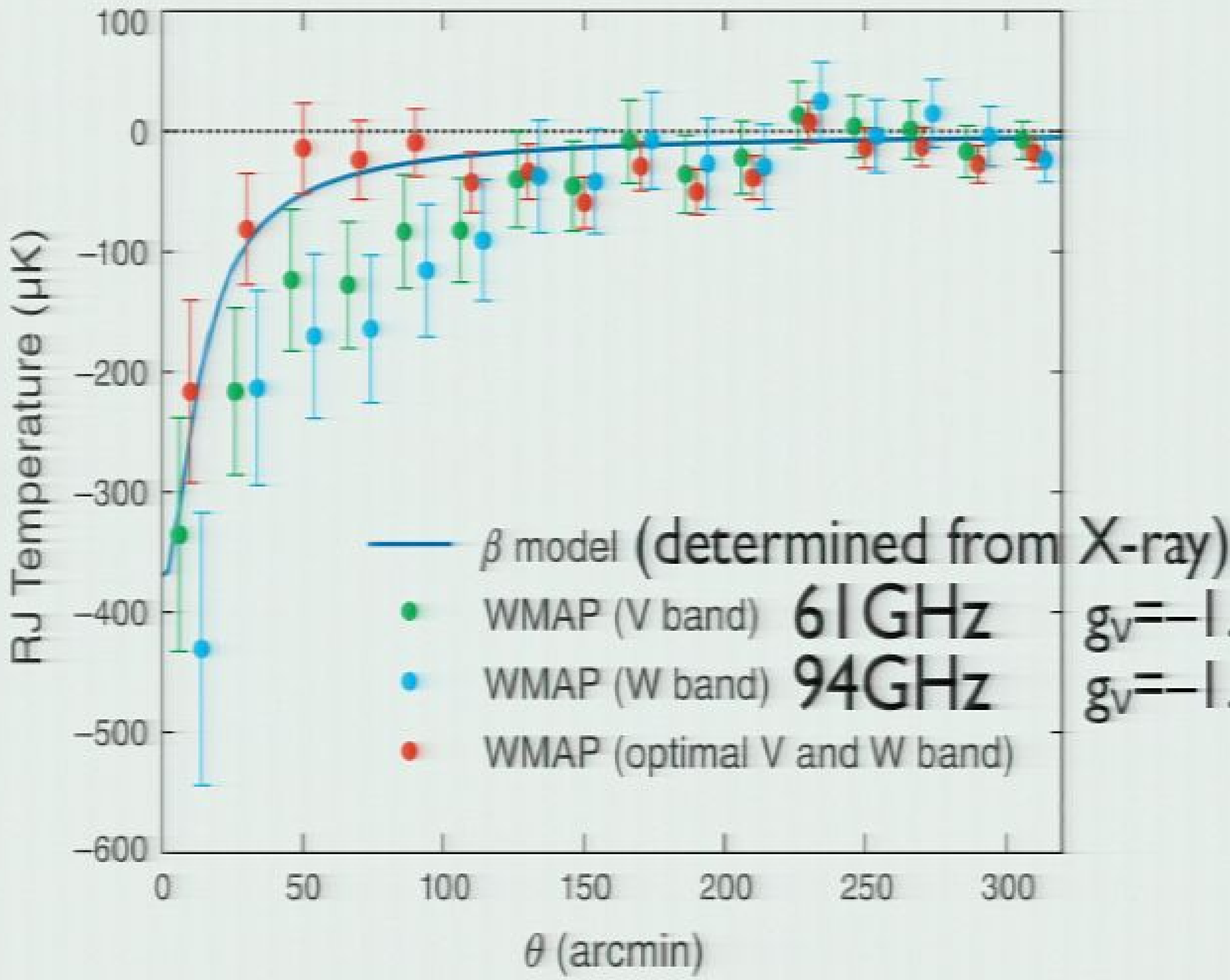

g_ν=–1.81

g_ν=–1.56

- "Optimal V and W band" analysis can separate SZ and CMB. The SZ effect toward Coma is detected at **3.6σ**.

Coma Cluster (z=0.023)

We find that the CMB fluctuation in the direction of Coma is ≈ −100uK. (This is a new result!)

$y_{coma}(0)=(7\pm2)\times10^{-5}$ (68%CL)

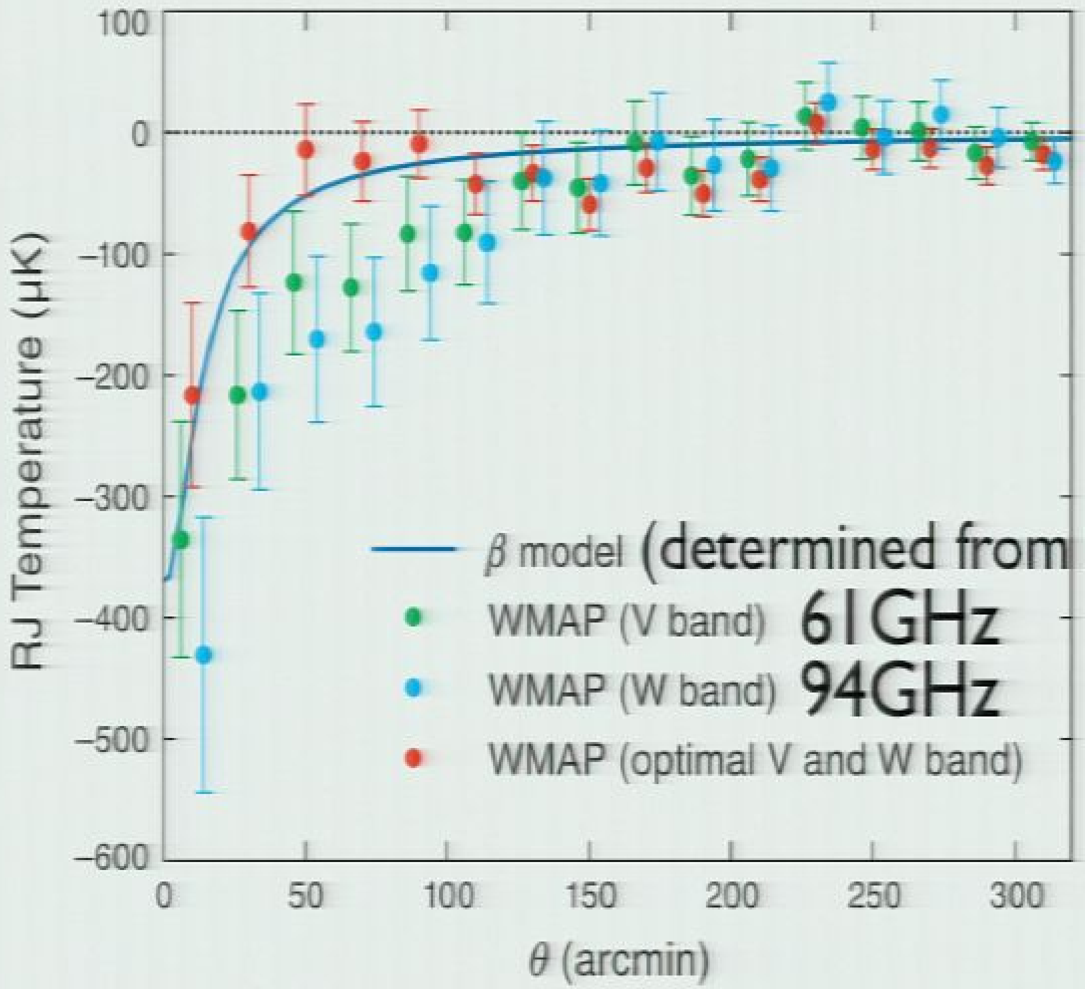

$g_V=-1.81$

$g_V=-1.56$

- "Optimal V and W band" analysis can separate SZ and CMB. The SZ effect toward Coma is detected at **3.6σ**.

A Question

- Are we detecting the ***expected*** amount of electron pressure, P_e, in the SZ effect?
  - Expected from X-ray observations.
  - Expected from theory.

Three approaches

- 1. Compare the WMAP data and X-ray data on individual clusters individually.
  - But, not all clusters are detected individually by the WMAP data...
- 2. Compare the stacked WMAP data and the expected average X-ray profiles.
  - Systematic effects in the stacking analysis must be carefully studied.
- 3. Compare the stacked WMAP data and the expected profiles from theory (hydro simulation etc).

Arnaud et al. Profile

- A fitting formula for the average electron pressure profile as a function of the cluster mass (M_{500}), derived from 33 nearby ($z<0.2$) clusters.

Three approaches

- 1. Compare the WMAP data and X-ray data on individual clusters individually.
  - But, not all clusters are detected individually by the WMAP data...
- 2. Compare the stacked WMAP data and the expected average X-ray profiles.
  - Systematic effects in the stacking analysis must be carefully studied.
- 3. Compare the stacked WMAP data and the expected profiles from theory (hydro simulation etc).

Arnaud et al. Profile

- A fitting formula for the average electron pressure profile as a function of the cluster mass (M_{500}), derived from 33 nearby ($z<0.2$) clusters.

Arnaud et al. Profile

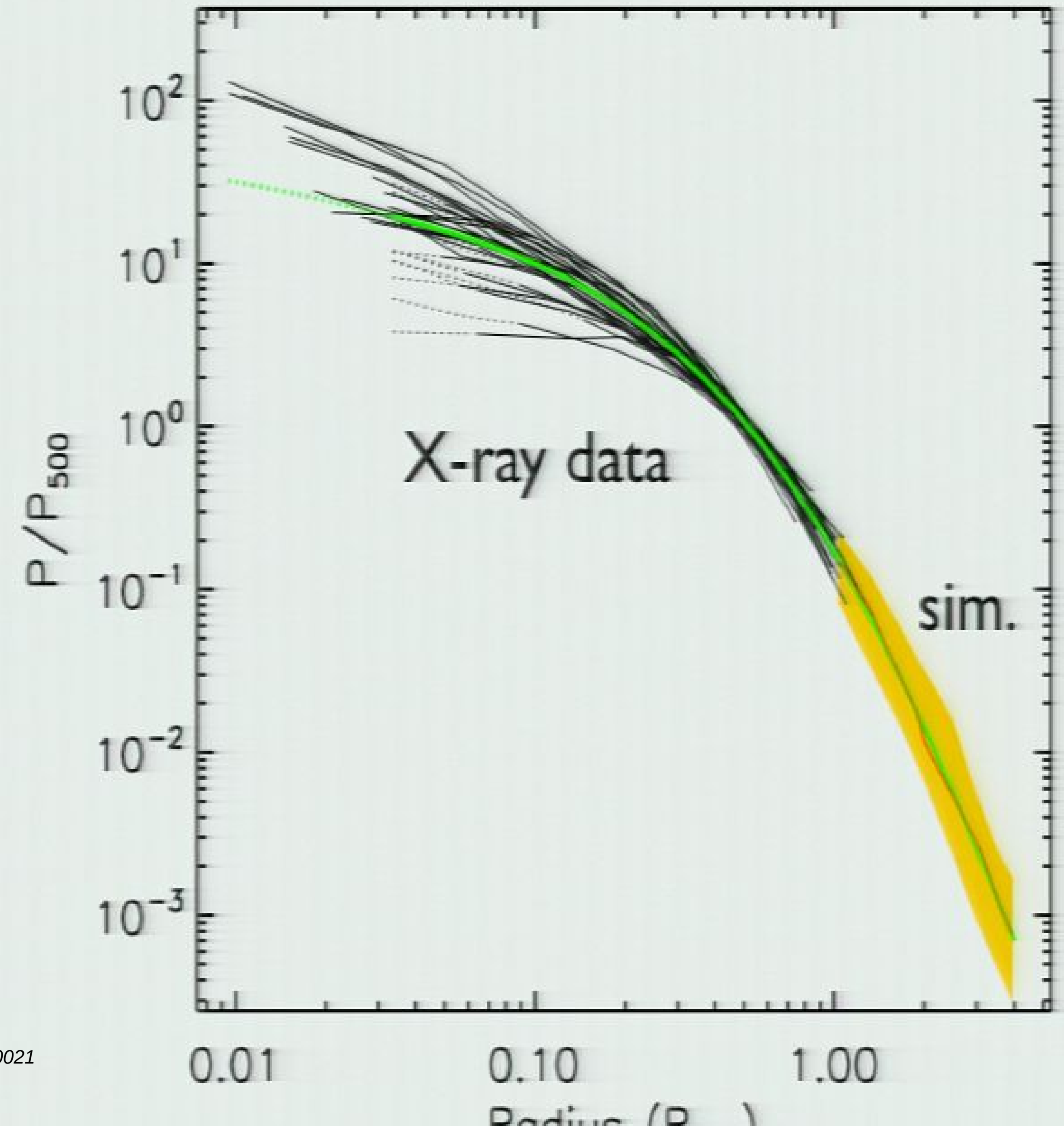

- A significant scatter exists at $R<0.2R_{500}$, but a good convergence in the outer part.

Coma Data vs Arnaud

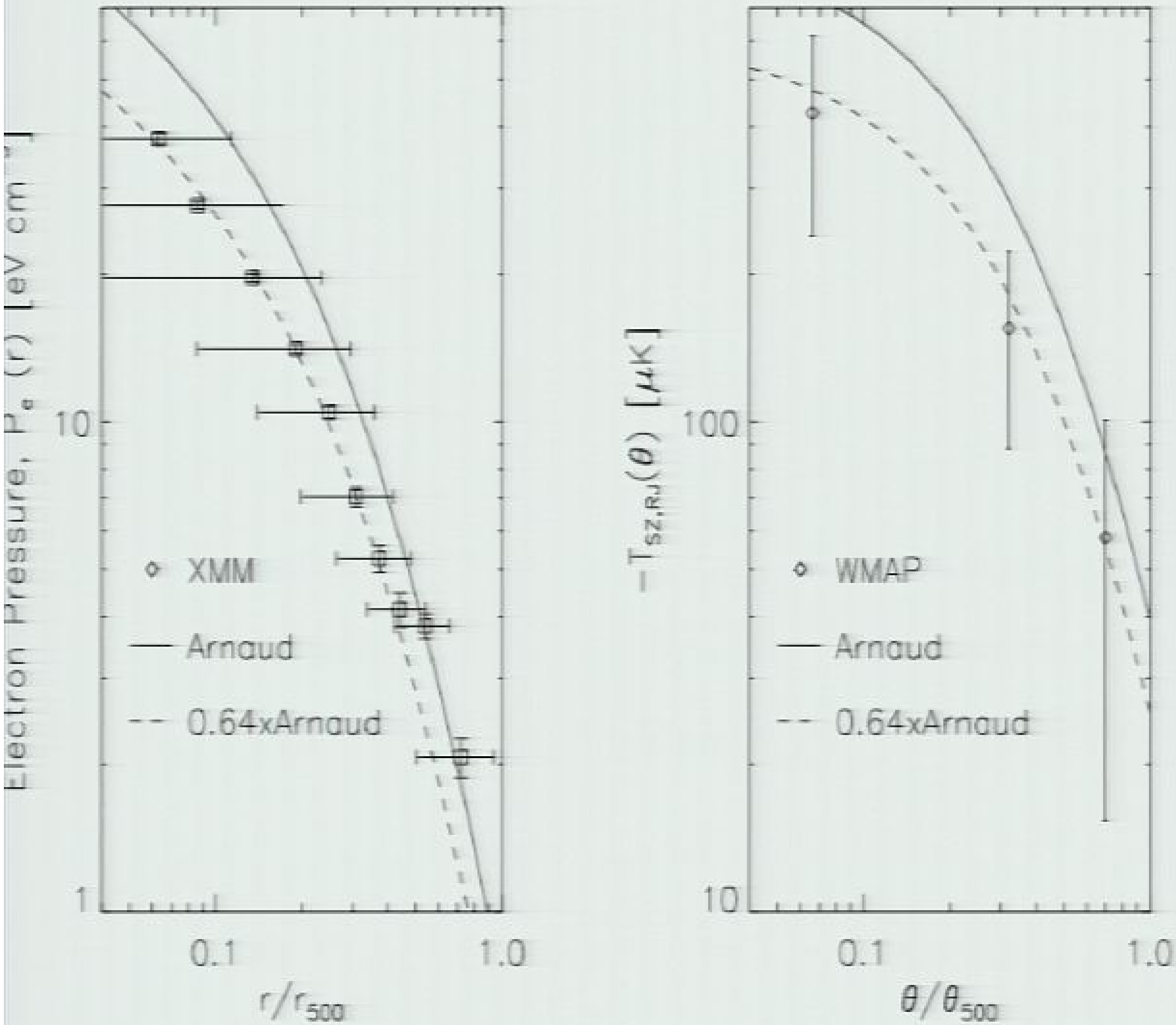

- $M_{500}=6.6\times10^{14}h^{-1}M_{sun}$ is estimated from the mass-temperature relation (Vikhlinin et al.)
  - $T_X^{coma}=8.4$keV.
- Arnaud et al.'s profile overestimates both the direct X-ray data and WMAP data by the same factor (0.64)!
  - To reconcile them, $Tx^{coma}=6.5$keV is required, but that is way too low.

The X-ray data (XMM) are provided by A. Finoguenov.

Well...

- That's just one cluster. What about the other clusters?
  - We measure the SZ effect of a very nice sample of well-studied nearby clusters compiled by Vikhlinin et al.

New results! (Prelim.)

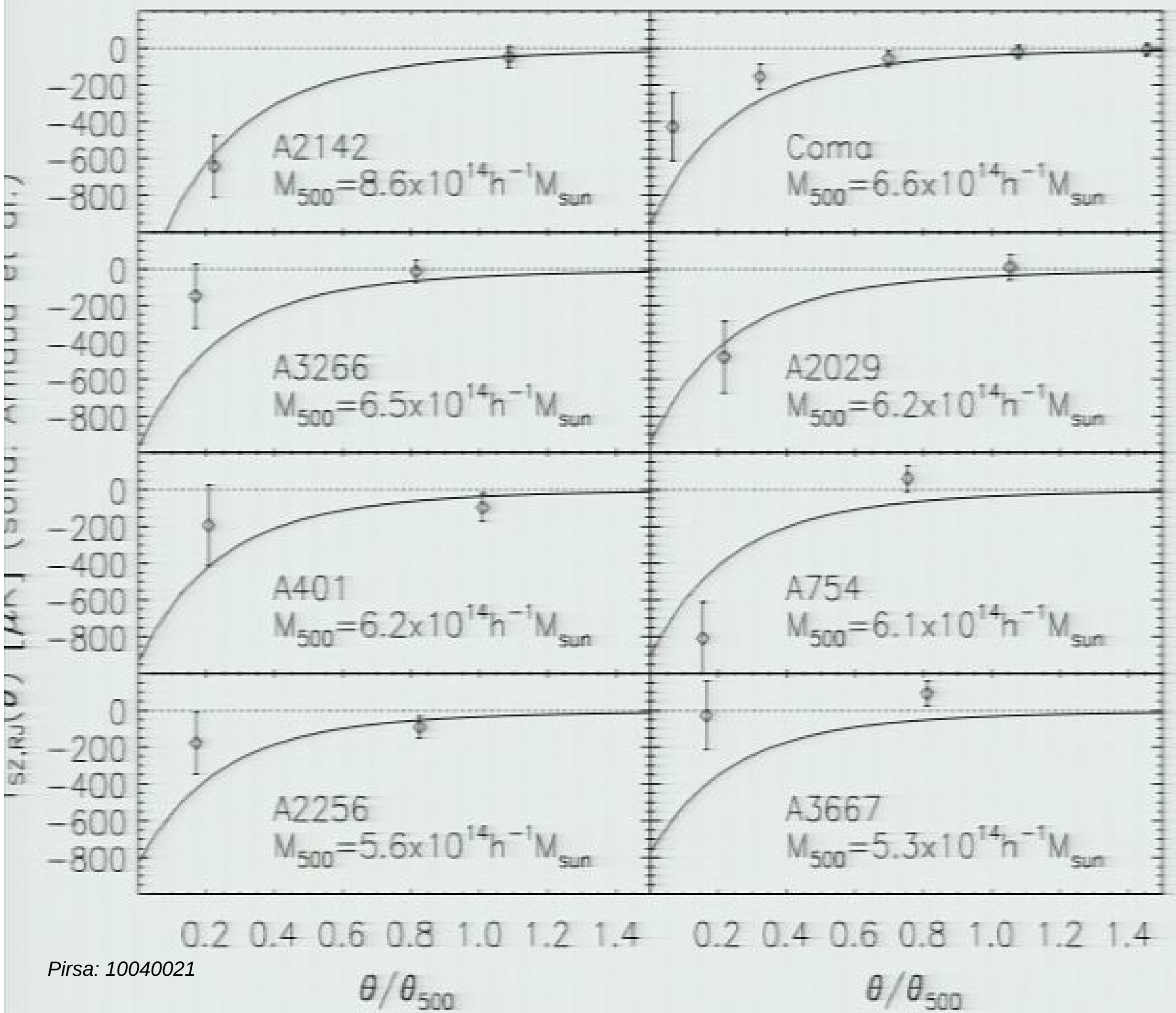

- Normalization for the 5 very high-mass clusters ($M_{500}>6\times10^{14}h^{-1}M_{sun}$) is 0.72±0.13.
- Normalization for the 12 high-mass clusters ($M_{500}>4\times10^{14}h^{-1}M_{sun}$) is 0.68±0.11.
- Arnaud et al. profile systematically overestimates the electron pressure!

Small-scale CMB Data

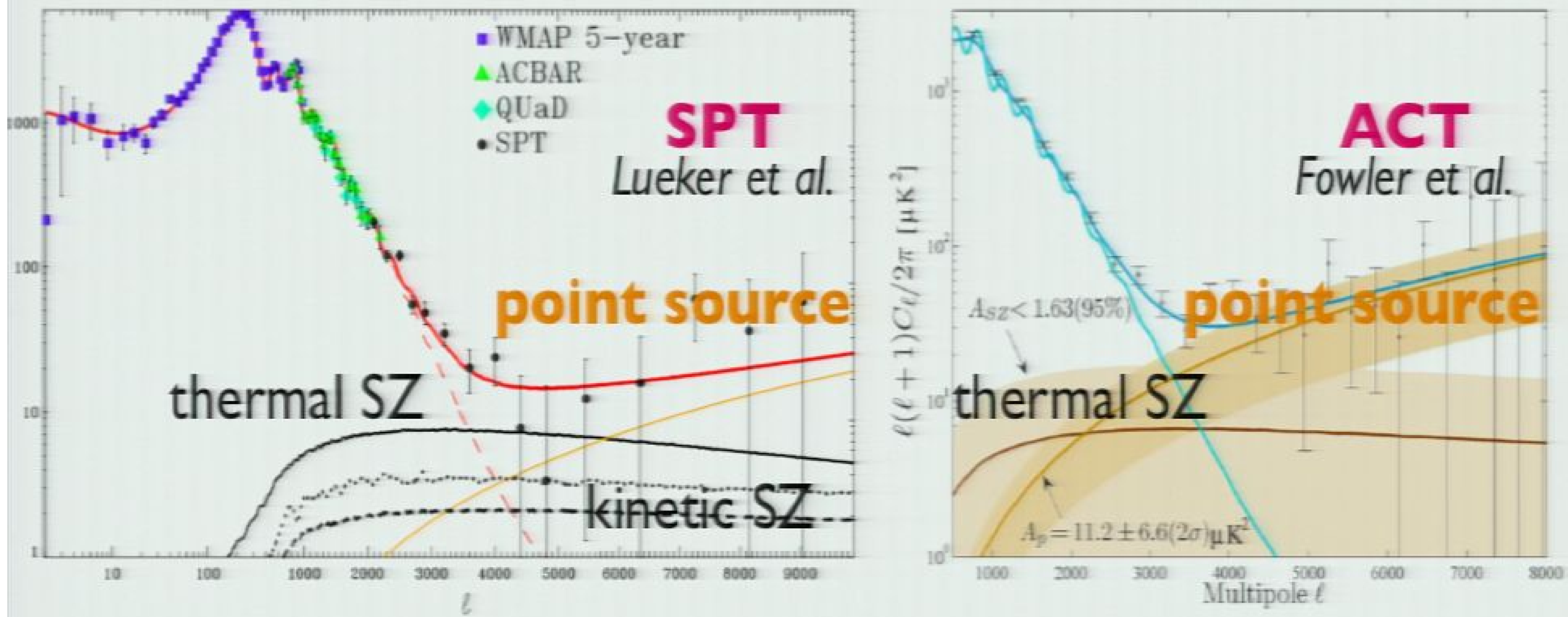

- The SPT measured the secondary anisotropy from (possibly) SZ. **The power spectrum amplitude is A_{SZ}=0.4–0.6 times the expectations.** Why?

Mass Distribution

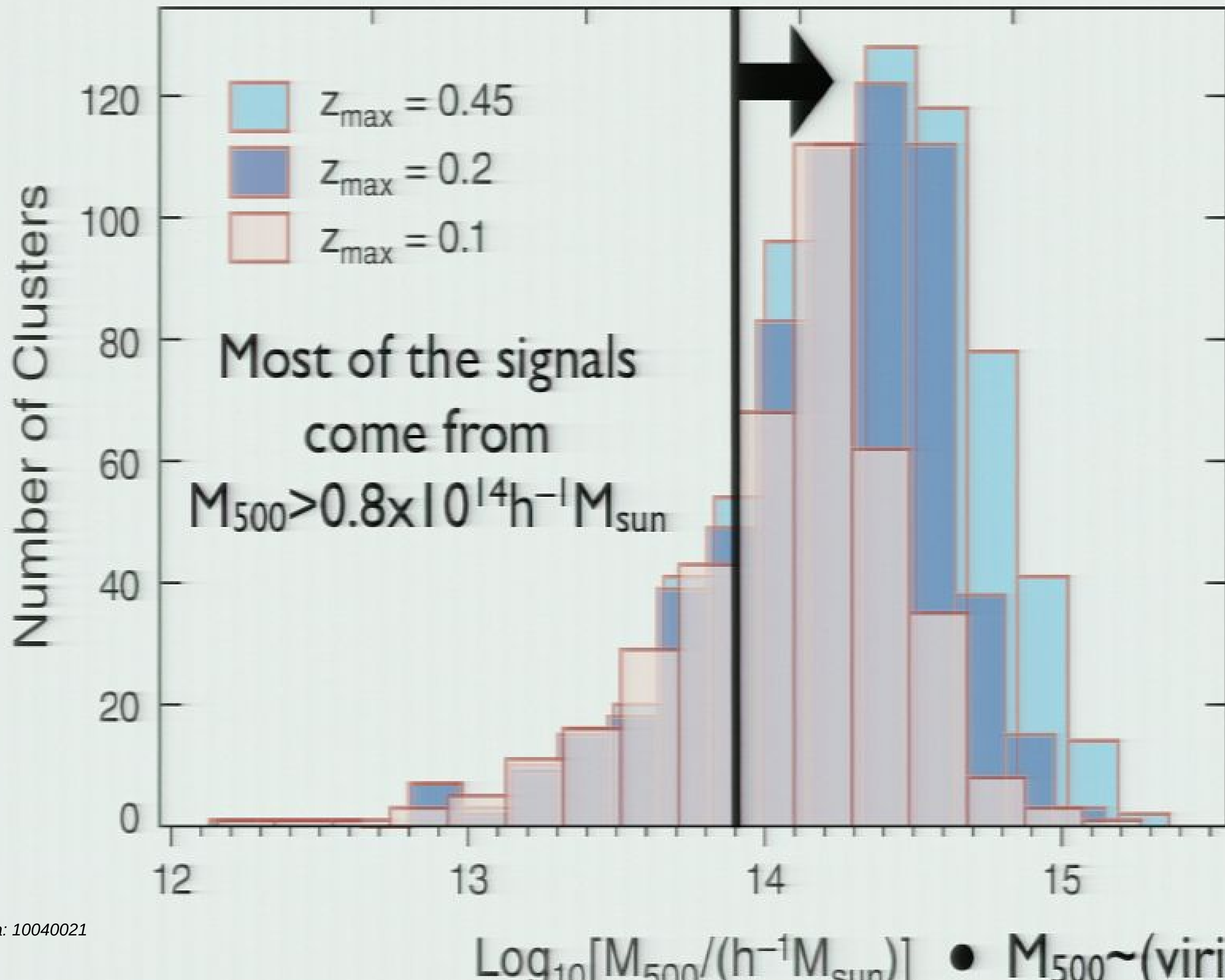

- $M_{500} \sim$ (virial mass)/1.6

Small-scale CMB Data

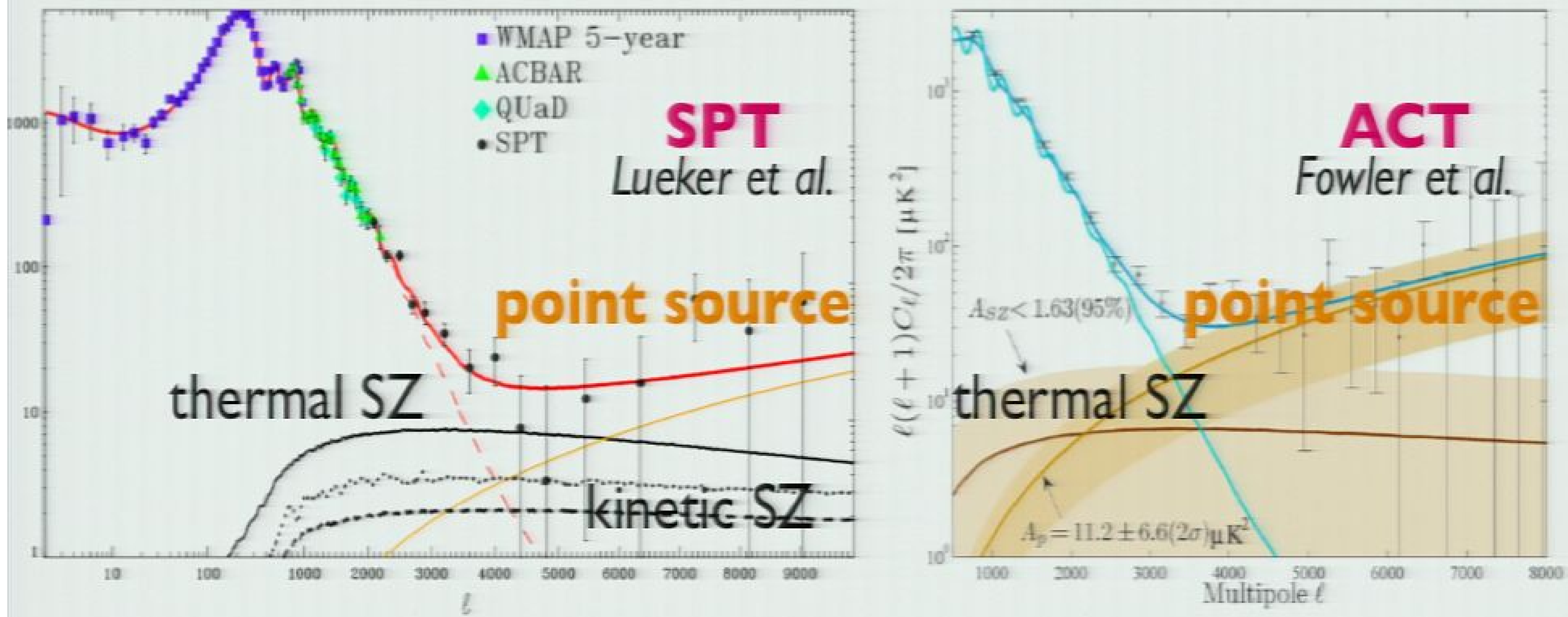

- The SPT measured the secondary anisotropy from (possibly) SZ. **The power spectrum amplitude is A_{SZ}=0.4–0.6 times the expectations.** Why?

Lower A_{SZ}: Two Possibilities

$$C_l = g_\nu^2 \int_0^{z_{\max}} dz \frac{dV}{dz} \int_{M_{\min}}^{M_{\max}} dM \frac{dn(M,z)}{dM} |\tilde{y}_l(M,z)|^2$$

$$\frac{l(l+1)C_l}{2\pi} \simeq 330\,\mu\mathrm{K}^2\, \sigma_8^7 \left(\frac{\Omega_b h}{0.035}\right)^2$$ x [gas pressure]

- The SZ power spectrum is sensitive to the number of clusters (i.e., σ_8) and the pressure of individual clusters.
- Lower SZ power spectrum can imply:
  - σ_8 is 0.77 (rather than 0.8): $\sum m_\nu$~0.2eV?
  - Gas pressure per cluster is lower than expected

WMAP measurement favors this possibility.

Size-Luminosity Relations

- To calculate the expected pressure profile for each cluster, we need to know the size of the cluster, r_{500}.
- This needs to be derived from the observed properties of X-ray clusters.
  - The best quantity is the gas mass times temperature, but this is available only for a small subset of clusters.
  - We use r_{500}–L_X relation (Boehringer et al.):

$$r_{500} = \frac{(0.753 \pm 0.063)\ h^{-1}\ \mathrm{Mpc}}{E(z)} \times \left(\frac{L_X}{10^{44}\ h^{-2}\ \mathrm{erg\ s^{-1}}} \right)^{0.228 \pm 0.015}$$

Uncertainty in this relation is the major source of sys. error.

$$E(z) \equiv H(z)/H_0 = \left[\Omega_m (1+z)^3 + \Omega_\Lambda \right]^{1/2}$$

Summary

- Significant improvements in the **high-l temperature** data, and the **polarization data at all multipoles**.
  - High-l temperature: $n_s<1$, detection of helium, improved limits on neutrino properties.
  - Polarization: polarization on the sky!
    - Polarization-only limit on r: $r<0.93$ (95%CL).
    - All data included: $r<0.24$ (95%CL; w/o SN)
    - $\Delta\alpha = -1.1 \pm 1.3$(statistical) ± 1.5(systematic) deg.

Puzzle?

- SZ effect: Coma's radial profile is measured, several massive clusters are detected, and the statistical detection reaches 8σ.
  - Evidence for lower-than-expected gas pressure.
  - The X-ray data are fine? We just need to revise the existing models.

Puzzle?

- SZ effect: Coma's radial profile is measured, several massive clusters are detected, and the statistical detection reaches 8σ.
  - Evidence for lower-than-expected gas pressure.
  - The X-ray data are fine? We just need to revise the existing models.

Puzzle?

- SZ effect: Coma's radial profile is measured, several massive clusters are detected, and the statistical detection reaches 8σ.
  - Evidence for lower-than-expected gas pressure.
  - The X-ray data are fine? We just need to revise the existing models.

Well...

- That's just one cluster. What about the other clusters?
  - We measure the SZ effect of a very nice sample of well-studied nearby clusters compiled by Vikhlinin et al.

Coma Data vs Arnaud

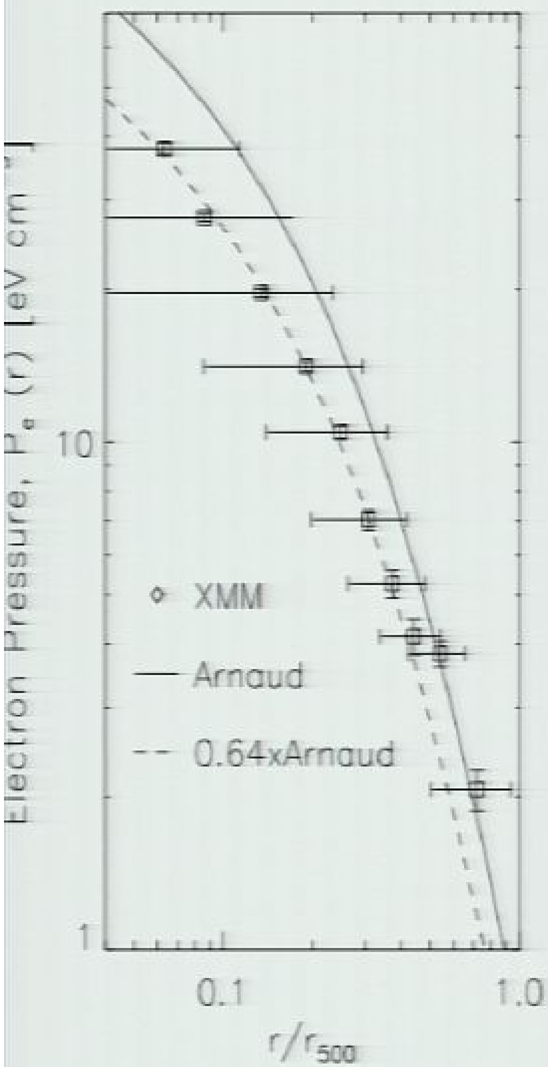

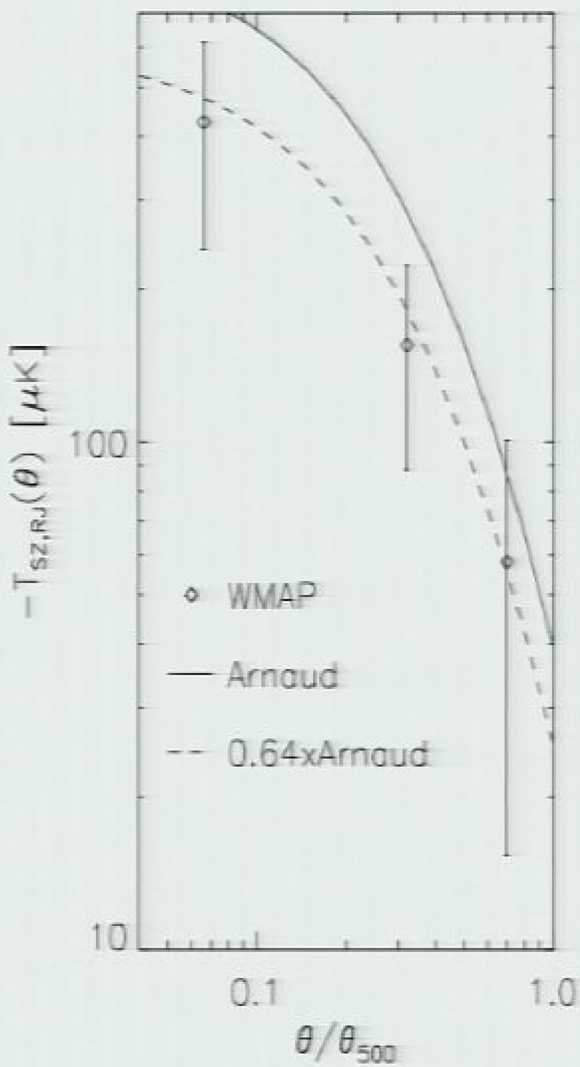

- $M_{500}=6.6\times10^{14}h^{-1}M_{sun}$ is estimated from the mass-temperature relation (Vikhlinin et al.)
  - T_X^{coma} =8.4keV.
- Arnaud et al.'s profile overestimates both the direct X-ray data and WMAP data by the same factor (0.64)!
  - To reconcile them, Tx^{coma}=6.5keV is required, but that is way too low.

The X-ray data (XMM) are provided by A. Finoguenov.

New results! (Prelim.)

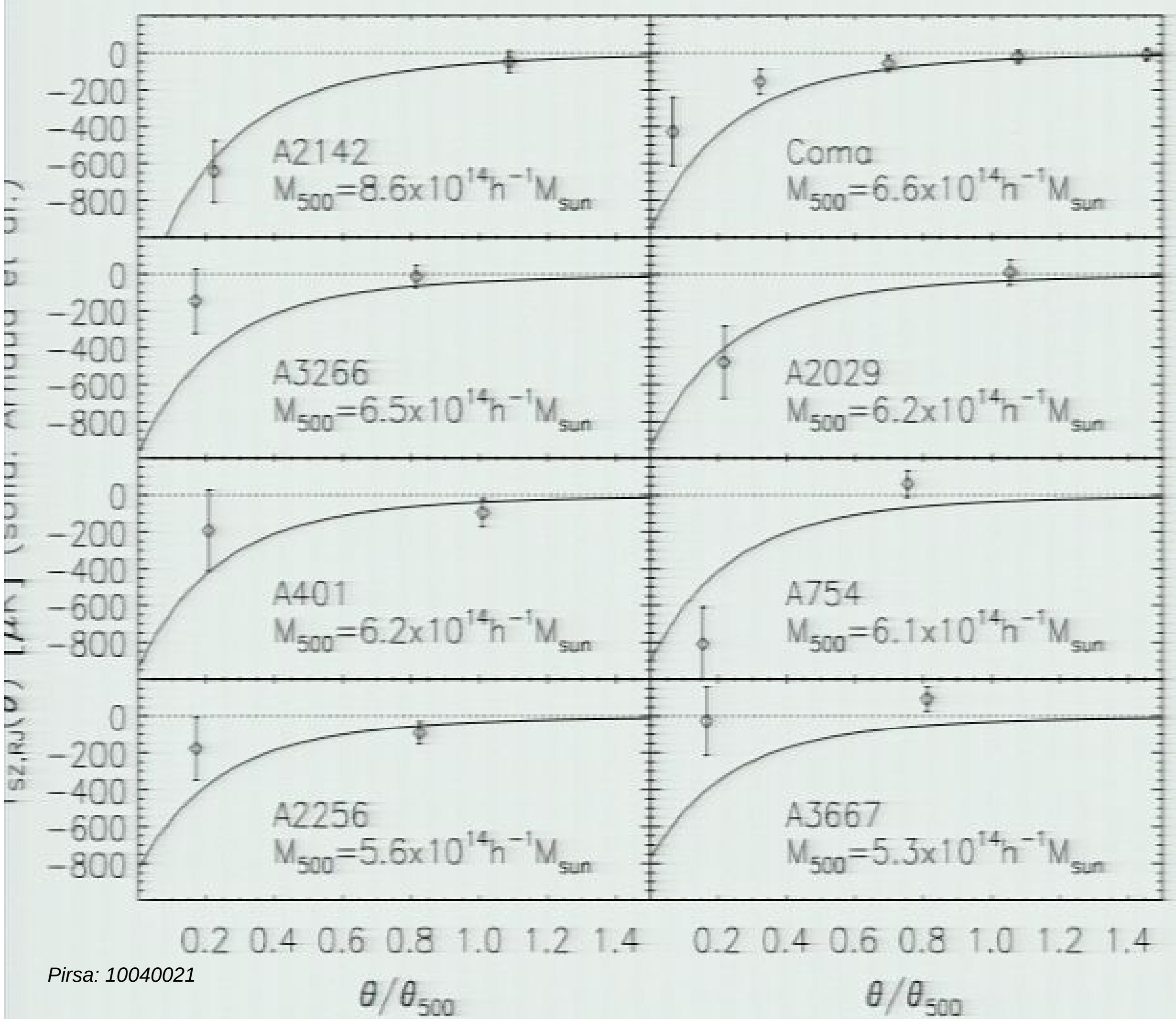

- Normalization for the 5 very high-mass clusters ($M_{500}>6\times10^{14}h^{-1}M_{sun}$) is 0.72±0.13.
- Normalization for the 12 high-mass clusters ($M_{500}>4\times10^{14}h^{-1}M_{sun}$) is 0.68±0.11.
- Arnaud et al. profile systematically overestimates the electron pressure!

Lower A_{SZ}: Two Possibilities

$$C_l = g_\nu^2 \int_0^{z_{\max}} dz \frac{dV}{dz} \int_{M_{\min}}^{M_{\max}} dM \frac{dn(M,z)}{dM} |\tilde{y}_l(M,z)|^2$$

→ $\frac{l(l+1)C_l}{2\pi} \simeq 330\,\mu\mathrm{K}^2\,\sigma_8^7 \left(\frac{\Omega_b h}{0.035}\right)^2$ x [gas pressure]

- The SZ power spectrum is sensitive to the number of clusters (i.e., σ_8) and the pressure of individual clusters.
- Lower SZ power spectrum can imply:
  - σ_8 is 0.77 (rather than 0.8): $\sum m_\nu \sim 0.2$eV?
  - Gas pressure per cluster is lower than expected

→ WMAP measurement favors this possibility.

52

Small-scale CMB Data

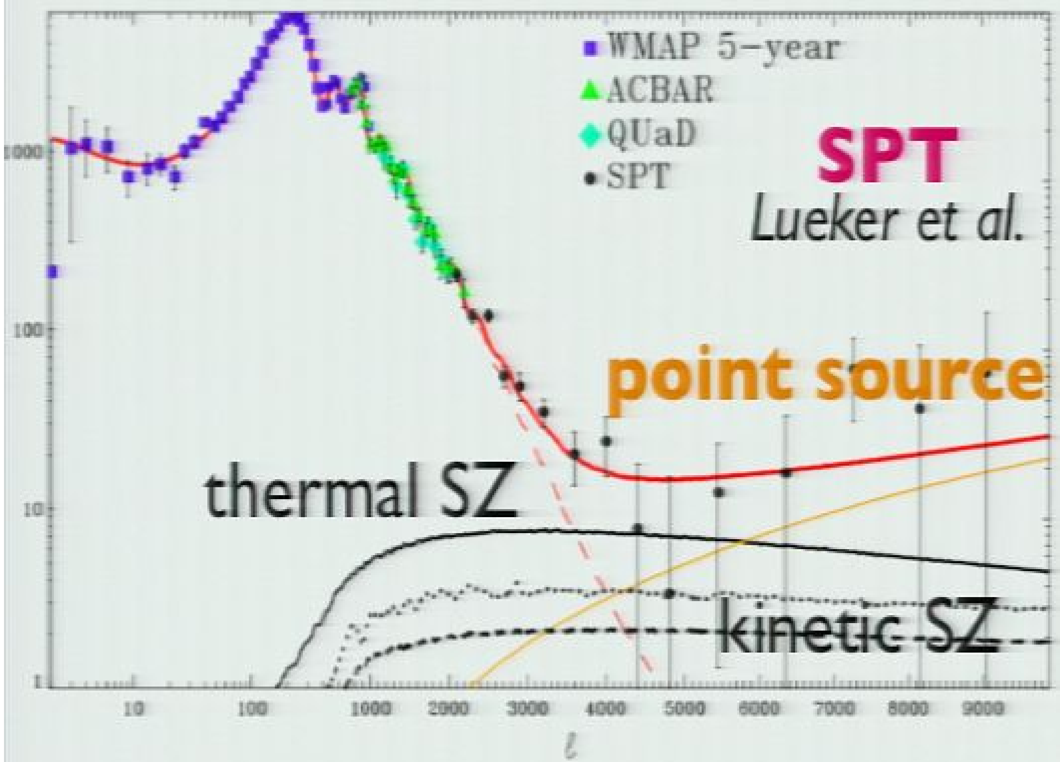

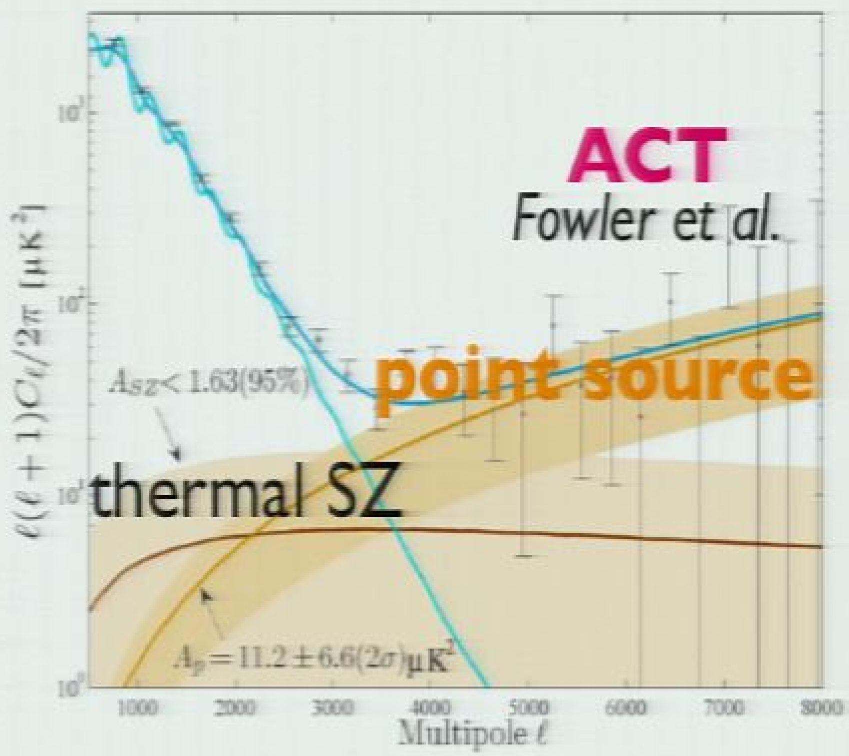

- The SPT measured the secondary anisotropy from (possibly) SZ. **The power spectrum amplitude is A_{SZ}=0.4–0.6 times the expectations.** Why?

Lower A_{SZ}: Two Possibilities

$$C_l = g_\nu^2 \int_0^{z_{\max}} dz \frac{dV}{dz} \int_{M_{\min}}^{M_{\max}} dM \frac{dn(M,z)}{dM} |\tilde{y}_l(M,z)|^2$$

$$\frac{l(l+1)C_l}{2\pi} \simeq 330\,\mu\mathrm{K}^2\,\sigma_8^7 \left(\frac{\Omega_b h}{0.035}\right)^2$$ x [gas pressure]

- The SZ power spectrum is sensitive to the number of clusters (i.e., σ_8) and the pressure of individual clusters.
- Lower SZ power spectrum can imply:
  - σ_8 is 0.77 (rather than 0.8): $\sum m_\nu \sim 0.2$eV?
  - Gas pressure per cluster is lower than expected

WMAP measurement favors this possibility.